Technical Report No. 195

3674-18-T

INTERSYMBOL INTERFERENCE IN BINARY COMMUNICATION SYSTEMS

by

Christopher V. Kimball

Approved by: Theodore G. Birdsall

T. G. Birdsall

COOLEY ELECTRONICS LABORATORY
Department of Electrical Engineering
The University of Michigan
Ann Arbor, Michigan

for

Contract No. Nonr-1224(36)
Office of Naval Research
Department of the Navy
Washington, D.C. 20360

August 1968

ABSTRACT

When a binary communication system transmits symbols through a bandlimited channel, the received symbols will generally overlap in time, giving rise to intersymbol interference. In the presence of noise, intersymbol interference produces a significant increase in the system probability of error. The problem of intersymbol interference and noise is considered here for known, linear, time invariant channels and with added white Gaussian noise. Although a particular underwater acoustic channel is used as a source of motivation, the results presented are equally applicable to other communication channels.

Traditional approaches to the intersymbol interference problem--spectrum and transversal (time) equalization are examined. A basis for the comparison of intersymbol interference problems using the concept of phase equalization, is given. A major assumption which limits the interference to that caused by adjacent symbols is made. This assumption is shown to be equivalent to restricting the transmitter to reasonable signalling rates relative to the bandwidth of the channel power spectrum. All subsequent analysis and evaluation are done under this assumption.

Several linear filter receivers prevalent in the literature--the matched filter receiver, the transversal filter receiver, and the optimized linear filter receiver--are reviewed and evaluated. Two easily implemented nonlinear receivers, the switched-mode receiver and

the iterated switched-mode receiver, are considered as alternatives to the more complex optimized linear filter receivers. The iterated switched-mode receiver, which is described for the first time here, is shown to perform better than any optimized linear receiver when intersymbol interference is moderate. Finally, the optimum (likelihood ratio) receiver is described and evaluated to provide an absolute lower bound on error probability for a given intersymbol interference problem.

A comparison of the error performance of the receivers shows that if intersymbol interference is reduced to moderate amounts by proper choice of signalling rate, then the easily implemented iterated switched-mode receiver gives near intersymbol interference free performance. For higher signalling rates and consequently larger amounts of intersymbol interference more complicated receivers are required to achieve near optimum performance and even the performance of the optimum receiver is significantly worse than intersymbol interference free performance.

FOREWORD

This report considers a practical problem in underwater communications--intersymbol interference. Four major contributions are presented. First, the extent of intersymbol interference in a given situation is shown to be dependent on the autocorrelation function of the received symbol instead of the received symbol itself. Examination of the received symbol usually indicates more intersymbol interference than is actually present. Second, several traditional and proposed receivers are compared on a consistent basis, indicating the trade-offs between system error performance and system complexity. The optimum (likelihood ratio) receiver is included in the comparison to provide a lower bound on error performance. Third, an easily implemented nonlinear receiver whose performance is close to that of the optimum receiver in many practical cases is described. Finally, a rule-of-thumb is given which relates transmission rate, error performance, and system complexity. The above contributions should be of considerable importance to a designer of an underwater communication system.

ACKNOWLEDGMENTS

I would like to thank the members of my committee, Professor T. G. Birdsall (Chairman), Professor W. A. Ericson, Professor K. B. Irani, Professor A. B. Macnee, and Professor M. P. Ristenbatt for their helpful suggestions. Credit is also due to my colleagues at the Cooley Electronics Laboratory, The University of Michigan, for their many comments and suggestions during the course of the research.

The research reported in this dissertation was supported by the Office of Naval Research, Department of Navy, under Contract No. Nonr-1224(36), "Acoustic Signal Processing."

Particular thanks are due to Mrs. Dianne Bohrmann and Miss Heather Sawler for their fine preparation of the manuscript.

TABLE OF CONTENTS

TABLE OF CONTENTS Cont.

LIST OF ILLUSTRATIONS

LIST OF ILLUSTRATIONS Cont.

LIST OF ILLUSTRATIONS Cont.

LIST OF ILLUSTRATIONS Cont.

LIST OF TABLES

LIST OF APPENDIXES

LIST OF SYMBOLS

Symbol	Definition	Page
$A(\omega)$	magnitude spectrum of $\rho'(t)$	26
b_k	value of the kth transmitted symbol	51
B_k	set of m dimensional vectors $b_0 \ldots b_i \ldots b_n$ $i \neq k$ $b_i = \pm 1$	54
$\bar{b}$	$(b_{k-q-1} \ldots b_i \ldots b_{k+q+1})$ $i \neq k$	81
b	(b_{j-1}, b_j)	116
b_k^{∞}	"large" magnitude with sign of b_k	123
$\lvert B_k \rvert$	any set $\{\bar{b} \in B_k \mid \bar{b} \in \lvert B_k \rvert \Rightarrow -\bar{b} \notin \lvert B_k \rvert\}$	175
CW	continuous wave	5
$C(\omega)$	channel (complex) spectrum	24
C_i	weight of jth delay in canonical form of the linear filter receiver	59
c_0, c_1	coefficients used in TFR	73
d_k	decision value on the kth symbol	51
D_k	hyperplane through the origin for kth symbol	54
d	index of signal detectability $2E/N_0$ for a single symbol	68
d_k^0	"first guess" decision on kth symbol for ISMR	98
d_k^1	final decision on kth symbol for ISMR	99
d_k^i	"ith guess" decisions made by ISMR	101
E	energy in a single noise free symbol	26
$EF(\omega)$	equalizer filter (complex) spectrum	27

Symbol	Definition	Page
$e(t)$	response of transversal filter to $\rho'(t)$	32
$E(\omega)$	Fourier transform of $e(t)$	32
$E[\cdot]$	expected value	56
$\hat{e}_0, \hat{e}_1, \hat{e}_2$	orthonormal unit vectors used to represent x^k	66
f	frequency (Hz)	7
FL	linear filter	23
$FL_{OPT}(\omega)$	complex spectrum of the optimum post equalizer filter	27
$FL(\omega)$	overall transfer function of a linear filter receiver	29
$FL_{MF}(\omega)$	complex spectrum of a matched filter	32
$FL_{TF}(\omega)$	complex spectrum of a transversal filter	32
F, F^{-1}	Fourier transform, inverse Fourier transform	39
$G_0(x_j, L_{k-1}^k)$	see Eq. 5.19	119
$G_1(x_j)$	see Eq. 5.22	120
$G_2(x_j, L_{j-1}^j(+1), L_{j-1}^j(-1))$	see Eq. 5.26	121
$G_0^1(x_0)$	see Eq. 5.34	123
G_0^{-1}	inverse (given $x_k^0, L_{k-1}^k, L_k^{k+1}$) of the G_0 mapping	143
h	impulse response of linear filter	52
$H(\omega)$	complex spectrum of linear filter in a linear filter receiver	52
$\tilde{h}^k$	$h(kT - t)$	53

Symbol	Definition	Page
H_1	subspace spanned by $\{\rho^i \mid i = 0 \ldots m\}$	58
H_2	orthogonal complement of H_1	58
$\tilde{h}_1^k$, $\tilde{h}_2^k$	components of $\tilde{h}^k$ in the H_1^k, H_2^k subspaces	58
ISMR	iterated switched mode receiver	97
$J(x_k^0, x_k^1)$	Jacobian of the G_0 mapping with x_k^0 as the auxiliary variable	143
k_i	transversal filter tap weights	31
K	normalizing constant for $p(x_j \mid b_{j-1} b_j)$	118
L^2	Hilbert space of finite energy waveforms	23
L_k	decision variable for the kth symbol	51
L_k''	output of the first adder for canonical linear receiver	61
L_k'	output of the matched filter for nonlinear receivers	92
$l_k(x)$	likelihood ratio of the reception x for the kth symbol	111
L_k^j	log odds ratio for the kth symbol given X_j	112
$lnl_k(x_j)$	log likelihood ratio of x_j for the kth symbol	113
$lnl_k(X_j)$	log likelihood ratio of X_j for the kth symbol	114
$L_{j-1}^j(b_k)$	conditional log odds ratio (Eq. 5.25)	122
$lnl_j(x_j \mid b_k)$	conditional log likelihood ratio (Eq. 5.29)	122
$\tilde{L}_k^j$	reverse log odds ratio, the log ratio of $\tilde{X}_j$ for the kth symbol	133

LIST OF SYMBOLS Cont.

Symbol	Definition	Page
M	degree of intersymbol interference	42
m	$m+1$ is the number of transmitted symbols	52
MFR	matched filter receiver	69
N	noise power	12
$\|N''(\omega)\|^2$	noise power spectrum at the output of equalizer filter	27
n(t)	noise waveform	52
N_0	noise power density	52
n'	internal noise waveform of canonical linear receiver	59
$OLFR_i$	optimized linear filter with i taps	83
OLFR(2T)	optimized linear filter receiver for impulse response having duration 2T	88
PR	psuedo random	5
$PEF(\omega)$	complex spectrum of phase equalizing filter	35
P	probability	54
$P_e(k)$	probability of error for the kth symbol	57
P_e	average system probability of error	58
$P_e(\bar{w})$	probability of error for OLFR with tap coefficients given by $\bar{w}$	82
P_0, P_1	conditional probabilities of error for SMR	93
$P_e(\alpha, \beta)$	probability of error when L_k has the form of Eq. 9.7	94

Symbol	Definition	Page
P_e^0	probability of error for the "first guess" decision of ISMR	98
$P_{00}, P_{01}, P_{10}, P_{11}$	conditional probabilities of error for the evaluation of ISMR	99
P_e^1	probability of error for ISMR final decisions	99
P_e^i	probability of error for ith decision level in the logical extension of ISMR	101
p	probability density function	111
Q	ratio of center frequency to bandwidth	3
$q_1(t), q_2(t)$	binary symbol waveforms	10
q(t)	transmitted binary simplex signal	24
$Q(\omega)$	Fourier transform of q(t)	24
$\mathscr{R}$	binary receiver	23
R(t)	autocorrelation function of the noise free received signal	68
r(t)	normalized autocorrelation function = R(t) / R(0)	68
R	$\rho_0^k \cdot \rho_1^{k-1} = R(T)$	183
S/N	average signal-to-noise power ratio	5
SMR	switched mode receiver	91
s_b	signal components in x_j given b	118
$S(u_1, u_2)$	$u_1\phi(u_1) + u_2\phi(u_2)$	175
t	time	7

LIST OF SYMBOLS Cont.

Symbol	Definition	Page
T	duration of the transmitted symbol	10
TFR	transversal filter receiver	72
TOOR	truncated observation optimum receiver	128
$\hat{u}_0, \hat{u}_1$	orthonormal vectors used to represent x_k	139
Var	variance	56
w_i	weight of the i th tap for $OLFR_{2q+1}$	79
$\overline{w}$	$(w_{-q} \ldots w_{+q})$	81
$\overline{w}^*$	optimum tap coefficients for OLFR	83
w'_{-1}, w'_{+1}	coefficients used in OLFR(2T)	87
x	total received waveform	52
x^k	portion of the reception x in $(kT, (k+2)T)$	64
X_j	portion of the reception in the time interval $(0, jT)$	112
x_j	portion of the reception in the time interval $(jT, (j+1)T)$	112
$\tilde{X}_j$	portion of the reception in the time interval $(jT, (n+2)T)$	133
x_k^0, x_k^1	components of x_k in the $\hat{u}_0$, $\hat{u}_1$ directions	140
$\bar{x}_k$	representation of x_u in plane defined by $\hat{u}_0$, $\hat{u}_1$	140

Symbol	Definition	Page
y_1	$\tilde{h}_1^k \cdot \rho^k$	174
y_2	$\sum_{i \neq k} b_i \rho^i \cdot \tilde{h}_1^k$	174
y_3	$1/\sqrt{N_0(\lvert \hat{h}_1^k \rvert^2 + \lvert \hat{h}_2^k \rvert^2)/2}$	174
$Z_1(\bar{b},\bar{w})$, $Z_2(\bar{b},\bar{w})$	functions used in computing $P_e(\bar{w})$ for OLFR	82
α, β	constants used in evaluation of SMR, ISMR	94
$\Gamma(d_{k-1})$	threshold for SMR	96
$\Gamma(d_{k-1}^0, d_{k+1}^0)$	threshold for ISMR	100
$\gamma(L_{k-1}^k, L_k^{k+1})$	integration path for determination of $p(L_k^{k+1} \mid L_{k-1}^k, b_k = +1)$	144
$\Delta_{b_{k-1}b_k}^k$	interference component of x_k given b_{k-1}, b_k	65
ζ	$1/2\,[\, L_k^{k+1} - 2x_k^0 \rho'_{00}]$	184
η	percentage of total energy of $\rho(t)$ in an interval of duration $2T$	44
ξ	$1/2[\, L_{k-1}^k + 2x_k^0 \rho'_{10}]$	184
$\rho'_1(t), \rho'_2(t)$	noise-free channel outputs due to symbols $q_1(t), q_2(t)$	13
$\rho'(t)$	uncompensated, noise-free channel output for simplex symbols	15
$\rho'(\omega)$	Fourier transform of $\rho'(t)$	26
$\rho''(\omega)$	complex spectrum of the noise-free output of the equalizer filter due to a single symbol	27

Symbol	Definition	Page
ρ	noise-free phase-equalized received symbol	36
ρ^i	$\rho(t-iT)$	56
ρ_0^k, ρ_1^k	$\rho_0^i(t - kT)$, $\rho_1^i(t - kT)$	64
ρ_0	$\rho_0 = \rho \quad 0 \leq t < T$ $= 0$ elsewhere	64
ρ_1	$\rho_1 = \rho \quad T \leq t < 2T$ $= 0$ elsewhere	64
$\rho_s(t)$	a selected segment of $\rho(t)$	70
$\tilde{\rho}^i$	$\rho(iT - t)$	61
ρ'_{ij}	component of ρ_i^{k-i} in the $\hat{u}_j$ direction	139
τ_c	time center of a waveform	26
τ_{RMS}	RMS time duration of a waveform	26
$\phi(u)$	zero mean, unit variance Gaussian density function	56
$\Phi(u)$	cumulative distribution function of $\phi(u)$	57
$\psi(\omega)$	phase spectrum of $\rho'(t)$	26
ω	radian frequency	24
superscript *	complex conjugate	27
$\cdot$ operator	L^2 inner product	53
$\perp$	L^2 orthogonality relation	65
$\circledast$	convolution operator	136

CHAPTER I

INTRODUCTION

This paper is the result of a study of the general underwater acoustic communications problem, using experimental results from a comparatively well-known channel. Because of the complexity of the general problem, a specific, but important aspect of the problem, is considered: intersymbol interference in binary signalling systems. Restriction to binary signalling systems provides considerable simplification in both analysis and implementation. Intersymbol interference occurs in such systems when the received symbols overlap one another in time, increasing the probability of error. Channel phenomena which produce irregularities in the received power spectrum, such as multipath and selective fading, are sources of intersymbol interference. Although underwater acoustic channels are the frame of reference for this study, application to other channels is easily accomplished.

For binary communication systems in the absence of intersymbol interference, the classical theory of signal detectability provides the basis for the design of the optimum (likelihood ratio) receiver (Ref. 1). Only a limited number of studies have been made which consider the intersymbol interference problem, however. These studies deal with the determination of the optimum linear filter receiver for a given situation (Refs. 2, 3, 4). Aein and Hancock have demonstrated an easily

implemented nonlinear receiver which is superior in performance to their optimum linear receiver (Ref. 2). A major objective of this paper is to extend the theory of signal detectability to intersymbol interference problems by analysing and evaluating the optimum (likelihood ratio) receiver. A comparison of the above receivers with those used in practice is also made.

In subsequent discussion, we often refer to experimental results from the Miami to Bimini test facility of the Michigan-Miami ("Mimi") project as a source of motivation (Ref. 5). Some significant aspects of the Mimi channel are sketched in the next section. We then discuss the working assumptions of the paper and ways in which these assumptions may be relaxed. Finally, the major conclusions and contributions of the thesis are summarized.

1.1. The Mimi Channel

The Mimi project is a joint effort by the Institute of Marine Science of the University of Miami and Cooley Electronics Laboratory of the University of Michigan. The Mimi test facility has two features which distinguish it from other facilities. First, both the transmitter and receiver hydrophones are in permanently fixed positions. This allows repetitive study of exactly the same physical channel. Second, very stable (1-2 parts in 10^{10}) oscillators are available at both the transmitting and receiving sites, which allow coherent averaging and analysis of the receptions. In this section we will sketch the

physical structure of the channel and several of its features which are relevant to the communications problem.

The basic Mimi channel consists of a transmitting transducer and reflector at Fowey Rocks near Miami, Florida, and receiving hydrophones at North Bimini Islands, Bahamas, 43 miles to the east as shown in Fig. 1.1. For the first 13 miles from Fowey Rocks the depth is sloping to 400 meters. Near the end of this shelf is the mean center line for the Gulf Stream, which is a source of turbulence. Beyond the first 13 miles the depth drops off abruptly to 800 meters until Bimini is reached. Ray path computations indicate bottom reflection combined with surface reflected and/or refracted modes of propagation in the channel.

Two fundamental limitations are placed on the channel by the transmitting transducer and reflector. The first is that the nominal bandwidth of the transducer is 100 Hz centered at a 420 Hz carrier frequency. This limitation is due to the construction of the transducer and the beam forming reflector. One can view the bandwidth restriction by considering the "Q" (center frequency/bandwidth) of the system, which indicates the system is wide band, i.e., 1.0 MHz at 4.2 MHz would be a wide band in HF radio. Alternatively, when typical information rates are considered, the system appears narrowband, i.e., a 100-wpm teletype requires a bandwidth of at least 80 Hz. We see that, relative to common information rates, bandwidth is a significant limitation.

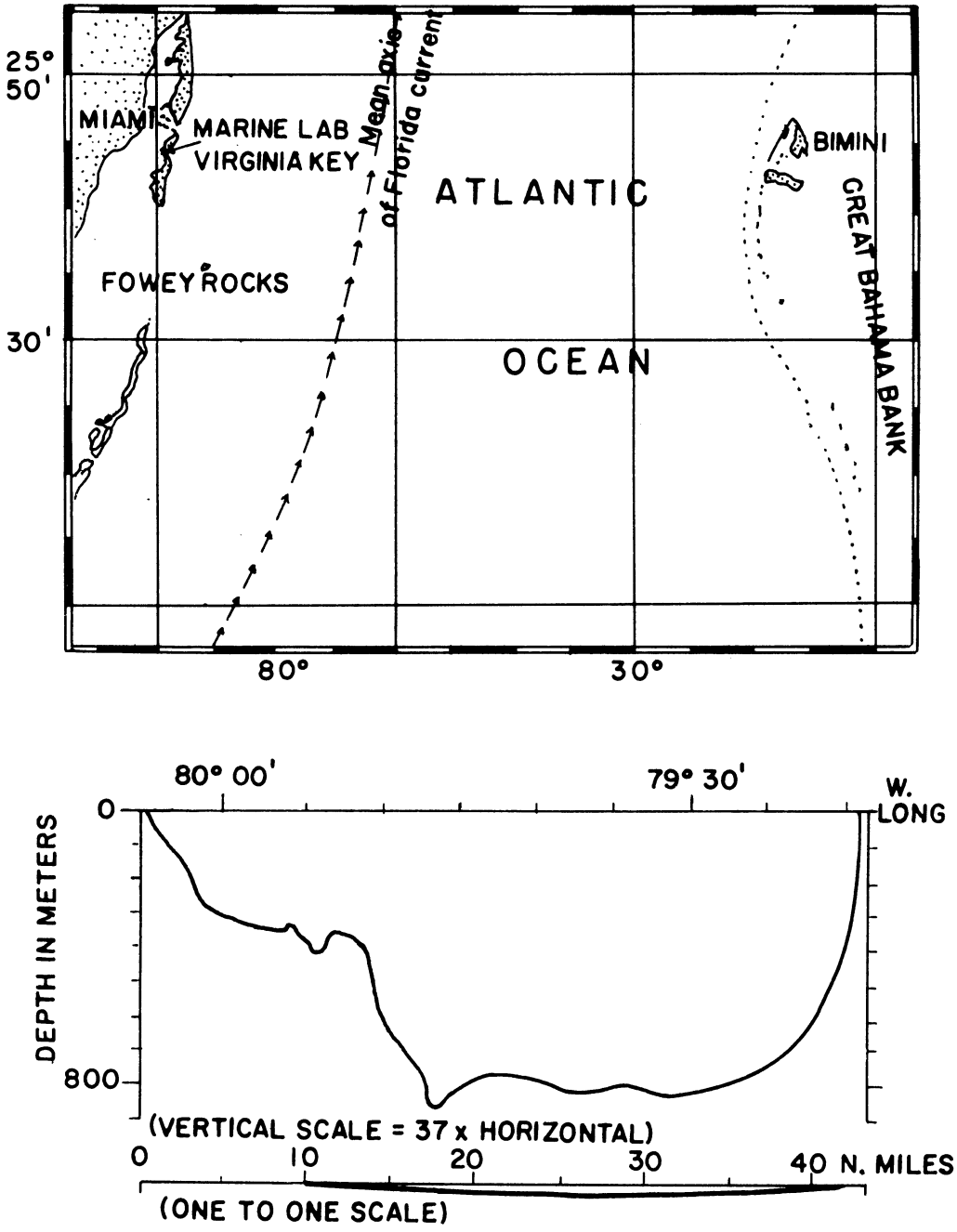

Fig. 1.1 Physical configuration of the Mimi channel

The second limitation due to the transmitting transducer is a peak power limitation. Ceramic elements in the transducer are subject to fracture and/or fatigue at high power levels. Because of the great difficulty and expense involved in obtaining a replacement transducer, the system is normally operated well below its specified rating. Even if more durable transducers were available, cavitation in the water surrounding the transducer would provide a peak power limitation. The effect of the peak power limitation on the communications problem is to severely limit the waveforms which may be transmitted.

Noise is a major problem in the Mimi channel. In travelling the 43 mile distance a signal is attenuated by 105 to 135 db, yielding S/N ratios in the range -10 db to + 20 db in a 100 Hz band. The precise form of the noise is largely unknown at the present time. Non-thermal noise such as ship or biological noise is known to be present, and hence an accurate description of the noise would be difficult.

Two types of signals have been used to measure the channel spectral characteristics: continuous wave (CW) signals and periodic pseudo-random (PR) signals. CW signals allow high S/N analysis of a single spectral line, usually at the 420 Hz center frequency. Results of these CW transmissions indicate very slow (less than 10 cycles per day) phase changes of the received signal relative to the coherent reference. During these same tests the amplitude of the reception was noted to fluctuate considerably, occasionally becoming undetectable. Two

tone (two simultaneous CW) tests indicate similar phase characteristics on both spectral lines, but with independent amplitude characteristics. Both forms of the CW experiment suggest the Mimi channel is amazingly phase stable and subject to a time variant frequency selective fading.

The wide band PR signals can be employed to measure the spectrum of the Mimi channel. This spectral analysis is done by cross-correlating the received signal with the original pseudo-random signal and then performing deconvolution techniques to obtain the complex channel spectra. Figure 1.2 shows a typical complex impulse response and corresponding spectrum based on a 5-minute coherent time average of data taken in February 1965.* Figure 1.3 shows the autocorrelation of the impulse response and the corresponding spectrum, which is the channel power spectrum.** The plotted data (which has been subjected to discretionary filtering) is believed representative of the form of the spectra to be expected in the Mimi channel.

From the spectra of Figs. 1.2 and 1.3, the selective fading effects of multipath are apparent. Two distinct null frequencies in the effective 50 Hz bandwidth are indicative of selective fading. The linear

---

*In this and subsequent discussions of the channel, we represent the real bandpass waveform as a complex low pass waveform as is usually done. The complex low pass waveform is given by $M(t)e^{j\theta(t)}$ where $M(t)$ is the magnitude waveform and $\theta(t)$ is the phase waveform. The physical bandpass waveform is given by $M(t)\cos[2\pi(420)t - \theta(t)]$.

**The autocorrelation function is a conjugate symmetric complex waveform because of the complex low pass representation of the impulse. The autocorrelation of the physical bandpass waveform is given by one-half the real part of the complex autocorrelation.

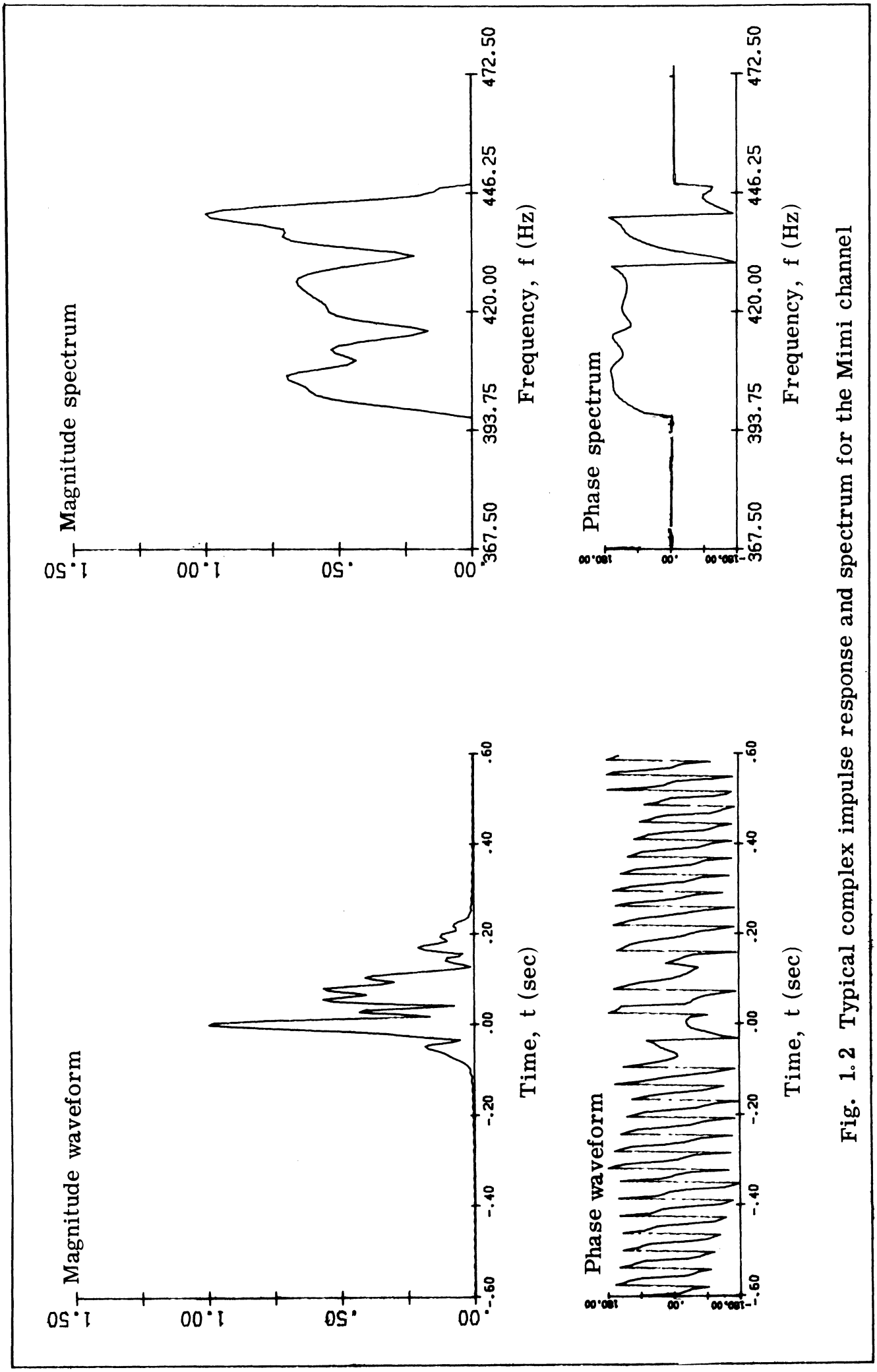

Fig. 1.2 Typical complex impulse response and spectrum for the Mimi channel

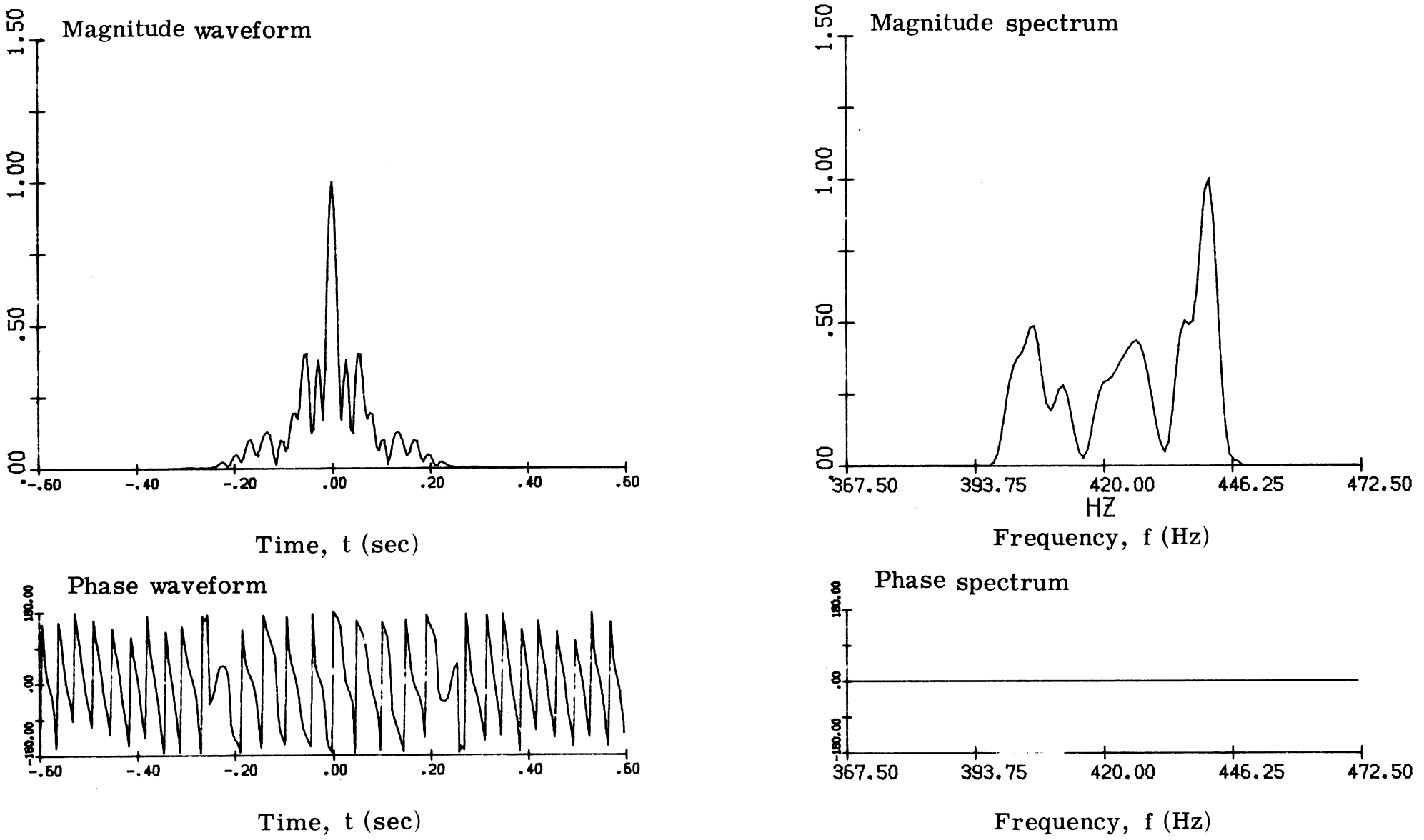

Fig. 1.3 Typical autocorrelation of the complex impulse response and power spectra for the Mimi channel

phase characteristic in the third (highest frequency) sub-band suggests that energy in this sub-band arrives later than that in the other two sub-bands. This assertion is borne out in the time domain by the delayed peaks in the impulse response. Such a late arrival may also be attributed to multipath.

Another significant feature of the Mimi channel is the presence of time variations of different time orders. Long term variations dependent on the time of day; tides and weather have been observed in both the CW and PR sequence transmissions. Sequence transmissions have shown very slight changes in the channel spectrum over a 5-minute interval. Studies using receiving hydrophones close (3 miles) to the transmitting site indicate the presence of an amplitude modulation effect caused by wave height. The time order of this effect is of the order of 1 to 10 seconds. More rapid time variations in the channel may also be present, but are difficult to distinguish from the noise.

Other interesting features of the channel are known to exist. Indeed, further analysis of the Mimi channel is a continuing project. We summarize the major features of the channel below:

1. Limited bandwidth: $\sim$ 100 Hz
2. Transmitter peak power limitation
3. Low received S/N ratios: -10 to +20 db
4. Multipath/Selective fading effects: Figs. 1.2, 1.3
5. Time variations of different durations: 5 min., 5 sec.

Although the Mimi channel is a very specific channel, the above effects are generally encountered in underwater acoustics and hence we expect to be able to generalize results obtained for the Mimi channel to other situations.

1.2. Assumptions

In order to study the communication problem on a firm theoretical basis, several simplifying assumptions are made. These assumptions take on varying degrees of importance and many of them may either be relaxed or considered worst case assumptions. In this section we state the working assumptions for the Mimi channel discussed previously.

Transmitter

A major assumption of this work is that the transmitter is restricted to binary signalling. That is, in any one time interval, T , the transmitter may transmit only one of two signals $q_1(t)$ or $q_2(t)$. The signals $q_1(t)$ and $q_2(t)$ considered will usually have low peak to average power ratios. More important, however, we assume that a detailed knowledge of the channel spectrum (beyond bandwidth and center frequency) is not available to the transmitter. This precludes the use of signals which are carefully chosen to smooth out irregularities in the channel spectrum.

Restriction of the problem to binary signalling has two desirable effects. The first is to simplify the analysis by allowing the use of

likelihood ratio procedures. The second is that the implementation of the transmitter is significantly simplified. Furthermore, studies have shown that binary signalling is a reasonable method of signalling at the S/N ratios encountered in the Mimi channel (Ref. 6).

The assumption that details of the channel spectrum are unknown to the transmitter is a realistic assumption in most underwater acoustic channels. In order to have the transmitter know the channel spectrum in detail, either the spectrum must not change at all with time or the communications system must have a feedback link. Even when the communications system is capable of two-way operation, the problem of maintaining an adequate, up-to-date knowledge of the channel at the transmitter is comparable to the original communications problem in difficulty.

Channel

The simplifying assumptions on the channel are comparatively numerous; however, most of them are acceptable from a practical viewpoint. We will assume that the channel is a time invariant, band limited, linear system with white Gaussian noise added at its output. Let us discuss these assumptions one by one.

As mentioned in the previous section, the Mimi channel (and other underwater acoustic channels) has significant time variations occurring in it. These variations, however, occur at a much slower rate than the information rate at which a communication system

could be expected to operate. For example, the fastest time variation in the Mimi channel observed to date has a time order in the range of 1 to 10 seconds, while the duration of a single symbol at 100 wpm, for example, is approximately 20 ms. Thus, over the time duration of a single symbol the channel is expected to change very little. Time variations in the channel spectrum have been observed to have even a longer time order, nearly 5 minutes.

The assumptions that the channel is bandlimited and linear are also borne out in practice. As mentioned earlier the transmitting transducer-reflector imposes a definite bandwidth restriction on the channel. The linearity assumption can be considered a reasonable approximation since, with the exception of the region immediately adjacent to the transmitter, signal energies throughout the physical channel are very small. The transmitter peak power limitation mentioned earlier also tends to reduce the chances of nonlinear behavior by the channel.

The added white Gaussian noise assumption is more difficult to justify. Although only limited noise studies have been made to date, evidence is available to indicate the actual noise is both non-white and non-Gaussian. Because of the lack of a good description of the channel noise and the obvious advantages of a white Gaussian noise model, this assumption is made anyway. We note, however, that for a given noise power, N, white Gaussian noise is a "worst case" form of noise. That

is, if a system is designed on the basis of white Gaussian noise of power N , then its performance in different noise of the same power will be no worse than its computed performance. The potential of using peculiarities of the noise to obtain better performance is eliminated by this assumption. Nevertheless, the added white Gaussian noise assumption allows us to gain considerable insight into the overall problem.

Receiver

We will assume that the operation of the receiver is coherent and synchronized with respect to the transmitter. Moreover, we assume that the noise-free outputs of the channel, $\rho'_1(t)$ and $\rho'_2(t)$ due to both transmitted symbols, $q_1(t)$ and $q_2(t)$ are known exactly. If the transmitted symbols are known, as they usually would be, this assumption is equivalent to a knowledge of the channel spectrum. The assumption that the noise-free received symbols are known exactly greatly simplifies subsequent analysis.

Since the availability of highly stable oscillators is one of the key features of the Mimi channel, the coherency and synchronization assumption is immediately valid for the Mimi channel. The problem of incoherent communications is somewhat more difficult than the coherent problem; however, the results for the coherent problem provide a basis for the study of the incoherent problem. Synchronization is a well-studied problem from other communications work.

The assumption that the noise-free received symbols $\rho'_1(t)$ and

$\rho'_2(t)$ are known exactly can be well approximated in practice through transmitted reference techniques similar to those used in HF radio (Ref. 7). In a transmitted reference technique the transmitted signal has two components: an information component and an unchanging reference component. Usually the two components are made orthogonal. At the receiver, the reference component is processed over a long (relative to the symbol duration) time to achieve a high S/N estimate of the noise-free channel response. In such systems a weighting factor is often introduced to allow the estimate to "track" slow time variations. Although more elegant methods of obtaining an estimate of the channel response warrant further study, the transmitted reference technique currently appears to be adequate. Incidentally, the estimate of the channel response afforded by this technique may in some systems (i. e., Mimi project) be of interest by itself.

The above assumptions sufficiently simplify the basic communication problem to allow a rigorous analysis. In summary we list these assumptions and their motivations below:

Transmitter:

Binary signalling	Easy to implement and efficient
Peak power limitation	Common transducer property
No detailed knowledge of channel	True unless feedback is used

Channel:	
Time Invariant	True over short times
Bandlimited	Common transducer/reflector property
Linear	First order approximation
Added white Gaussian noise	A "worst case" assumption
Receiver:	
Coherent and Synchronized Operation	Available at Mimi facility
Exact knowledge of noise free symbol	Possible with transmitted reference

The objective of the systems considered here is to minimize the average probability of error at the receiver for long sequences of transmitted symbols.

Two other relatively trivial assumptions are also being made for convenience in the analysis. The first is that the transmitted symbol values are equiprobable and independent, a very common and reasonable assumption in a communication system. The second is that the noise free input symbols to the receiver are binary simplex symbols; that is, the noise-free input symbol to the receiver is either $\rho'(t)$ or $-\rho'(t)$. If the actual received symbols $\rho'_1(t)$, $\rho'_2(t)$ are not binary simplex, but are known exactly as assumed above, one can obtain simplex symbols by subtracting $\frac{\rho'_1(t) + \rho'_2(t)}{2}$ from the reception.

1.3. Intersymbol Interference

When binary symbols are transmitted through a band limited channel, the received symbols in general will overlap in time, giving rise to intersymbol interference. We will later see that irregularities in the channel power spectrum such as selective fading notches increase intersymbol interference beyond that encountered in an ideal bandpass channel. If noise is not present at the output of the channel, a simple linear filter often called an equalizer, can be used to reduce intersymbol interference to a large degree. On the other hand, if noise is present in the systems, the use of the equalizer may severely degrade system error performance. This second problem of intersymbol interference in the presence of noise is the key problem of the idealized Mimi channel described in the preceding section and is the subject of this study.

To demonstrate the importance of the intersymbol interference problem, we will consider a heuristic example using the Mimi channel. Inspection of the power spectrum of Fig. 1.3 suggests the useful bandwidth of the channel is approximately 50 Hz. By using biphase signalling with a signal duration of 40 ms, the major lobe of the transmitted signal spectrum will be passed by the channel.* Figure 1.4 depicts the time waveform and spectrum of a single 40 ms symbol on the same scale as the earlier figures. By multiplying the complex spectra of the 40 ms symbol

---

*In biphase signalling, the transmitted symbols are pulses of carrier, 180^{o} degrees out of phase with each other.

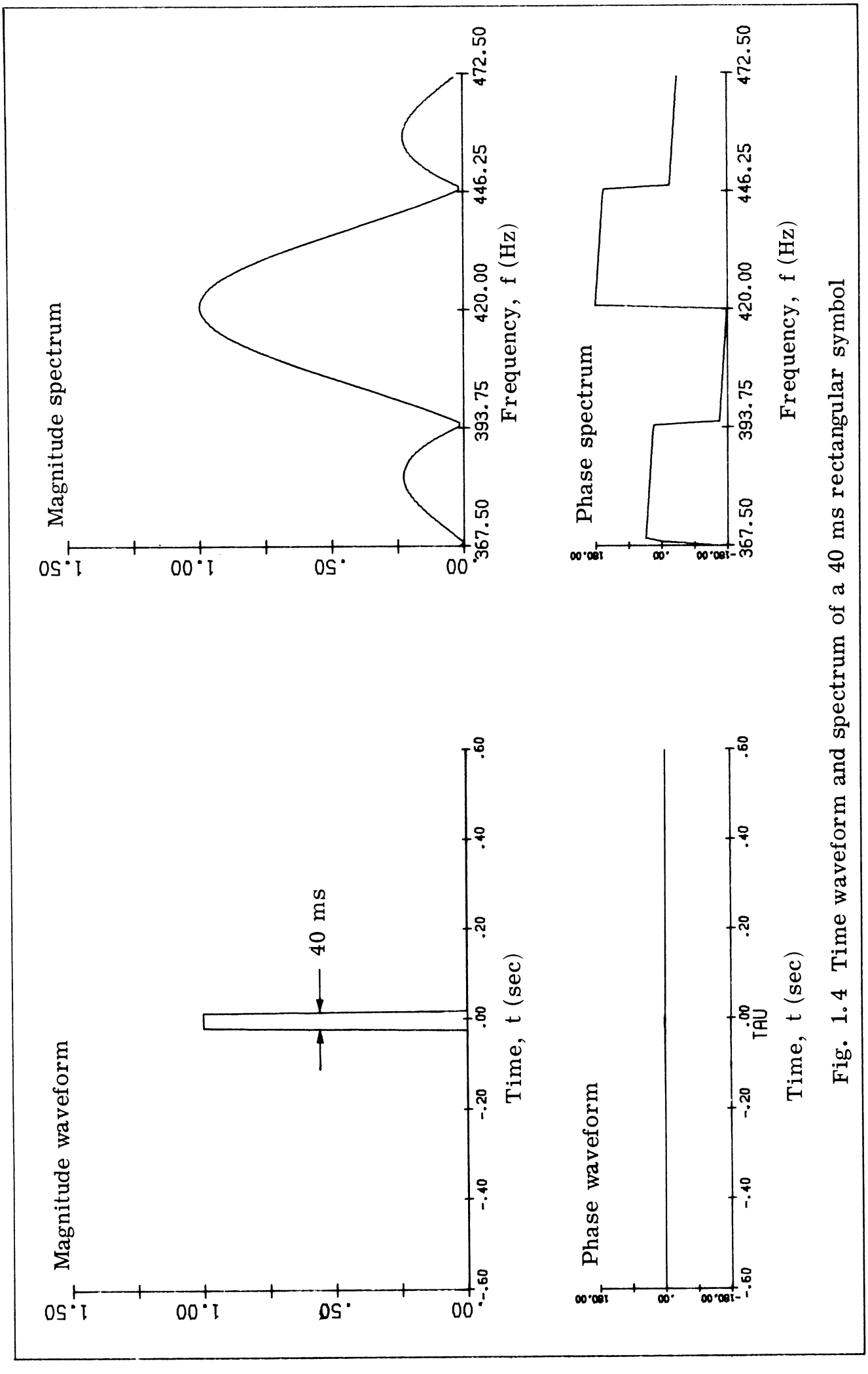

Fig. 1.4 Time waveform and spectrum of a 40 ms rectangular symbol

and the channel, the spectrum of the received symbol is found. Figure 1.5 depicts the spectrum of the received symbol and the complex time waveform of the received symbol. From Fig. 1.5 we note that the received symbol has significant energy over more than 200 ms.

If the 40 ms symbol is used in the heuristic biphase modulation communication system, there will be portions of at least five symbols in every 40 ms interval at the receiver. Depending on the particular values of the interfering symbol, this overlap will bias the decision on the symbol in question one way or the other. The net effect, of course, is to increase the probability of error for the system beyond that expected from the added noise. An increase by a factor of ten or more in the probability of error is typical.

In the second chapter we deal with the general intersymbol interference problem in detail. Until then the above discussion will provide an adequate background.

1.4. Summary and Contributions

In the next chapter, we discuss several traditional approaches to the intersymbol interference problem and their limitations. The notion of phase equalization is introduced to characterize the problem in terms of the power spectrum of the received symbol. The degree of intersymbol interference is defined and a major assumption concerning it is made. This assumption is shown to be equivalent to the limitation of signalling rates to reasonable values.

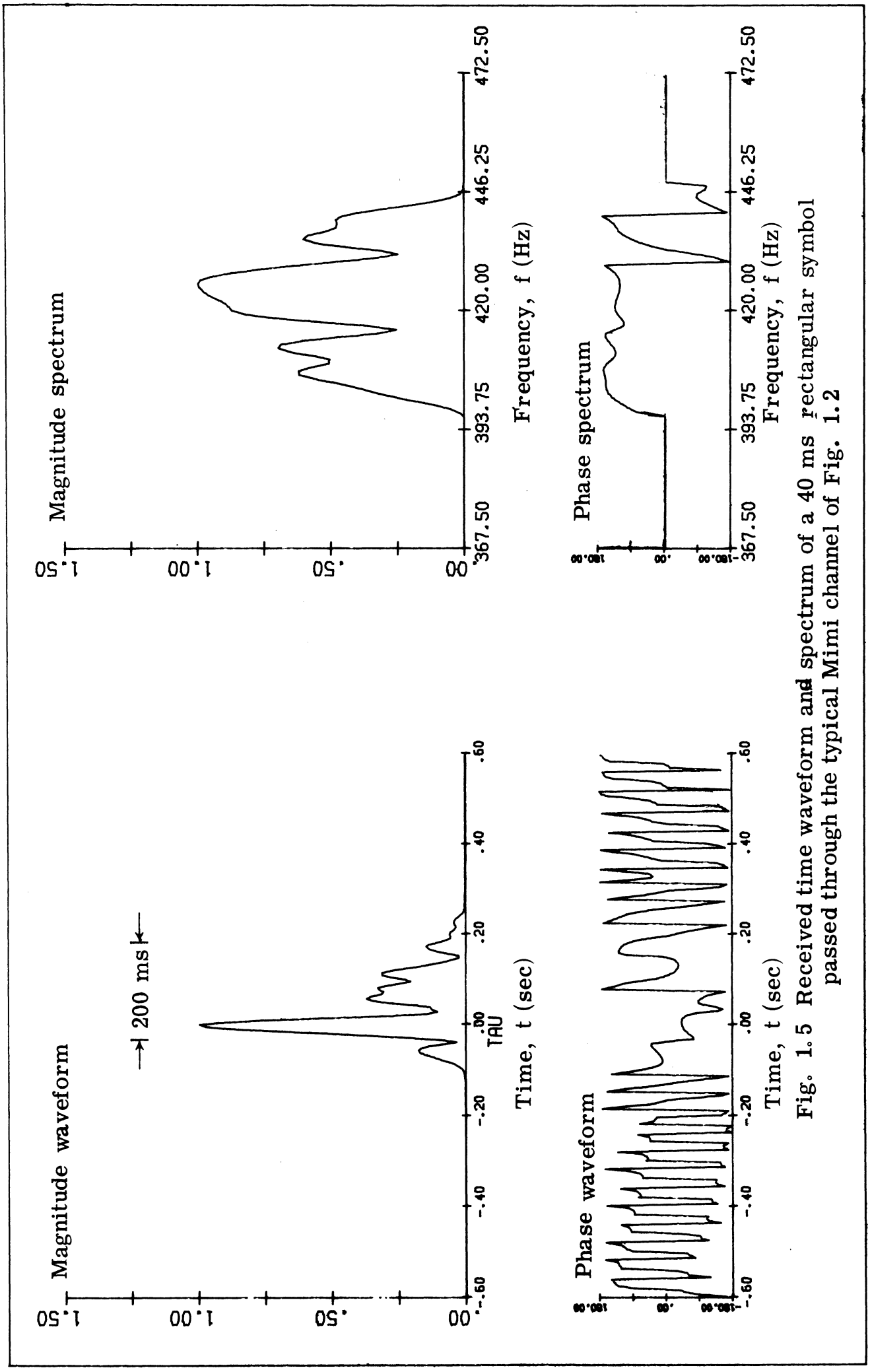

Fig. 1.5 Received time waveform and spectrum of a 40 ms rectangular symbol passed through the typical Mimi channel of Fig. 1.2

The third chapter reviews the class of linear receivers using a convenient vector space notation which allows meaningful visualization of receiver operation. Three types of linear receiver prevalent in the literature are considered, the matched filter receiver derived from classical detection theory, the traditional transversal filter and the optimized receiver. The optimization involved in the third receiver is done for a number of different classes of varying degree of complexity in implementation. Finally, comparisons are made between the linear receiver types.

In the fourth chapter two nonlinear receivers are described and evaluated. These receivers are of interest because of their ease of implementation and good performance. The first receiver is due to Aein and Hancock (Ref. 2), the second is described for the first time in this paper. The performance of the nonlinear receivers is compared with that of various linear receivers. In many instances the second nonlinear receiver performs better than the difficult-to-implement optimized linear receiver.

The fifth chapter describes and evaluates the optimum receiver for the intersymbol interference in noise problem. This receiver computes the likelihood ratio for each received symbol and bases its decision on it. The optimum receiver is significant because of the absolute bound on performance and the insight it provides.

In the sixth chapter the conclusions of the paper are summarized

and topics for future study are suggested.

Contributions

This study emphasizes the importance of the power spectrum of the received symbol as opposed to the complex spectrum of the received symbol on the intersymbol interference problem. By working with power spectrum and limiting the amount of intersymbol interference to a reasonable amount, a common basis for the comparison of traditional and proposed receivers is found.

A new nonlinear receiver is suggested as a practical alternative to the complicated optimum linear receiver. This receiver is simple to implement and performs remarkably well.

The major contribution of this thesis, however, is the design and evaluation of the optimum (likelihood ratio) receiver. The optimum (likelihood ratio) receiver is important for two reasons. First, its performance provides a lower bound on the error probability for any other receiver and hence provides an absolute measure how a given receiver performs. Secondly, the basic form of the optimum (likelihood ratio) receiver shows the necessity of using information on both past and future symbols in making each decision. This provides a basis for future design of easily implemented, near optimum receivers.

A comparison of the optimum receiver with various linear and nonlinear receivers is made. This comparison provides a useful rule

of thumb for the system designer who wishes to trade off error performance, ease of implementation, and information rate.

CHAPTER II

INTERSYMBOL INTERFERENCE

The general problem of intersymbol interference in binary systems with noise is considered in this chapter. We first note several approaches to the intersymbol interference problem which are frequently used in practice. The important concepts of phase equalization and the dependence of receiver performance on power spectrum are introduced. A convenient characterization of the intersymbol interference problem and a measure of the degree of intersymbol interference are also given. Finally, a key assumption regarding the degree of intersymbol interference in practical systems is made and justified.

In this and subsequent chapters it will be helpful to distinguish between the terms "filter" and "receiver." By a filter, FL , we mean a linear, time invariant system which maps finite energy waveforms into finite energy waveforms, $FL: L^2 \rightarrow L^2$. The question of realizability of the filters described here will be ignored, since adequate approximations are usually possible. A receiver, $\mathscr{R}$, maps finite energy waveforms (the received signal) into binary decisions on symbol values $\mathscr{R}: L^2 \rightarrow \{\pm 1\}$. Although a receiver may have a linear filter within it, a receiver is inherently a nonlinear device.

2.1. Traditional Approaches

Most of the traditional approaches to the intersymbol interference

problem involve the use of a single linear filter followed by a sampler and threshold device as the receiver. This class of receivers will be referred to as the linear filter receiver class. The third chapter deals with this class in detail. Figure 2.1 shows a block diagram of a binary communication system in which the symbols $\pm q(t)$ are transmitted through a channel, $C(\omega)$, (meeting the assumptions of Section 1.2) and are received using a linear filter receiver.* It is easily shown that for the equiprobable binary simplex signals assumed here the best decision threshold is zero.

Spectrum Equalization

Spectrum equalization methods arose from applications where the reception was essentially noise-free; i.e., land-line teletype. Designers realized that variations in the amplitude and phase spectra led to distortion of the received symbol and, consequently, intersymbol interference. The obvious solution was to introduce filters, appropriately called equalizers, to flatten the amplitude spectrum and to linearize the phase spectrum. The design of such filters has been the subject of much study by circuit designers.

The basic objective of traditional spectrum equalization techniques has been to reduce the time duration of the received symbol, and hence, intersymbol interference. This simple notion can be put on a quantitative

---

*We represent time waveforms using small letters and represent their Fourier transforms by corresponding capital letters. For example, the Fourier transform of the symbol $q(t)$ is $Q(\omega)$.

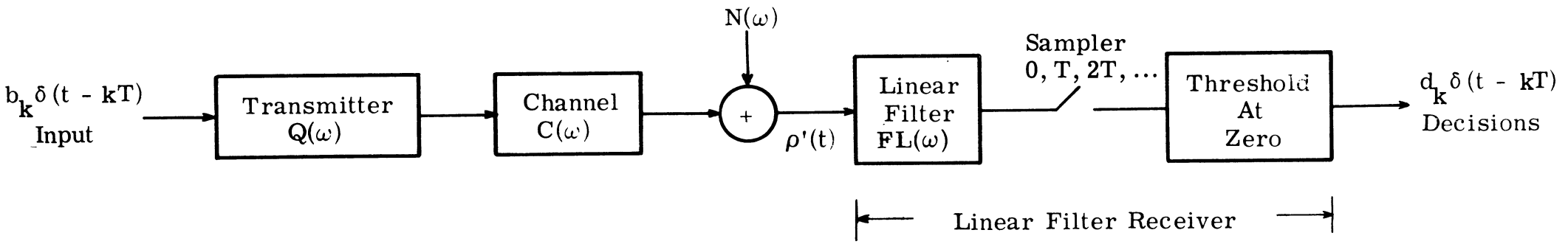

Fig. 2.1. Block diagram of channel and linear filter receiver

basis by considering the RMS time duration, τ_{RMS}, of the received symbol, $\rho'(t)$. The time center τ_c of $\rho'(t)$ is defined by

$$\tau_c \triangleq \frac{1}{E} \int_{-\infty}^{+\infty} t\,|\rho'(t)|^2\,dt \tag{2.1}$$

$$E \triangleq \int_{-\infty}^{+\infty} |\rho'(t)|^2\,dt \tag{2.2}$$

Then the RMS time duration of $\rho'(t)$, τ_{RMS} is defined as the deviation of $|\rho'(t)|^2$ about τ_c, normalized by E.

$$\tau_{RMS}^2 \triangleq \frac{1}{E} \int_{-\infty}^{+\infty} (t - \tau_c)^2\,|\rho'(t)|^2\,dt \tag{2.3}$$

Thus τ_{RMS} is a measure of how compact the energy of $\rho'(t)$ is in time. We will choose our time origin so that $\tau_c = 0$ in the following discussion.

A convenient equality derived from Fourier transform theory allows us to relate the RMS time duration of $\rho'(t)$ and its complex spectrum, $\rho'(\omega) = Q(\omega)C(\omega)$. Let $A(\omega)$ be the magnitude spectrum of $\rho'(\omega)$, and let $\psi(\omega)$ be the phase spectrum of $\rho'(\omega)$. Using Parseval's theorem, one may show that:

$$\frac{1}{E} \int_{-\infty}^{+\infty} t^2\,|\rho'(t)|^2\,dt = \frac{1}{2\pi E} \int_{-\infty}^{+\infty} \left(\frac{dA(\omega)}{d\omega}\right)^2 + A^2(\omega) \left(\frac{d\psi(\omega)}{d\omega}\right)^2 d\omega \tag{2.4}$$

where we have chosen the time origin so that $\tau_c = 0$, (Ref. 8, page 62).

We see that by reducing the magnitude of the derivative $\frac{dA(\omega)}{d\omega}$ or the derivative $\frac{d\psi(\omega)}{d\omega}$ the RMS time duration of $\rho'(t)$ is reduced. This, of course, is the purpose of the traditional spectrum equalizer.

Figure 2.2 shows a receiver using spectrum equalization. We will assume that intersymbol interference is completely eliminated at the output of the equalizer, $EF(\omega)$. Then the classical theory of signal detectability indicates the (matched filter) form of the optimum post-equalizer receiver. Let the spectrum of the equalizer output be $\rho''(\omega) = Q(\omega)C(\omega)EF(\omega)$, then the transfer function of the optimum post-equalizer receiver, $FL_{OPT}(\omega)$ is given by

$$FL_{OPT}(\omega) = \frac{[\rho''(\omega)]^*}{|N''(\omega)|^2} \tag{2.5}$$

where * indicates complex conjugate and $|N''(\omega)|^2$ is the power spectrum of the noise at the input to the post equalizer receiver (Ref. 9). Since the equalizer generally has a non-white spectrum $|N''(\omega)|^2$ will not usually be white.

Let us compute the overall transfer function $FL(\omega)$ of the linear filter portion of the receiver shown in Fig. 2.2. We have

$$\left(\rho''(\omega)\right)^* = [Q(\omega)C(\omega)EF(\omega)]^* \tag{2.6}$$

and

$$|N''(\omega)|^2 = |EF(\omega)|^2 \tag{2.7}$$

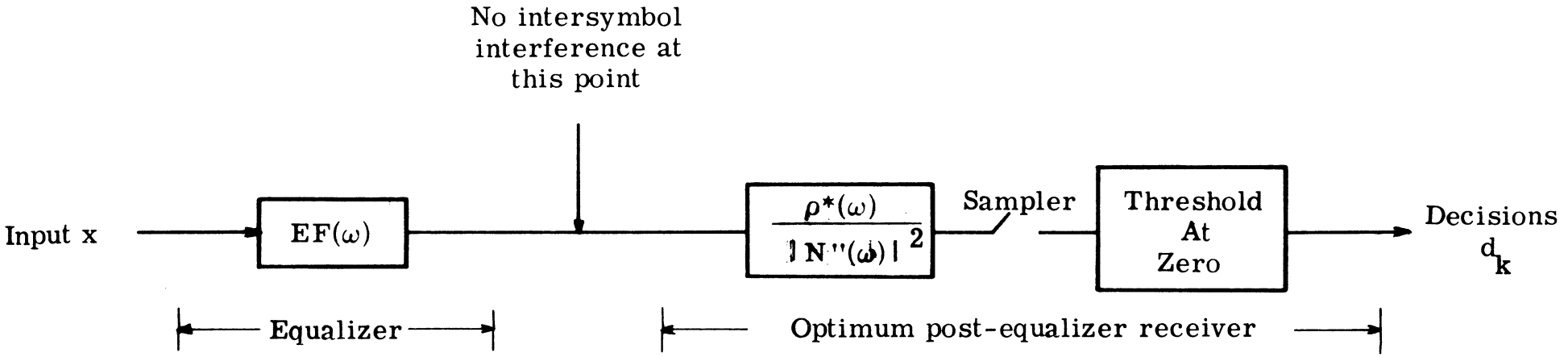

Fig. 2.2. A receiver using spectrum equalization

since the noise at the input to the equalizer is white. The overall transfer function $FL(\omega)$ is then

$$FL(\omega) = EF(\omega)Q^*(\omega)C^*(\omega)EF^*(\omega)/|EF(\omega)|^2 \qquad (2.8)$$

$$= Q^*(\omega)C^*(\omega) = \left[\rho'(\omega)\right]^* \qquad (2.9)$$

The above reduced transfer function $FL(\omega)$ is seen to be that of a filter matched directly to the output of the channel.

The result given by Equation 2.9 is very interesting. Even when the equalizing filter $EF(\omega)$ is completely successful in eliminating intersymbol interference and when the optimum post equalizer receiver is used, the optimum post equalizer filter $FL_{OPT}(\omega)$ contains a factor $1/|N''(\omega)|^2$ which cancels out the effect of the equalizer. The overall transfer function after this cancellation, given in Equation 2.9, is that of a filter matched to the channel output and does not contain any distinct equalization factor. Furthermore, the performance of the receiver given by Equation 2.9 is very poor.* Thus the spectrum equalization technique is not effective in reducing the effects of intersymbol interference in a communication system.

Transversal (Time) Equalization

Another approach to the intersymbol interference problem is to

---

*This is shown in Section 3.2

use a transversal filter receiver (Ref. 10). Such a receiver evolves from consideration of the system time response rather than its spectrum and has the advantage that intersymbol interference is completely eliminated. As with spectrum equalization techniques, noise performance is not taken into account in the design.

The basic notion of the transversal filter receiver is very simple. If receiver decisions are to be based on the filter output sampled every T seconds, then if the superimposed responses of consecutive symbols go through zero every T seconds, intersymbol interference is eliminated. Figure 2.3 depicts the response of a typical transversal filter to

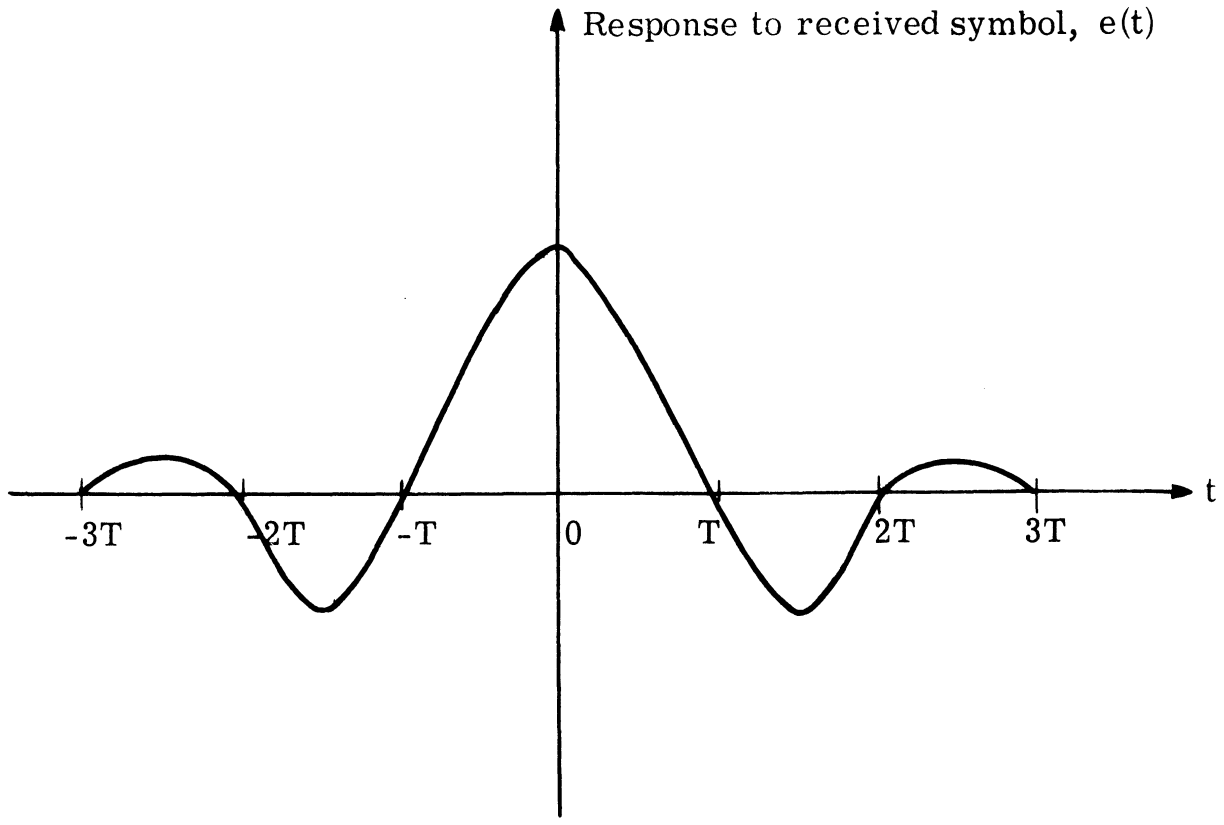

Fig. 2.3. Typical transversal filter response to a received symbol

a received symbol. Since the superposition of such waveforms shifted by multiples of T has a non-zero component from only one symbol every T seconds, intersymbol interference has been completely eliminated.

Transversal filter receivers are used because of their effectiveness in eliminating intersymbol interference and the ease with which they may be implemented using a tapped delay line. Figure 2.4 shows a simple seven-tap transversal filter receiver. The outputs of the delay

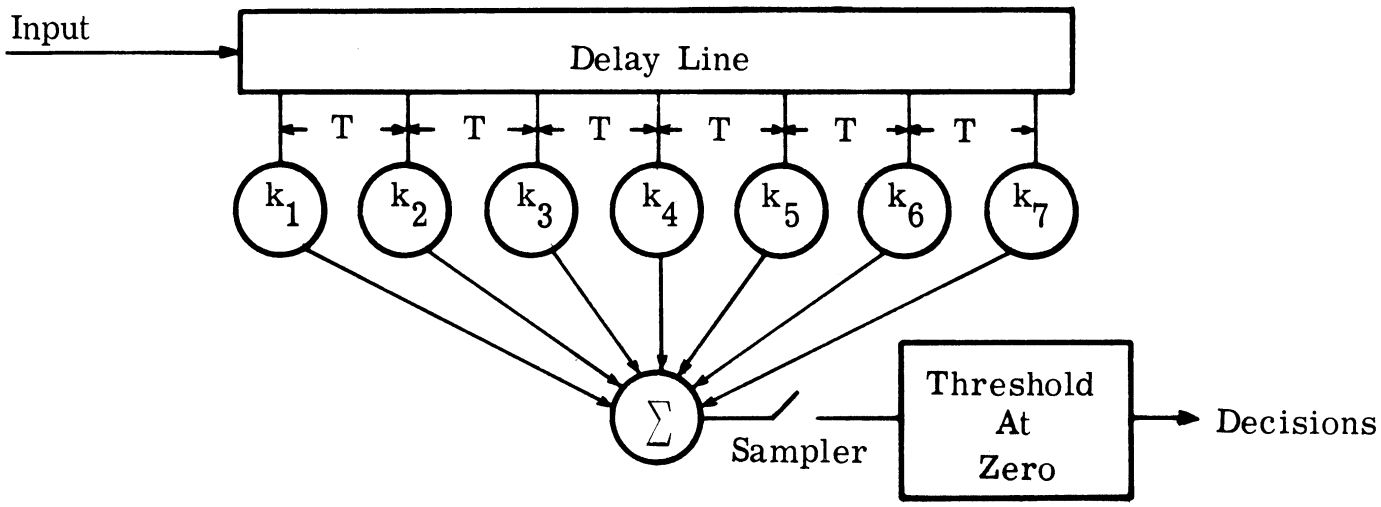

Fig. 2.4. Seven tap transversal filter receiver

line taps (spaced T seconds apart) are weighted with adjustable coefficients and then added. The tap coefficients may be set by cycling a noise-free received symbol through the delay line with T second delays and adjusting the coefficients to obtain zero output at all but one delay. Considerable study has been done to achieve "automatic equalization" by

having the receiver continuously adjust the tap coefficients to compensate for slow channel variations (Ref.10).

Since the transversal filter receiver completely eliminates intersymbol interference, it is the optimum receiver in the absence of noise. One might be optimistic and hope that good intersymbol interference performance and good noise performance go hand-in-hand. Unfortunately, this is not the case and one must trade noise performance and intersymbol interference performance against each other in order to obtain the best overall system error performance. The following brief discussion illustrates the necessity of compromise.

Consider the system shown in Fig. 2.1. If no intersymbol interference is present, classical signal detection theory indicates the use of a matched filter receiver, that is,

$$FL_{MF}(\omega) = \left[Q(\omega)C(\omega)\right]^* \tag{2.10}$$

For a transversal filter receiver with a filter symbol response e(t) having the required zeros at all but one multiple of T seconds, we must have:

$$E(\omega) = Q(\omega)C(\omega)FL_{TF}(\omega) \tag{2.11}$$

Thus the transfer function of the transversal filter, which is optimum in the absence of noise, is given by

$$FL_{TF}(\omega) = \frac{E(\omega)}{Q(\omega)C(\omega)} \tag{2.12}$$

Comparing Equations 2.10 and 2.12 shows that the matched filter and the transversal filter are equal only if

$$E(\omega) = |Q(\omega)C(\omega)|^2 \qquad (2.13)$$

which implies that e(t) is the autocorrelation of the channel symbol response. This is an unlikely occurrence in realistic channels and, in general, $FL_{MF}(\omega)$ and $FL_{TF}(\omega)$ are different. Thus the optimum no-intersymbol interference receiver derived from detection theory and the optimum no-noise receiver derived above are different and a compromise between the approaches is needed.

Transmission of Special Signals

The above discussion suggests an effective but impractical method of handling the problem of intersymbol interference in noise. Suppose that the transmitted symbol, q(t), is carefully constructed so that

$$|Q(\omega)|^2 = \frac{E(\omega)}{|C(\omega)|^2} \qquad (2.14)$$

where e(t) has the desired zeros at all but one multiple of T seconds. Then Equation 2.13 is satisfied and the optimum interference-free receiver $FL_{MF}(\omega)$ and the optimum noise-free receiver $FL_{TF}(\omega)$ are identical. Hence, we have achieved both optimum noise performance and optimum intersymbol interference performance.

Although appealing from a receiver design point of view, the above approach does not meet the specified assumptions given earlier. Contrary to our assumptions, this approach requires that the transmitter know the channel power spectrum and also that the transmitter be unrestricted in terms of peak power capability. These drawbacks eliminate this system from further consideration here.

Transmission at Slower Rate

Perhaps the simplest method of coping with intersymbol interference is to increase the symbol duration T to the point where the interference becomes tolerable in some sense. Although this is a simple and common method of avoiding the problem, it forces the system designer to accept a loss in rate without indicating the trade-off in error performance. Another disadvantage to this approach is that longer symbol durations may be contrary to other aspects of system design. For example, to reduce the effects of sudden channel fades it may be desirable to send one symbol in several short pieces separated in time (time diversity). The use of long transmitted symbols would impose a severe limitation on such a time-diversity system.

A major result of this study is that intersymbol interference is essentially due to a bandwidth limitation on the received power spectrum and that the transmission rate should be chosen in the light of this bandwidth limitation. We will provide analysis, however, which indicates the initial trade off between transmission rate, intersymbol interference

and system error performance.

2.2. Characterization of the Problem

In this section we describe measures of the severity of a given intersymbol interference problem. We will show that the amount of intersymbol interference is directly related to the power spectrum of the received symbol, and hence, can be viewed in terms of a bandwidth limitation. We also define an integer **M**, known as the degree of intersymbol interference, to indicate the amount of overlap of the received symbols.

Phase Equalization

An important problem for the system designer is to determine the actual extent of intersymbol interference in a given practical situation. One approach to this problem is simply to measure the duration of the received symbol -- the longer the duration of the symbol the more severe the intersymbol interference problem would be expected to be. As we will soon see, this approach can be very misleading for a practical channel because it usually indicates more severe intersymbol interference than is actually present.

To provide a consistent measure of the extent of intersymbol interference in a given situation, we consider the equalization of the phase spectrum of the received symbol. Let $\rho'(\omega)$ be the complex spectrum of the received symbol. Then the phase-equalizing filter $\mathrm{PEF}(\omega)$ is defined by:

$$\rho'(\omega)\,\mathbf{PEF}(\omega) = |\rho'(\omega)| = \rho(\omega) \qquad (2.15)$$

That is, the spectrum $\rho(\omega)$ of the output $\rho(t)$ of the phase-equalizing filter is equal to the magnitude spectrum $|\rho'(\omega)|$ of the input $\rho'(t)$ to the filter. Since $|\rho'(\omega)|$ is always positive and real, the phase spectrum of $\rho(\omega)$ has a constant value of zero and thus the term phase equalization is appropriate.

Consider the two systems shown in Fig. 2.5. The phase-equalizing filter $\mathbf{PEF}(\omega)$ in system No. 2 equalizes the phase spectrum of the received symbol, and hence, system No. 2 is called the phase-equalized system. Because the phase-equalizing filter has a white magnitude spectrum, the noise at the receiver input to system No. 2 has exactly the same statistics as that of system No. 1. On the other

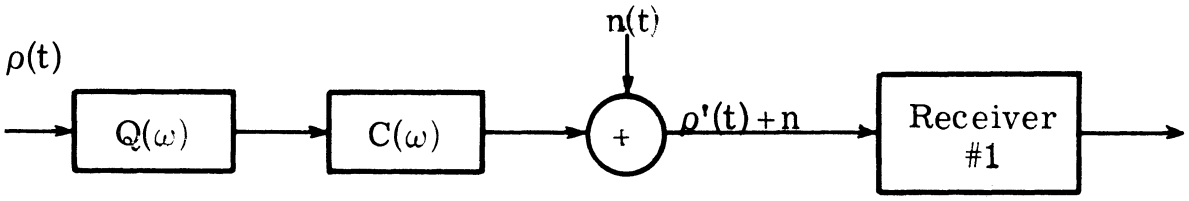

System #1 (Unequalized)

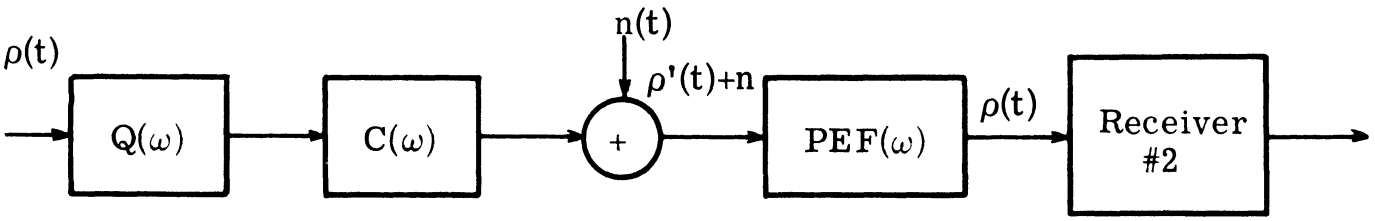

System #2 (Phase equalized)

Fig. 2.5. Unequalized and phase-equalized systems

hand, since the spectrum $\rho(\omega)$ of the output of the phase-equalizing filter has a constant phase, $d\psi(\omega)/d\omega$ is zero and, from Equation 2.4, the RMS time duration of $\rho(t)$ is less than or equal to that of $\rho(t)$. Thus by using phase equalization we can reduce the RMS time duration of the received symbol without changing the noise problem. This is in contrast with the general spectrum equalization technique described earlier, in which the noise power spectrum is changed as the RMS time duration is reduced.

Figure 2.6 depicts the response of the Mimi channel to a 40 ms rectangular symbol with and without phase equalization. Analysis of the unequalized received symbol indicates the symbol has 90% of its energy within 165 ms and that there will be components of at least four symbols in each 40 ms time interval. The phase-equalized symbol has 90% of its energy within 50 ms indicating much less intersymbol interference than one would expect from inspection of the unequalized received symbol. By phase equalization the RMS time duration of the received symbol is reduced from 48 ms to 26 ms.

The relationship between the unequalized received symbol $\rho'(t)$ and the phase-equalized symbol ρ is interesting in that it relates the amount of intersymbol interference after phase equalization to power spectrum. Since the magnitude spectrum of $PEF(\omega)$ is white, the power spectrum of $\rho'(t)$, $|\rho'(\omega)|^2$ is identical to that of $\rho(t)$, $|\rho(\omega)|^2$.

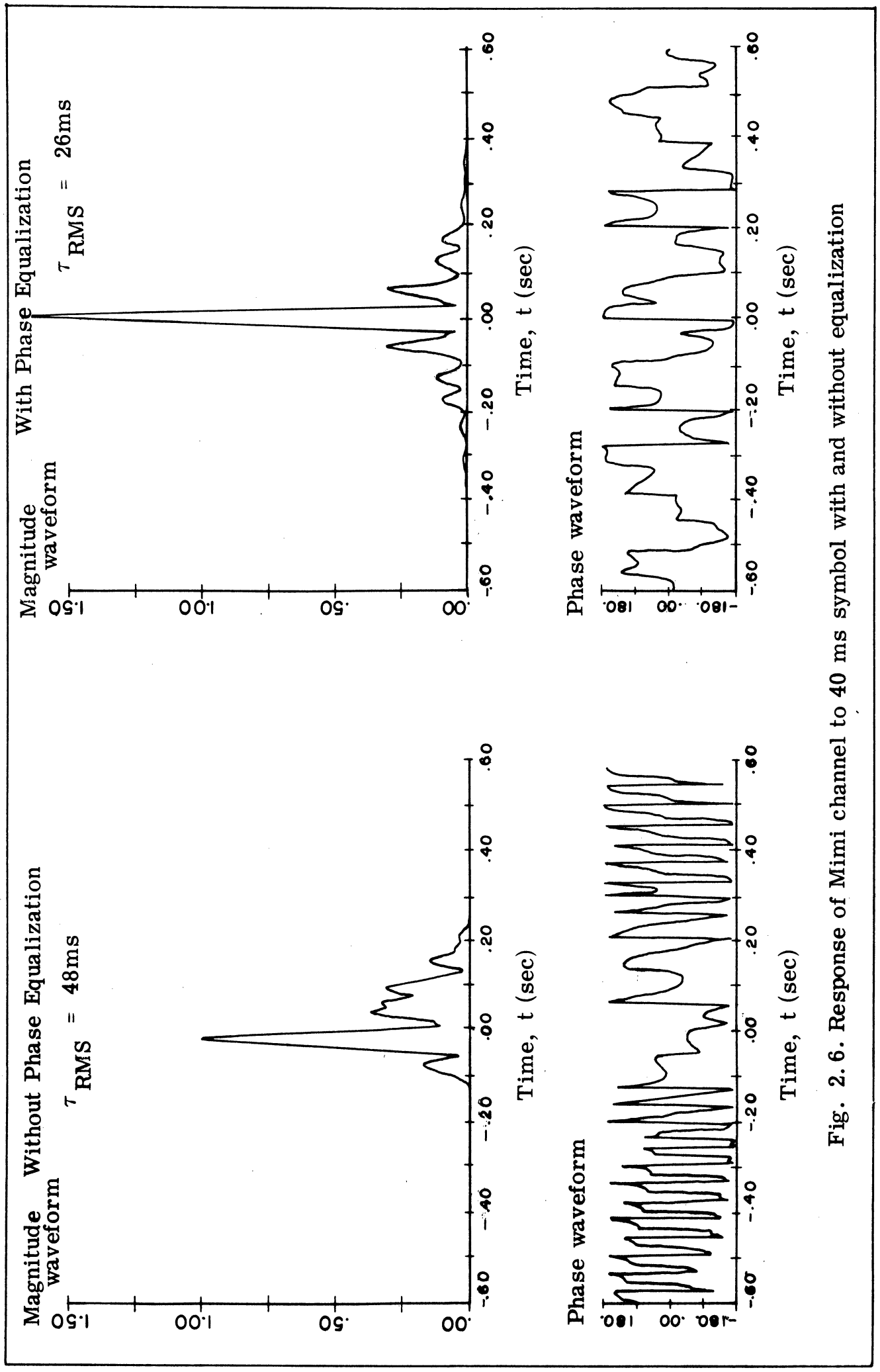

Fig. 2.6. Response of Mimi channel to 40 ms symbol with and without equalization

From Equation 2.4 we see that any waveform for which $d\psi / d\omega$ is zero will have the smallest possible RMS time duration of all waveforms having the same magnitude spectrum, or equivalently, the same power spectrum. Since $d\psi(\omega) / d\omega$ is zero for a phase-equalized waveform, we conclude that among all waveforms having the same power spectrum, the phase-equalized waveform has the smallest possible RMS time duration.

From the power spectrum $|\rho'(\omega)|^2$ of the received symbol $\rho'(t)$, the waveform of the corresponding phase-equalized symbol $\rho(t)$ can be found

$$\rho(t) = F^{-1}\left[\sqrt{|\rho'(\omega)|^2}\right] \qquad (2.16)$$

where $F^{-1}[Z(\omega)]$ is the inverse Fourier transform of $Z(\omega)$. Since $|\rho'(\omega)|^2$ is a power spectrum, $\sqrt{|\rho'(\omega)|^2}$ is positive and real. The inverse transform of a positive and real spectrum is conjugate symmetric in time.

By relating intersymbol interference to the power spectrum of the received symbol, considerable insight is gained. For example, consider the phase-equalized magnitude response and power spectrum of a 40 ms rectangular symbol passed through the Mimi channel shown in Fig. 2.7. Figure 2.7 also shows these functions for a flat bandpass channel having the same nominal bandwidth. Because of the notches and irregularities in the Mimi channel power spectrum, one would

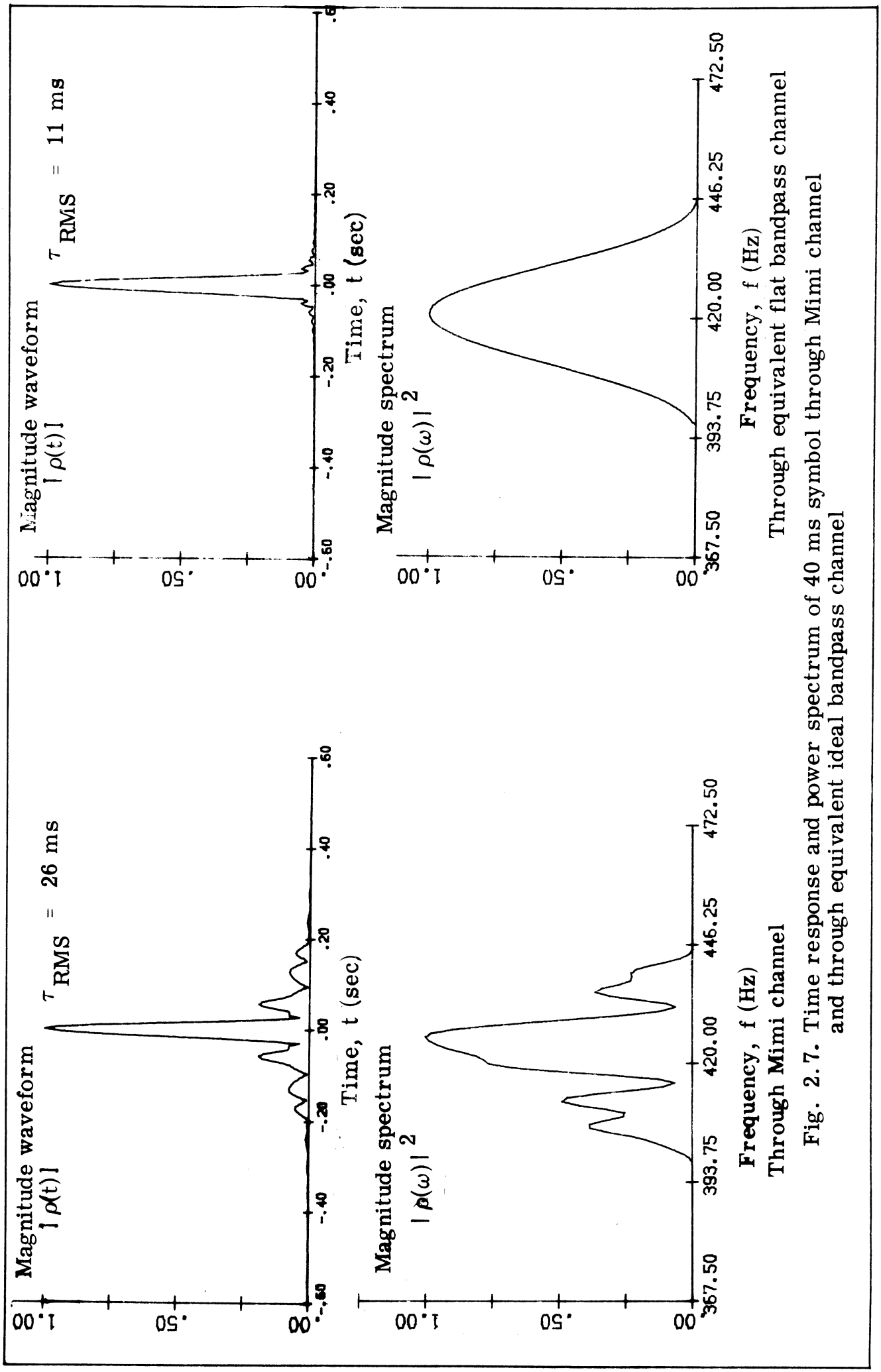

Fig. 2.7. Time response and power spectrum of 40 ms symbol through Mimi channel and through equivalent ideal bandpass channel

expect to achieve different system performance through the two channels. An intuitive way of expressing this is to say that the bandwidth of the Mimi channel is reduced by the notches and irregularities in its power spectrum. Because these same notches and irregularities in the channel power spectrum produce intersymbol interference, we are led to the intuitive, but productive conclusion that intersymbol interference (after phase equalization) is caused by signalling too fast for the bandwidth of the channel.

Before proceeding further, it is important to point out that it is seldom necessary to use a separate phase-equalizing filter $PEF(\omega)$ in a receiver. As will be seen later, most receivers perform a cross correlation of the reception with the noise-free received symbol $\rho'(t)$. Since the noise-free output of such a correlation process is the auto-correlation function of the received symbol, the output waveform of the correlator is the same whether or not phase equalization is used. Thus in many instances it is not necessary to realize a separate phase-equalizing filter.

In subsequent discussions we will assume that the received symbol is phase-equalized. This means that the received symbol ρ will have the minimum RMS time duration of all waveforms having the same power spectrum and that it will be conjugate symmetric in time.

Degree of Intersymbol Interference

In order to work with the intersymbol interference problem

conveniently, it is helpful to limit the amount of intersymbol interference due to a single received symbol. This may be accomplished by defining an integer M, known as the degree of intersymbol interference, as the smallest integer multiple of T completely contained in the "duration" of the phase-equalized received symbol. For example, if the phase-equalized received symbol duration is less than $3T$ but greater than $2T$, the degree of intersymbol interference is two, $M=2$. The $M=0$ case corresponds to no intersymbol interference.

Practically speaking, it is unlikely that a received symbol will have a finite time duration due to the bandlimited nature of the channels considered here. Because of this it is necessary to use some reasonable measure of symbol duration. Since signal energy plays such an important role in classical detection theory, a reasonable criterion is that some specified percentage of the energy, η, be within the received symbol duration. The effect of the energy outside of the symbol duration under this criterion depends on the particular power spectrum and receiver under consideration. At present, a requirement that 90% of the symbol energy be contained in the symbol duration, $\eta = 90\%$, is believed to be adequate.

2.3. The M = 1 Assumption

The remainder of this paper is concerned with intersymbol interference problems in which the degree of intersymbol interference is one ($M=1$). That is, the duration of the phase-equalized received symbol

is less than $2T$. This is a major assumption; however, it can be considered equivalent to a restriction to moderate signalling rates through the channel. The relation between the $M = 1$ assumption and signalling rate is discussed below.

Suppose that we are to use binary simplex signalling to communicate through a given channel, such as the Mimi channel. At the outset, both the transmitted symbol duration, T, and the waveform of the transmitted signal, $q(t)$, are free variables. Of course, restrictions such as bandwidth and peak power limitations impose constraints on these variables. It is important to note, however, that the symbol duration, T, and the bandwidth of $q(t)$ can be adjusted practically independently of one another. For example, by using a block-coded binary signal one can obtain a wide bandwidth signal having a long-time duration (Ref. 11).

From the earlier discussion on phase equalization we know that the time duration of the received symbol, and consequently intersymbol interference, is reduced if the power spectrum of the received symbol is nearly white. Furthermore, from Equation 2.16, we see that the duration of the phase-equalized symbol is reduced as the width of the power spectrum is increased. Thus the ideal power spectrum of the received symbol is wide band and white, independent of the duration of the transmitted symbol. Since the channel spectrum is unknown to the transmitter, the best transmitted signal also has a wide band and white power spectrum, again independent of its duration T. This is a well-known result.

Let us temporarily neglect the constraints on the possible transmitted waveforms in order to examine the effect of the channel alone on the intersymbol interference problem. Suppose that we use an impulse function as the transmitted signal and that the transmitted signal duration (in this case the time between impulses) is T. Then the transmitted power spectrum is white and the power spectrum of the received symbol is simply the channel power spectrum. The phase-equalized channel impulse response is then the waveform of the phase-equalized received symbol, using the widest possible transmitted waveform. Figure 2.8 depicts the phase-equalized impulse response for the Mimi channel.

Given the phase-equalized impulse response for a channel and an energy criterion, η, on the phase-equalized received symbol duration (i.e., 90% of the total energy is within the symbol duration), we can determine the "duration" of the received symbol. Figure 2.9 shows the duration of the phase-equalized impulse response for the Mimi channel as a function of the percentage of energy in the response duration. From the assumed duration of the received symbol found above, we can find the shortest transmitted signal duration for which the $M = 1$ assumption is valid.

For example, consider the Mimi channel with a duration criterion based on 90% of the total energy being within the phase-equalized received symbol duration. From Fig. 2.9 we see that the symbol duration is

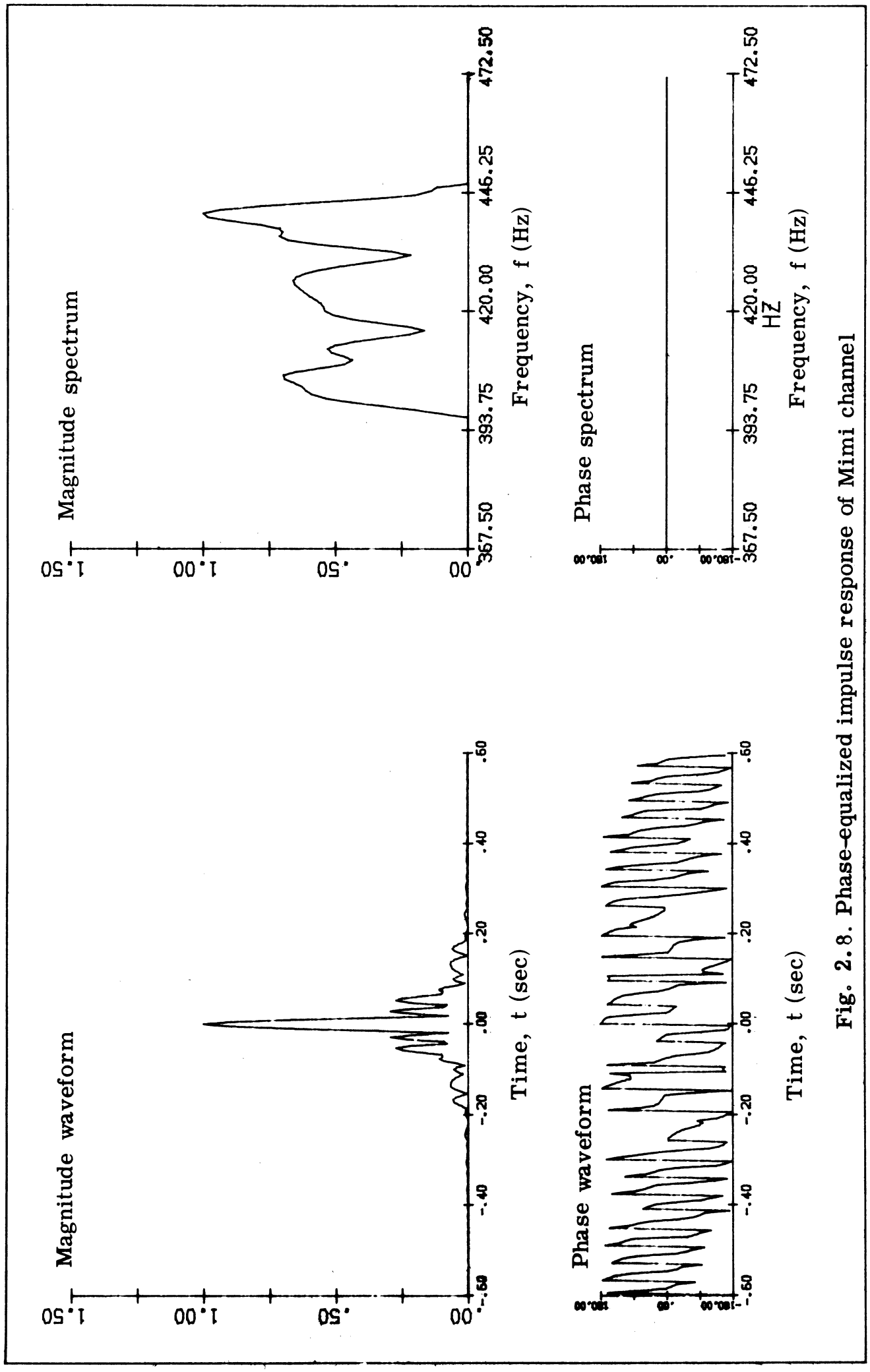

Fig. 2.8. Phase-equalized impulse response of Mimi channel

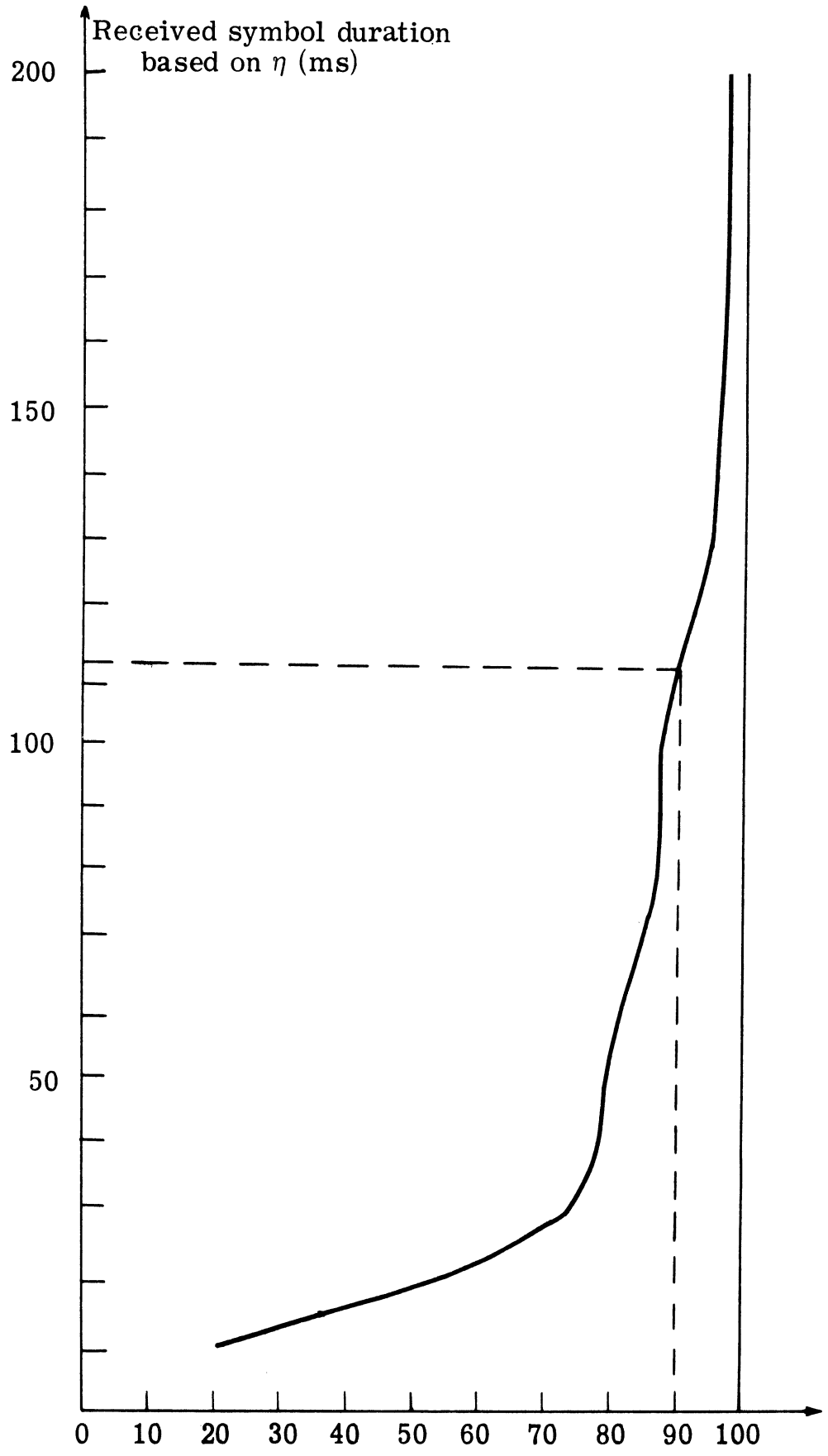

Fig. 2.9. Received symbol duration based on η as a function of η for the Mimi channel

approximately 112 ms, and hence, under this criterion the $M = 1$ assumption is valid, for $T > 56$ ms. The bandwidth of the channel power spectrum for the Mimi channel is less than 50 Hz, as can be seen from Fig. 1.3. If this bandwidth were that of a flat bandpass channel, a reasonable signalling rate would be 25 symbols per second, which requires a 40 ms symbol. Thus we see that for this particular example, the $M = 1$ restriction is equivalent to requiring that the signalling rate be slightly slower than for a flat bandpass channel. Because of the severe notches in the actual channel power spectrum, one would not expect to signal at the ideal channel rate.

The foregoing discussion was based on the use of ideal transmitted signals which cannot be used in practice. To go from this idealization to a practical peak power limited signal set is the relatively well studied problem of generating wide band, flat power spectrum signals having good peak-to-average power ratios (Ref. 11). Pseudo-random sequences are one convenient and common solution. Although we do not consider this problem in this thesis, we offer as a simple example, the three-digit, 60 ms "perfect word" symbol shown with its spectrum in Fig. 2.10. The phase-equalized received symbol (after the channel of Fig. 1.2) is shown in Fig. 2.11. Signalling with this particular symbol corresponds to $M = 1$ with more than 94% of the energy within the symbol duration.

In summary, limiting the intersymbol interference due to adjacent

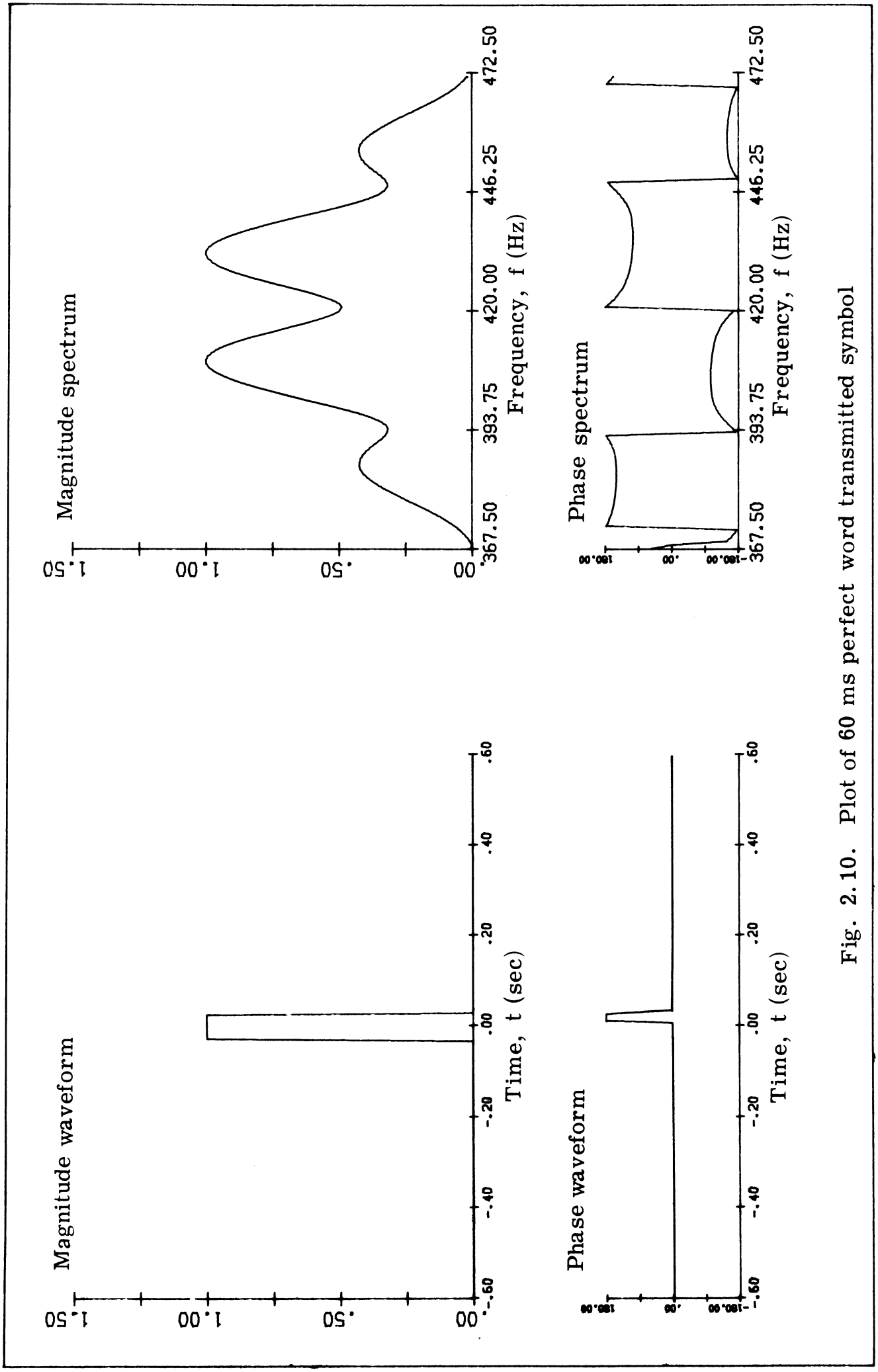

Fig. 2.10. Plot of 60 ms perfect word transmitted symbol

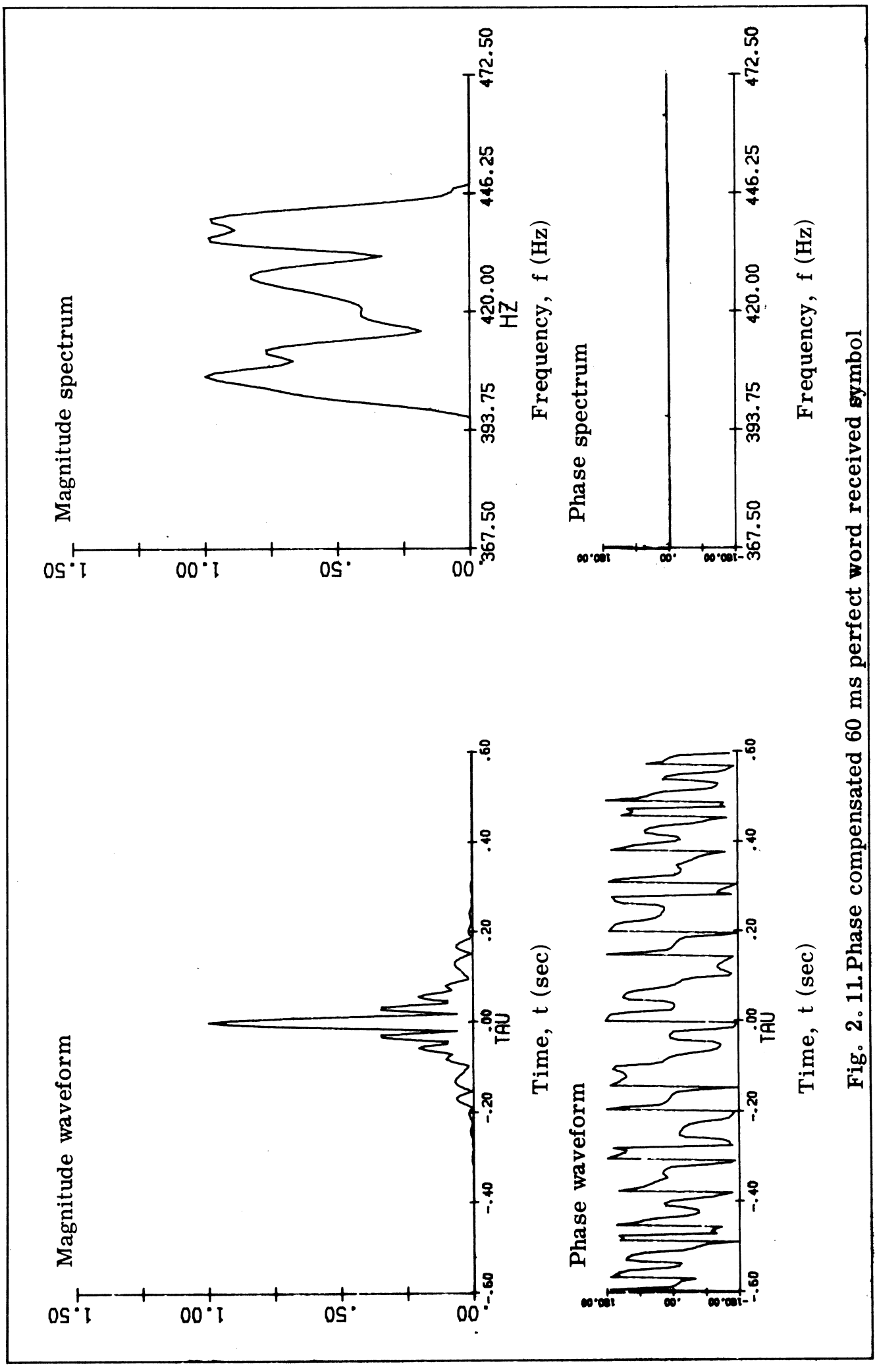

Fig. 2.11. Phase compensated 60 ms perfect word received symbol

symbols ($M = 1$) is equivalent to a restriction on the signalling rate. The phase-equalized channel impulse response and the "enclosed energy" criterion η, for the duration of the response provide the information required to calculate an upper bound on the signalling rate for which the $M = 1$ assumption is valid. We have seen that for the Mimi channel of Fig. 1.2 and an "enclosed energy" criterion of $\eta = 90\%$, the resulting upper bound on signalling rate is very close to the rate for a flat band-pass channel. Furthermore, the $M = 1$ restriction may be maintained using peak power limited signals with a relatively minor decrease in rate.

CHAPTER III

LINEAR FILTER RECEIVERS

A linear filter receiver or correlation receiver is a receiver in which decisions are made on the basis of the sampled output L_k of a linear, time invariant filter. If $L_k \geq 0$ the receiver makes a $d_k = +1$ decision indicating the value of the k^{th} symbol, b_k, was $+1$, if $L_k < 0$ a $d_k = -1$ decision is made.* Figure 3.1 depicts the general linear filter receiver.

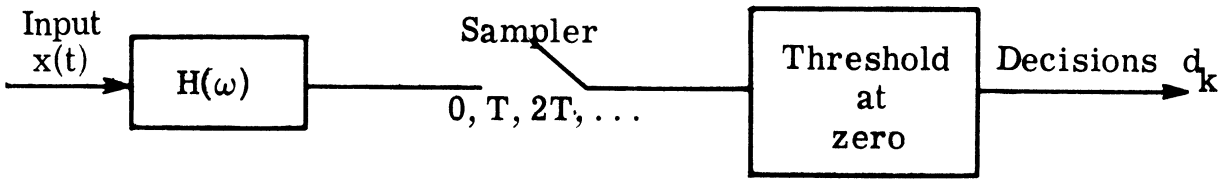

Fig. 3.1. General linear filter receiver

Linear filter receivers have been studied comparatively intensively in the literature (Refs. 2, 3, 4). The purpose of this chapter is to review these earlier efforts in a common frame of reference. We first consider the general operation of linear filter receivers and their

*This is simply a sign convention.

performance. Special forms of linear filter receivers, such as the transversal filter receiver are considered under the assumption of a phase-equalized, unit degree of intersymbol interference (M = 1) symbol. Finally, we consider the optimization linear filter receiver for various optimization constraints.

3.1. General Discussion

In this section we consider the operation, error performance and canonical form for the class of linear filter receivers. Although we will quickly return to our assumption of a unit degree of intersymbol interference, the material presented in this section is for the general problem.

Operation of the Receiver

Let $\rho(t)$ be the waveform of a single, noise-free received symbol due to the transmission of a symbol of value $+1$ at time $t = 0$. Let $b_0 \cdots b_m$, $b_i = \pm 1$ be the transmitted symbol values in a finite duration transmission. Then the actual reception, $x(t)$ is given by

$$x(t) = \sum_{0}^{m} b_i \rho(t - iT) + n(t) \qquad (3.1)$$

where $n(t)$ is white Gaussian noise of noise power density N_o watts/Hz.

Let $h(t)$ be the impulse response of the time invariant linear filter $H(\omega)$ which represents the linear filter portion of the receiver shown in Fig. 3.1. We will not require that $h(t)$ be physically realizable since an approximate realization of $H(\omega)$ can be generally obtained.

Then the response of the filter to the reception $x(t)$ at time kT, L_k, is given by

$$L_k = \int_{-\infty}^{+\infty} x(t)\, h(kT - t)\, dt \tag{3.2}$$

Define

$$\overset{\sim k}{h}(t) = h(kT - t) \tag{3.3}$$

then

$$L_k = \int_{-\infty}^{+\infty} x(t)\, \overset{\sim k}{h}(t)\, dt \tag{3.4}$$

If $x(t)$ and $h(t)$ are of finite energy (a realistic assumption), then $x(t)$ and $\overset{\sim k}{h}(t)$ are vectors in the Hilbert space L^2 which is referred to as signal space. In signal space Equation 3.4 defines the dot (or inner) product of $x(t)$ and $\overset{\sim k}{h}(t)$. Suppressing the time variables t, T we can write Equation 3.4 as

$$L_k = x \cdot \overset{\sim k}{h} \tag{3.5}$$

Equation 3.5 gives the geometrical interpretation that the correlator output at time kT is proportional to the projection of the received waveform vector x onto $\overset{\sim k}{h}$. This geometrical idea provides a simple visualization of the operation of a linear filter receiver. Since the receiver makes a $d_k = +1$ decision if $L_k \geq 0$ and a $d_k = -1$ decision if

$L_k < 0$, the hyperplane D_k through the origin defined by

$$x \cdot \overset{\sim k}{h} = 0 \tag{3.6}$$

partitions the signal space into two half spaces. If the reception x lies in the upper half space ($x \cdot \overset{\sim k}{h} \geq 0$) a $d_k = +1$ decision is made, if x lies in the lower half space ($x \cdot \overset{\sim k}{h} < 0$) a $d_k = -1$ decision is made. Figure 3.2 depicts a possible visualization of this operation. Subsequent decisions, $d_{k+1} \cdots$, are obtained by comparing x with the corresponding hyperplane $D_{k+1} \cdots$, etc.

Performance of the Linear Filter Receiver

The probability of error on the k^{th} symbol is the probability that L_k will be negative (and the resulting decision, $d_k = -1$) when, in fact, the transmitted symbol was positive, $b_k = +1$.* Let B_k be the set of all possible m dimensional vectors $b_0 b_1 \cdots b_i \cdots b_m$, $i \neq k$ where $b_i = \pm 1$. Then we can define

$$P_e(k) = P[L_k < 0 \mid b_k = +1] \tag{3.7}$$

$$= \frac{1}{2^m} \sum_{B_k} P[L_k < 0 \mid b_0 \cdots b_m, b_k = +1] \tag{3.8}$$

---

*Because of the symmetry of the problem, the probability that L_k is positive when $b_k = -1$ also equals the probability of error.

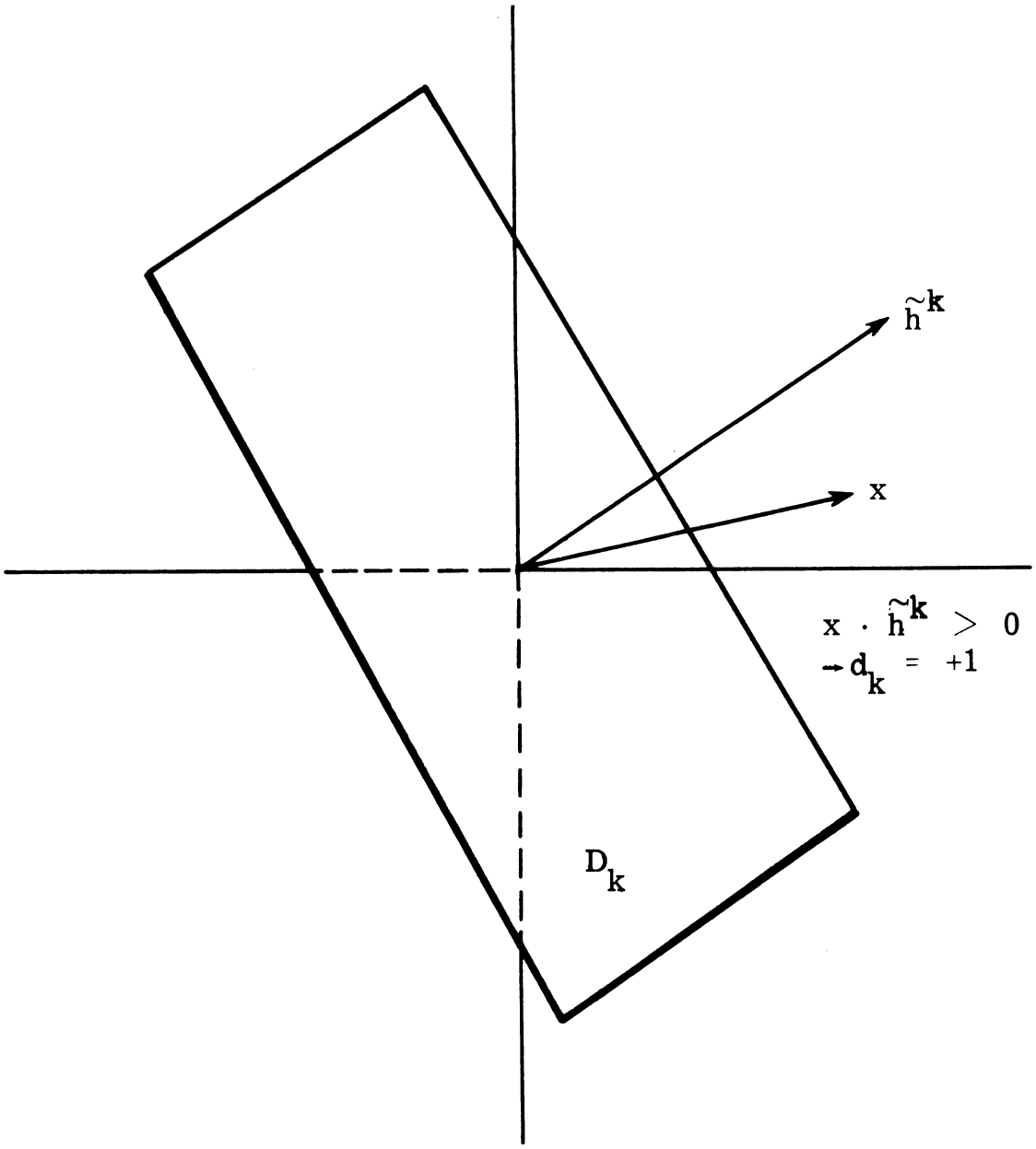

Fig. 3. 2. Decision plane of a linear filter receiver

since the symbol values, b_i , $i \neq k$ are assumed equiprobable. The probabilities $P[\, L_k < 0 \mid b_0 \ldots b_m, b_k = +1]$ are easily computed as we see below.

Suppose that the transmitted symbol values are $b_0 \ldots b_m$ where $b_k = +1$. Because the input noise is Gaussian, the sampled filter output L_k is a random variable having a Gaussian density function. Its mean is given by

$$E[\, L_k \mid b_0 \ldots b_m, b_k = +1] = E\left[(\rho^k + \sum_{i \neq k} b_i \rho^i + n) \cdot \tilde{h}^k \right] \tag{3.9}$$

where ρ^i denotes the L^2 waveform, $\rho(t - iT)$. Because the noise has a zero mean, we have

$$E[\, L_k \mid b_0 \ldots b_m, b_k = +1] = \tilde{h}^k \cdot \rho^k + \sum_{i \neq k} b_i \rho^i \cdot \tilde{h}^k \tag{3.10}$$

The variance of L_k is given by

$$\mathrm{Var}[\, L_k \mid b_0 \ldots b_m, b_k = +1] = N_0 \mid \tilde{h}^k \mid^2 / 2 \tag{3.11}$$

where N_0 is the one-sided noise power density of the white input noise. Let $\phi(u)$ be the zero mean, unit variance Gaussian density function, then

$$P[\, L_k < 0 \mid b_0 \cdots b_m, b_k = +1] = \int_{-\infty}^{0} \phi\left[\frac{u - \left(\overset{\sim k}{h} \cdot \rho^k + \sum_{i \neq k} b_i \rho^i \circ \overset{\sim k}{h} \right)}{\left(\sqrt{N_0 \left| \overset{\sim k}{h} \right|^2 / 2} \right)} \right] du \tag{3.12}$$

$$= \Phi\left[- \frac{\overset{\sim k}{h} \cdot \rho^k + \sum_{i \neq k} b_i \rho^i \cdot \overset{\sim k}{h}}{\left(\sqrt{N_0 \left| \overset{\sim k}{h} \right|^2 / 2} \right)} \right] \tag{3.13}$$

where $\Phi(u)$ is the cumulative distribution function of $\phi(u)$. Substituting Equation 3.13 into Equation 3.8, we obtain

$$P_e(k) = \frac{1}{2^m} \sum_{B_k} \Phi\left[- \frac{\overset{\sim k}{h} \circ \rho^k + \sum_{i \neq k} b_i \rho^i \cdot \overset{\sim k}{h}}{\left(\sqrt{N_0 \left| \overset{\sim k}{h} \right|^2 / 2} \right)} \right] \tag{3.14}$$

The above equation gives the probability of error for the k^{th} decision as a function of the received symbol ρ, the filter impulse response, h, and the noise power density, N_0.

In general, $P_e(k)$ will depend on where the k^{th} symbol is located

in the transmission. Since we are considering communications systems, it is reasonable to assume that the transmission consists of a very large number of consecutive symbols; i.e., $m \cong 10^3$. Under this assumption the effect of the beginning and end of the transmission on the system error probability (the average of $P_e(k)$ over k) is negligible. Hence, we will consider the k^{th} symbol to be located in the center of a very long sequence of transmitted symbols and that Equation 3.14 therefore gives the system probability of error P_e.

Canonical Form of Linear Filter Receivers

The foregoing discussion is sufficient to develop a canonical model of all linear filter receivers. This canonical model illustrates the effect of the filter impulse response h and suggests a convenient implementation for linear filter receivers.

Let $\tilde{h}^k$ be composed of two orthogonal components $\tilde{h}^k_1$ and $\tilde{h}^k_2$ where $\tilde{h}^k_1$ is in the $m+1$ dimensional subspace H_1 spanned by the time-shifted received symbols $\rho^i = \rho(t - iT)$, $i = 0 \ldots m$, and where $\tilde{h}^k_2$ is in the orthogonal complement, H_2, of the ρ^i. That is

$$\rho^i \cdot \tilde{h}^k_2 = 0 \qquad (i = 0 \ldots m) \tag{3.15}$$

if and only if $\tilde{h}^k_2 \in H_2$. The correlator output L_k is then given by

$$L_k = x \cdot (\tilde{h}^k_1 + \tilde{h}^k_2) \tag{3.16}$$

$$= \sum_{i=0}^{m} b_i \rho^i \cdot \tilde{h}^k_1 + n \cdot \tilde{h}^k_1 + n \cdot \tilde{h}^k_2 \tag{3.17}$$

The third term $n \cdot \tilde{h}^k_2$ is a zero mean Gaussian random variable with variance $N_0 \left|\tilde{h}^k_2\right|^2 / 2$.

We note that any vector $\tilde{h}^k_1$ in H_1 can be presented as

$$\tilde{h}^k_1 = \sum_{i=0}^{m} C_i \rho^i \tag{3.18}$$

since by definition, $\tilde{h}^k_1$ belongs to the subspace spanned by the ρ^i.

Consider the system shown in Fig. 3.3 in which a filter matched to ρ, $\rho^*(\omega)$ is followed by a tapped delay line. The output of the j^{th} delay line tap (which corresponds to a delay of jT seconds) is weighted by C_{m-j} and the weighted outputs are summed in the first adder. The output of the first adder, plus a zero mean Gaussian noise waveform $n'(t)$ having noise power $N_0 \left|\tilde{h}^k_2\right|^2 / 2$ is sampled at time kT to give L_k which is compared to a threshold in the usual manner. The noise n' is included in the system shown in order to simulate receivers in which $\left|\tilde{h}^k_2\right|$ is non-zero as we shall soon see.

The impulse response, h, of the matched filter-delay line-first adder section of the receiver is given by

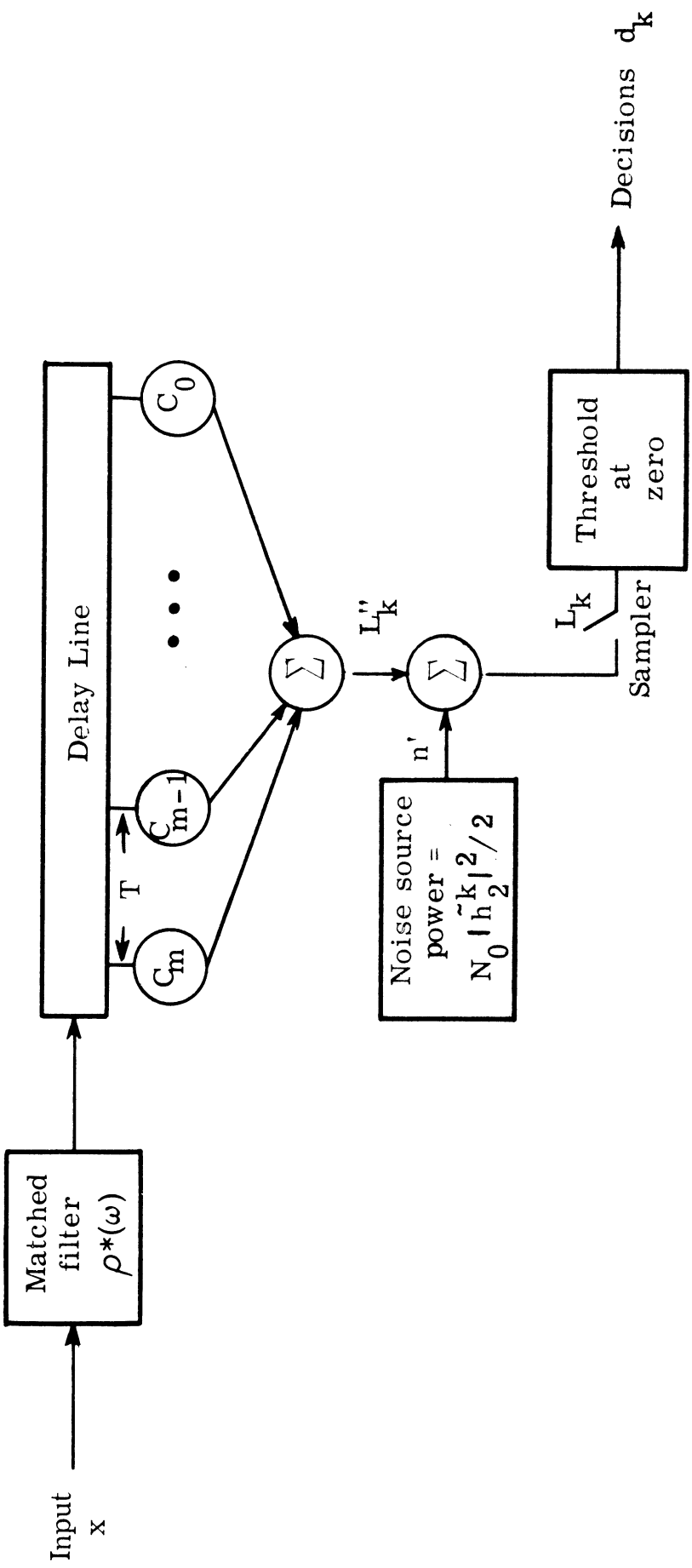

Fig. 3.3. Canonical linear filter receiver

$$h = \sum_{j=0}^{m} C_{m-j}\, \rho(-t + jT) \tag{3.19}$$

$$= \sum C_{m-j}\, \tilde{\rho}^{\,j} \tag{3.20}$$

where $\tilde{\rho}^{\,j} = \rho(jT - t)$.

Then the output L_k'' of this section of time kT due to the reception x is

$$L_k'' = \int x(t)\, h(kT - t)\, dt \tag{3.21}$$

$$= \int x(t) \sum_{j=0}^{m} C_{m-j}\, \rho(t - (k-j)\,T)\, dt \tag{3.22}$$

$$= x \cdot \tilde{h}_1^k \tag{3.23}$$

The sampled output of the second adder is then

$$L_k = \sum b_i\, \rho^i \cdot \tilde{h}_1^k + n \cdot \tilde{h}_1^k + n' \tag{3.24}$$

Since n' is simply zero mean Gaussian noise of noise power $N_0 \left|\tilde{h}_2^k\right|^2/2$, L_k is equal to the L_k given by Equation 3.17. From Equations 3.17 and 3.24, we see that the noise process n' internal to the canonical receiver simulates the contribution, $n \cdot \tilde{h}_2^k$, of the input noise in the H_2 subspace. Thus by proper adjustment of the coefficients $C_0 \ldots C_m$ and the noise power associated

with n' any linear filter receiver can be simulated in the form shown in Fig. 3.3.

We note in passing that no separate phase-equalizing filter is required with the canonical receiver. This is because the matched filter portion of the receiver $\rho^*(\omega)$ forms the autocorrelation of the noise-free symbol. Since the power spectrum (hence autocorrelation function) of a waveform and its phase-equalized version are identical, there is no need to precede the canonical receiver with a phase-equalizing filter. Nevertheless, the concept of phase equalization is confirmed--linear filter receiver performance depends on the power spectrum (autocorrelation function) of the received symbol.

One would expect that in any reasonable receiver design the magnitude $|\tilde{h}_2^k|$ would be zero since a non-zero $|\tilde{h}_2^k|$ serves to add noise to the decision variable L_k. This is indeed the case. In Appendix A we show that if $\tilde{h}^k \cdot \rho^k$ is positive then the probability of error $P_e(k)$ is reduced by decreasing $|\tilde{h}_2^k|$ to zero.* Any receiver in which $\tilde{h}^k \cdot \rho^k > 0$ and $|\tilde{h}_2^k| = 0$ will be referred to as an admissible receiver. Since the probability of error for any non-admissible receiver with $\tilde{h}^k \cdot \rho^k > 0$ can always be reduced by making $|\tilde{h}_2^k| = 0$, we will usually consider only admissible receivers in the remainder of this chapter. We note, however, that it is

*If $\tilde{h}^k \cdot \rho^k$ is negative, the receiver decisions are of the wrong polarity, even in the absence of noise and intersymbol interference.

possible for a receiver with a well-chosen set of coefficients $C_0 \ldots C_m$ and a non-zero $\left|\tilde{h}_2^k\right|$ to perform better than an admissible receiver with poorly chosen $C_0 \ldots C_m$.

3.2. Matched Filter and Transversal Filter Receivers

Two simple linear filter receivers are considered in this section: the matched filter receiver and the traditional transversal filter receiver. Unlike the previous section, we will assume that the received symbol ρ is of duration less than $2T$ ($M = 1$). Figure 3.4 depicts a stylized received symbol that will be used repeatedly to clarify the meaning of the notation.

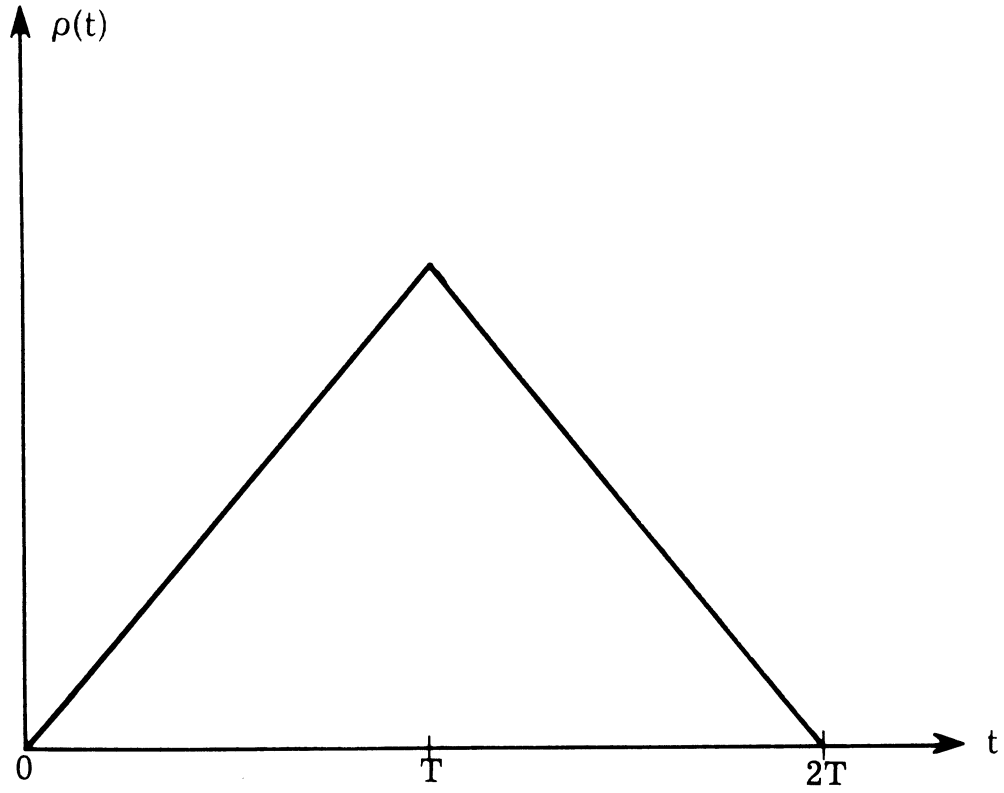

Fig. 3.4. Stylized phase-equalized received symbol ($M = 1$)

Note, however, that any realistic received symbol ρ will be time symmetric because of phase equalization. As a matter of convenience, the axis of symmetry for the symbol is $t = T$ as indicated in Fig. 3.4.

Vector Representation

Vector space representation of the reception x over an interval of length $2T$ is very helpful in understanding the matched filter and transversal filter receivers. Let ρ_0 be equal to ρ for $0 \leq t < T$ and zero elsewhere and let ρ_1 be equal to ρ for $T \leq t < 2T$ and zero elsewhere. Then the reception $\mathbf{x}^k$ in the interval $(kT, kT + 2T)$ where $k > 0$ is given by

$$x_k(t) = b_{k-1}\,\rho_1^{k-1}(t) + b_k\left[\rho_0^k(t) + \rho_1^k(t)\right] + b_{k+1}\,\rho_0^{k+1}(t) + n(t) \tag{3.25}$$

where b_i is the value (± 1) of the k^{th} symbol. This is illustrated in Fig. 3.5 for the symbol shown in Fig. 3.4.

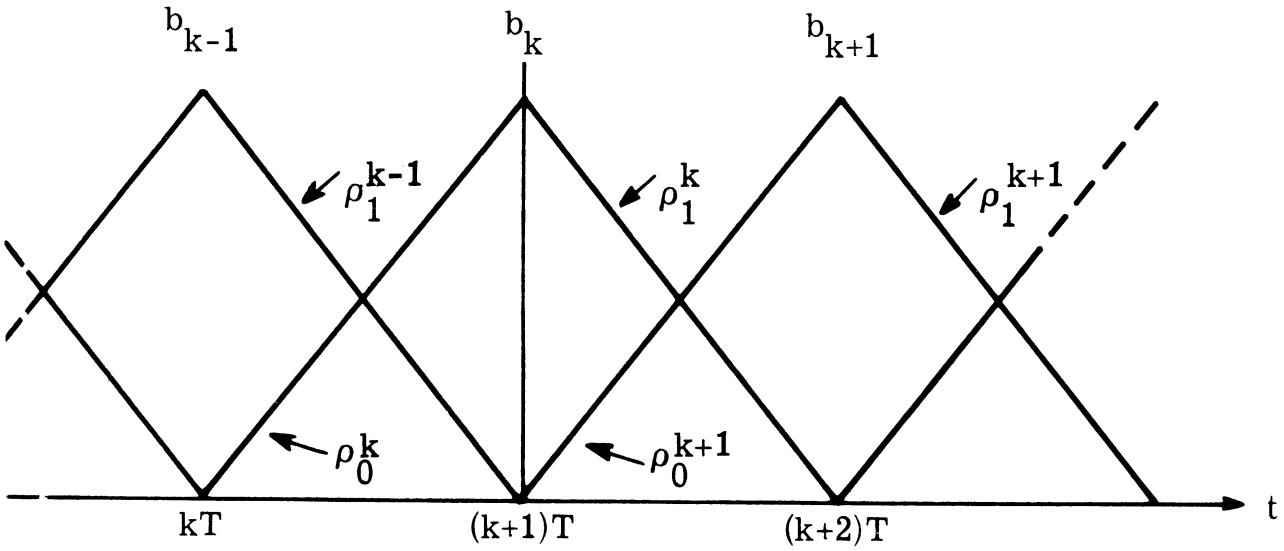

Fig. 3.5. Noise-free components in the interval (kT, (k+2)T)

Let us assume that $b_k = +1$. Then the noise free reception consists of a vector $\rho^k = \rho_0^k + \rho_1^k$ plus one of four "interference waveforms" dependent upon the values of b_{k-1} and b_{k+1}. Define the interference waveform for the k^{th} symbol as

$$\Delta^k_{b_{k-1}b_{k+1}} = b_{k-1}\rho_1^{k-1} + b_{k+1}\rho_0^{k+1} \tag{3.26}$$

Both Δ^k_{+1-1} and Δ^k_{-1+1} are orthogonal to ρ^k since

$$\rho^k \cdot \Delta^k_{b_{k-1}b_{k+1}} = b_{k-1}\rho_1^{k-1} \cdot \rho_0^k + b_{k+1}\rho_0^{k+1} \cdot \rho_1^k \tag{3.27}$$

and

$$\rho_0^k \cdot \rho_1^{k-1} = \rho_0^{k+1} \cdot \rho_1^k \tag{3.28}$$

We write $\Delta^k_{+1-1} \perp \Delta^k_{-1+1}$. However, Δ^k_{11} and Δ^k_{-1-1} are not orthogonal to ρ^k unless $\rho_1^{k-1} \cdot \rho_0^k = 0$

$$\Delta^k_{\pm 1 \pm 1} = \pm 2\rho_1^{k-1} \cdot \rho_0^k \tag{3.29}$$

from Equation 3.27. Furthermore $\Delta^k_{\pm 1 \pm 1}$ and $\Delta^k_{\pm 1 \pm 1}$ are orthogonal ($\Delta^k_{+1+1} \perp \Delta^k_{+1-1}$ and $\Delta^k_{-1-1} \perp \Delta^k_{-1+1}$) since

$$\Delta^k_{b_{k-1}b_{k+1}} \cdot \Delta^k_{b'_{k-1}b'_{k+1}} = b_{k-1}b'_{k-1}\left|\rho_1^{k-1}\right|^2 + b_{k+1}b'_{k+1}\left|\rho_0^{k+1}\right|^2 \tag{3.30}$$

and by symmetry due to phase equalization

$$\left| \rho_1^{k-1} \right|^2 = \left| \rho_0^{k+1} \right|^2 \tag{3.31}$$

Since ρ_1^{k-1} and ρ_0^{k+1} are orthogonal in time we have

$$\left| \Delta^{k}_{b_{k-1} b_{k+1}} \right|^2 = \left| \rho_1^{k-1} \right|^2 + \left| \rho_0^{k+1} \right|^2 \tag{3.32}$$

$$= \left| \rho \right|^2 \tag{3.33}$$

that is, all the interfering waveforms $\Delta^{k}_{b_{k+1} b_{k-1}}$ have the same magnitude.

The relations derived in the preceding paragraph can be represented very simply in 3-space. One convenient choice of orthonormal basis vectors $\hat{e}_0$, $\hat{e}_1$, and $\hat{e}_2$ is

$$\hat{e}_0 = \rho^k / \left| \rho^k \right| \tag{3.34}$$

$$\hat{e}_1 = \Delta_{+1-1} \Big/ \left| \Delta_{+1-1} \right| \tag{3.35}$$

$$\hat{e}_2 = \frac{\Delta_{+1-1} - \left[\Delta_{+1+1} \cdot \hat{e}_0 \right] \hat{e}_0}{\left| \Delta_{+1+1} - \left[\Delta_{+1+1} \cdot \hat{e}_0 \right] \hat{e}_0 - \left[\Delta_{+1+1} \cdot \hat{e}_1 \right] \hat{e}_1 \right|} \tag{3.36}$$

Figure 3.6 depicts the relations given above for a typical interference problem.

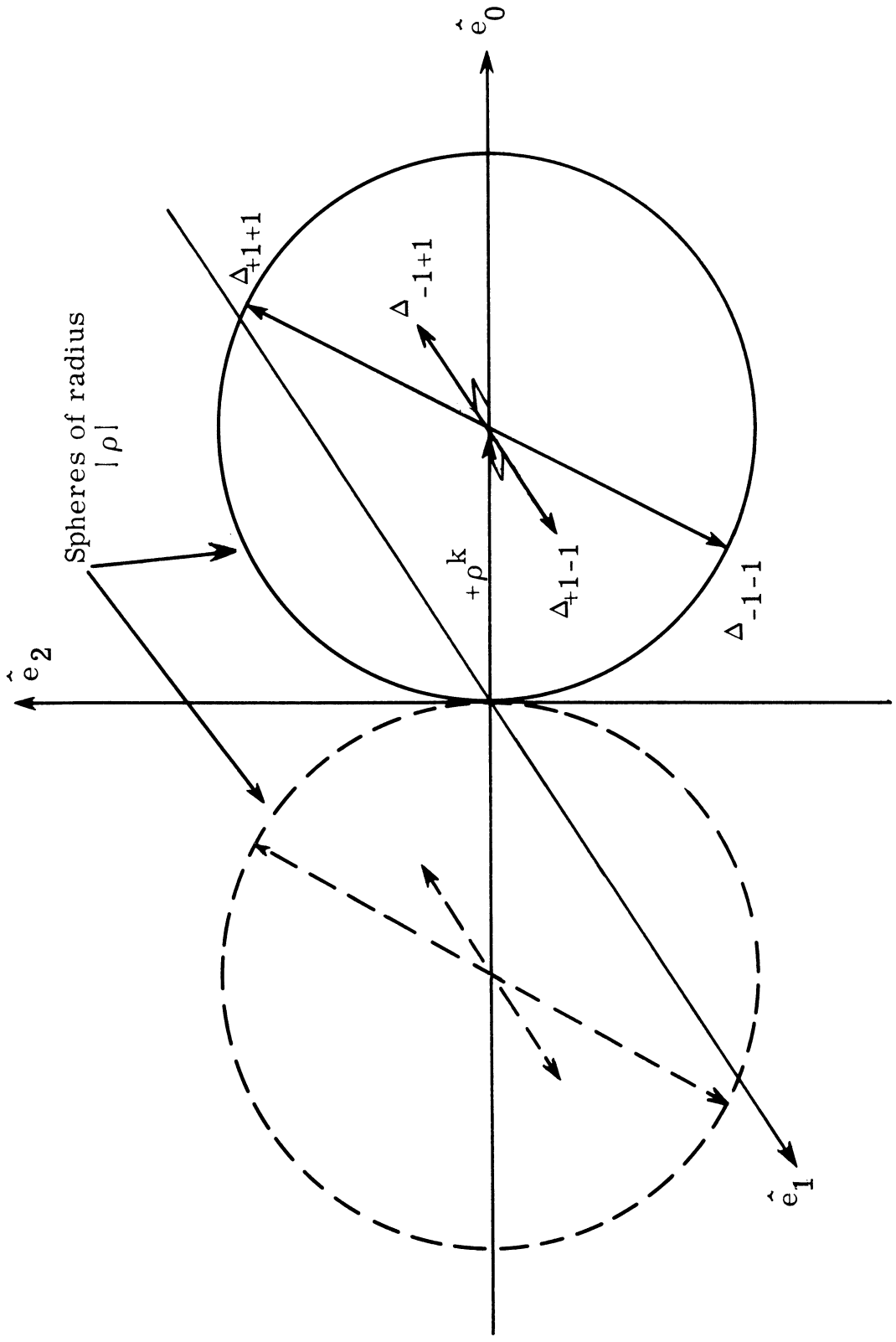

Fig. 3.6. Vector space representation of signal components in (kT, (k+2)T)

Before proceeding further, we will relate the quantities described above back to "real world quantities." The quantity $|\rho|^2$ is the energy of a single noise-free symbol, which is also the value of the autocorrelation function $R(\tau)$ of the received symbol at zero. From Fig. 3.5

$$\rho_0^k \cdot \rho_1^{k-1} = \rho_1^k \cdot \rho_0^{k+1} \tag{3.37}$$

$$= R(T) \tag{3.38}$$

Thus all of the quantities describing the phase-equalized, $M = 1$ received symbol are given by the autocorrelation function $R(\tau)$ evaluated at 0 and T. The normalized autocorrelation function $r(\tau)$ is

$$r(\tau) = R(\tau) / R(0) \tag{3.39}$$

From time symmetry and the $M = 1$ assumption one can show that $|r(T)| \leq .5$. The case when $r(T) = 0$ corresponds to the no-intersymbol interference case.

The effects of noise on the problem can be conveniently included by dividing the magnitudes of all waveform vectors by $\sqrt{N_0/2}$, making the resulting variance unity. Under this convention the magnitude of ρ becomes $\sqrt{d}$ where

$$d = 2E/N_0 \tag{3.40}$$

is the index of signal detectability used in classical detection theory. For

binary simplex signals in the absence of intersymbol interference, the smallest probability of error is given by classical detection theory as

$$P_e = \Phi(-\sqrt{d}) \tag{3.41}$$

This represents a lower bound on error probability for all systems with intersymbol interference.

Matched Filter Receiver (MFR)

The matched filter receiver (MFR) is the simplest possible solution to the intersymbol interference in noise problem. If intersymbol interference is not present, classical signal detection theory indicates the MFR to be the optimum (likelihood ratio) receiver. Because intersymbol interference is not considered in the design of the MFR, system performance is degraded when intersymbol interference is present.

We will define the MFR as the linear filter receiver for which

$$\underset{\sim}{h}^k = \rho^k \tag{3.42}$$

In terms of the canonical receiver given in the preceding section, this means that all but one of the delay line tap coefficients is zero, or equivalently, no delay line is used. Since $\underset{\sim}{h}^k$ is entirely within the subspace H_1, $|\underset{\sim}{h}_2^k| = 0$ and no noise source is required either. From this and the fact that $\underset{\sim}{h}^k \cdot \rho^k = |\rho^k|^2 > 0$ we see that the MFR is an admissible receiver.

There is another way of interpreting the term "matched filter

receiver," however. An intuitive approach is to carefully select a segment of the received symbol $\rho_s(t)$ having a duration less than or equal to T, and match a filter to it. The segment would be chosen so as to have a large amount of signal energy and little intersymbol interference in it. In general, a filter matched to $\rho_s(t)$ would not be an admissible receiver in the sense of the preceding section and we do not consider it here.

The operation of the MFR in terms of the 3-space representation of x^k is apparent. The equation of the decision plane is

$$x^k \cdot \rho^k = 0 \tag{3.43}$$

Note that the direction of the decision plane does not depend on the intersymbol interference, (see Fig. 3.7).

Equation 3.14 with $\tilde{h}_k = \rho^k$ gives the equation for the system error probability. Because of the unit degree of intersymbol interference ($M = 1$) assumption $\rho^i \cdot \tilde{h}^{\sim k} = 0$ for $i < k-1$ and $i > k+1$.

$$P_e = \frac{1}{2^m} \sum_{B_k} \Phi \left[- \frac{|\rho|^2 + b_{k-1}\rho_1^{k-1} \cdot \rho_0^k + b_{k+1}\rho_0^{k+1} \cdot \rho_1^k}{|\rho| \sqrt{N_0/2}} \right] \tag{3.44}$$

Combining terms we obtain:

$$= 1/4 \sum_{\substack{\text{all} \\ b_{k-1} b_{k+1}}} \Phi \left\{ - |\rho| \left[1 + r(T) \left(b_{k-1} + b_{k+1} \right) \right] \Big/ \sqrt{N_0/2} \right\} \tag{3.45}$$

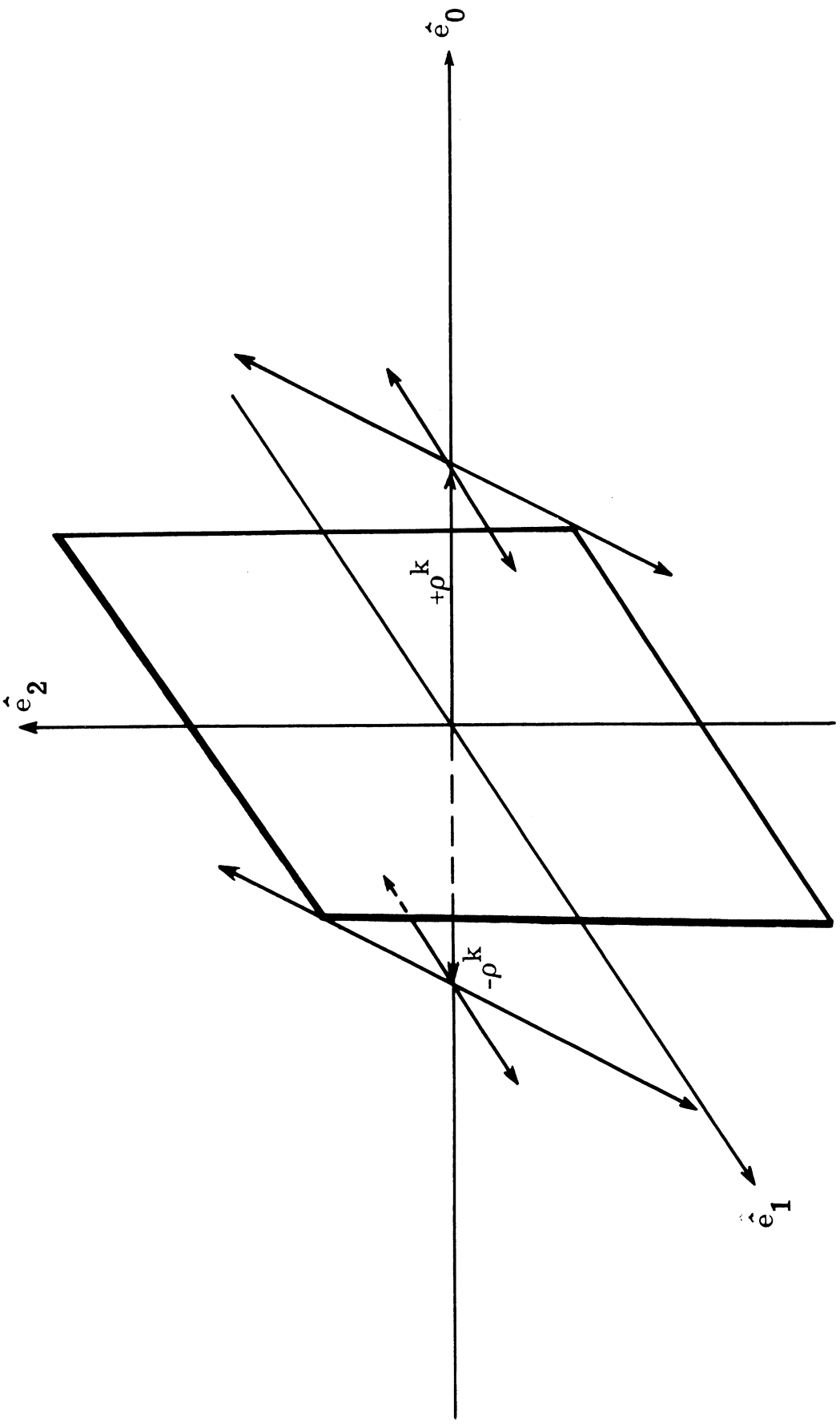

Fig. 3.7. Decision plane for matched filter receiver

Writing the above explicitly in terms of d

$$P_e = 1/4\,\Phi\left[-\sqrt{d}\,(1+2r(T))\right] + 1/2\,\Phi\left[-\sqrt{d}\right] + 1/4\,\Phi\left[-\sqrt{d}\,(1-2r(T))\right] \tag{3.46}$$

Note that for r(T) near zero the system probability of error approaches that for the interference free receiver, as one would expect.

Transversal Filter Receiver (TFR)

The transversal filter receiver (TFR) represents a traditional approach to the intersymbol interference problem. The TFR completely eliminates intersymbol interference but at the expense of performance against noise.

The defining characteristic of the TFR is that the linear filter output is uneffected by the interfering symbols, that is

$$\overset{\sim k}{h} \cdot x = L_k \tag{3.47}$$

does not depend on b_i , $i \neq k$. From Equation 3.1

$$\overset{\sim k}{h} \cdot x = b_k \rho^k \cdot \overset{\sim k}{h} + \sum_{i \neq k} b_i \rho^i \cdot \overset{\sim k}{h} + \overset{\sim k}{h} \circ n \tag{3.48}$$

In order to have the desired independence, we must have

$$\rho^i \cdot \overset{\sim k}{h} = 0 \tag{3.49}$$

for all $i \neq k$. If $\rho^1 \cdot \rho^k \neq 0$ for all $i \neq k$, this implies that $\overset{\sim k}{h}$

must have a non-zero component in the H_2 subspace and hence the TFR is not an admissible receiver in the sense of the preceding section.* Since the TFR is a traditional and commonly used receiver, it will be analyzed even though it is not an admissible receiver.

Since the probability of error can be expected to increase with the magnitude of the component of $\tilde{h}^k$ in the H_2 subspace, it is desirable to make this component as small as possible while satisfying Equation 3.49. This can be done by making $\tilde{h}^k$ zero outside the interval $(kT , (k+2)T)$ and making $\tilde{h}^k$ satisfy

$$\tilde{h}^k \cdot \rho_1^{k-1} = 0 \tag{3.50}$$

and

$$\tilde{h}^k \cdot \rho_0^{k+1} = 0 \tag{3.51}$$

The preceding equations describe a tilted plane in the 3-space representation of x^k which is parallel to the plane of the interference vectors, $\Delta^k_{b_{k-1}b_{k-1}}$. Figure 3.8 depicts the decision plane for the TFR.

Equations 3.50 and 3.51 above allow the determination of $\tilde{h}^k$. Let

$$\tilde{h}^k = \rho^k + c_1\rho_1^{k-1} + c_0\rho_0^{k+1} \tag{3.52}$$

then

---

*From the definition of $r(T)$ we see that $\rho^i \cdot \rho^k = 0$ for all $i \neq k$ if and only if $r(T) = 0$, that is, if there is no intersymbol interference.

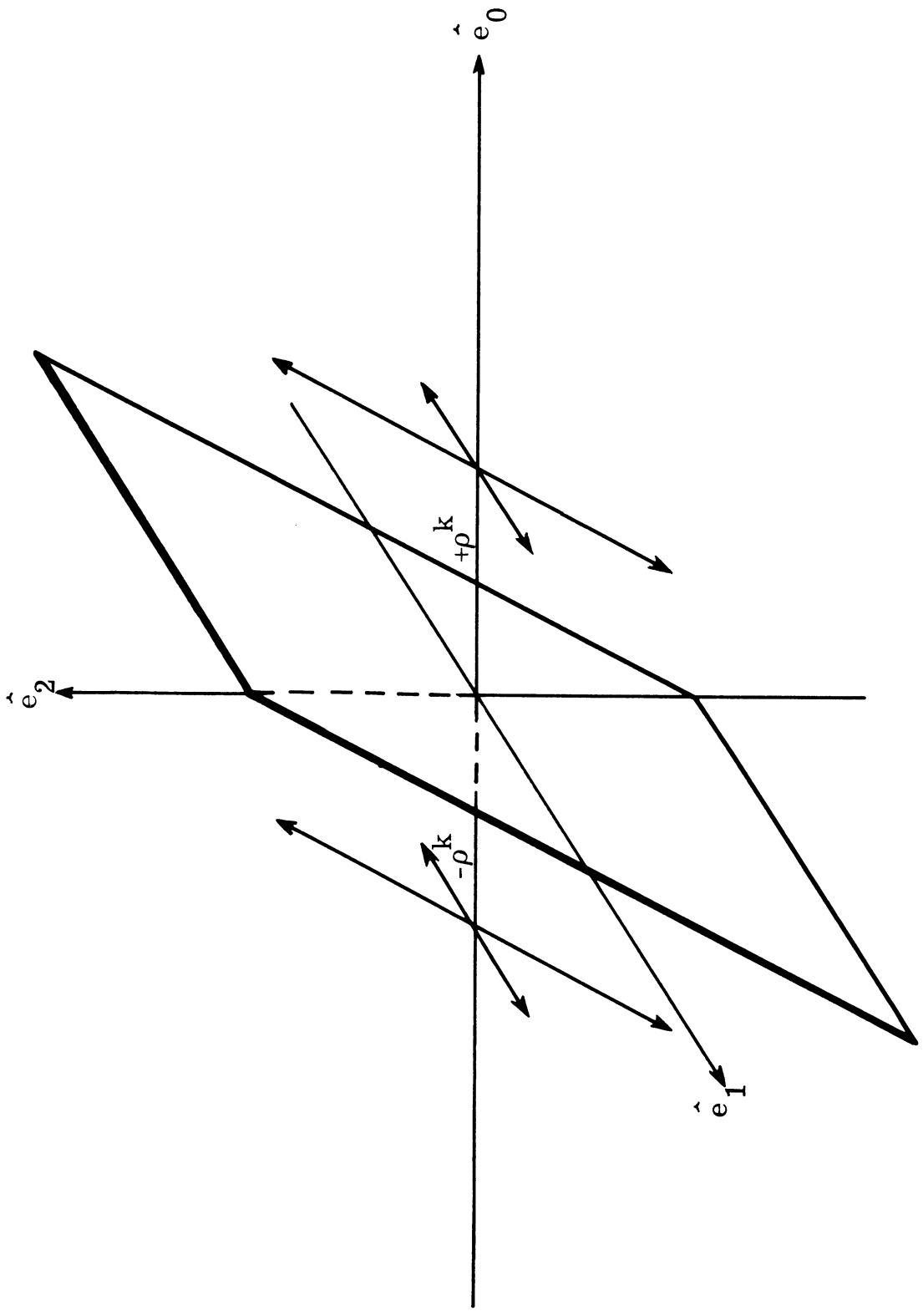

Fig. 3.8. Decision plane for transversal filter receiver

$$\underset{h}{\overset{\sim k}{}} \cdot \rho_1^{k-1} = \rho_0^k \cdot \rho_1^{k-1} + \rho_1^k \cdot \rho_1^{k-1} + c_1 \rho_1^{k-1\,2} + c_0 \rho_1^{k-1} \rho_0^{k+1} \tag{3.53}$$

$$= \rho_0^k \cdot \rho_1^{k-1} + c_1 \left| \rho_1^{k-1} \right|^2 = 0 \tag{3.54}$$

since $\rho_1^k \perp \rho_1^{k-1}$ and $\rho_1^{k-1} \perp \rho_0^{k+1}$. Solving for c_1

$$c_1 = -2r(T) \tag{3.55}$$

Similarly,

$$\underset{h}{\overset{\sim k}{}} \cdot \rho_0^k = \rho_0^k \cdot \rho_1^{k-1} + c_0 \left| \rho_0^k \right|^2 \tag{3.56}$$

and

$$c_0 = -2r(T) \tag{3.57}$$

The probability of error for the TFR is found directly from Equation 3.14; however, because of Equations 3.50 and 3.51, the expression is very simple

$$P_e = \Phi \left\{ \frac{-\underset{h}{\overset{\sim k}{}} \cdot \rho^k}{\sqrt{N_0 / 2}} \right\} \tag{3.58}$$

Now we have, from Equations 3.54 and 3.56 above

$$\tilde{h}^k \cdot \rho^k = |\rho^k|^2 - 2r(T)\rho_1^{k-1} \cdot \rho - 2r(T)\rho_0^{k+1} \cdot \rho^k \qquad (3.59)$$

$$= |\rho^k|^2 \left[1 - 4(r(T))^2\right] \qquad (3.60)$$

thus

$$P_e = \Phi\left[-\sqrt{d}\,\left(1 - 4(r(T))^2\right]\right] \qquad (3.61)$$

Note that as $r(T)$ goes to zero, the probability of error approaches that of an interference free receiver, as one would expect. As $r(T)$ approaches $.5$, however, the probability of error approaches $.5$, the worst possible error probability.

Figure 3.9 compares the error performances of the MFR and TFR as a function of $|r(T)|$ for a d of 10. Also shown in this plot is the performance of an interference-free receiver operating with a d of 5 and 10. Error probabilities of both the MFR and TFR increase rapidly with $|r(T)|$. With the exception of a very small region ($|r(T)| > .45$) the TFR performance is superior to that of the MFR.

A natural question arising from this comparison is why does the TFR, which is not an admissible receiver, perform better than the MFR which is an admissible receiver. The answer to this is that "admissible" means that components of $\tilde{h}^k$ which add only noise to L_k have been eliminated. By eliminating the component of $\tilde{h}^k$ in the H_2 subspace, a TFR can be converted into an admissible receiver and the probability

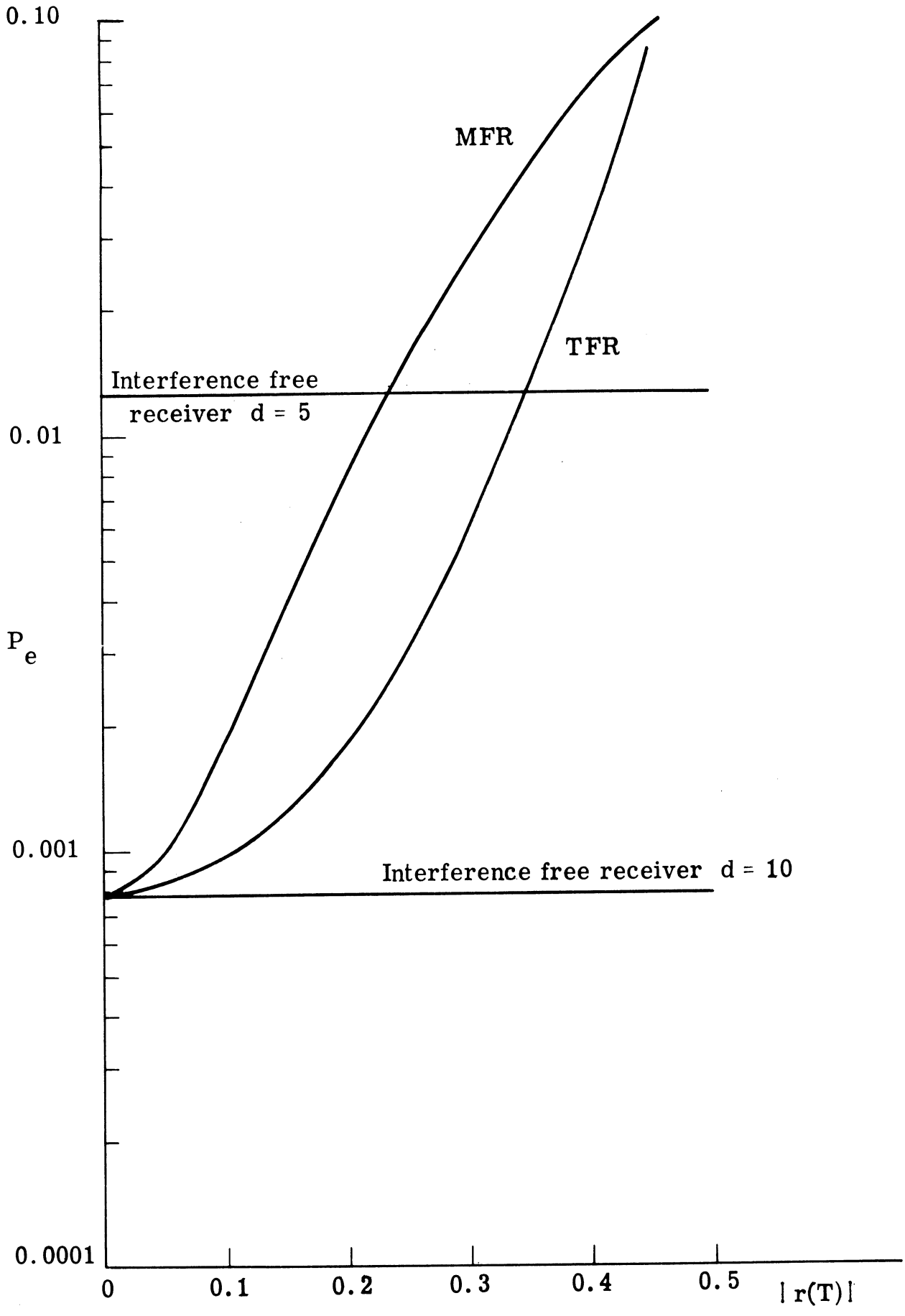

Fig. 3.9. Comparison of MFR and TFR for d = 10

of error reduced. Unfortunately, this modification destroys the characteristic of eliminating intersymbol interference and the receiver loses its identity.

A word of caution is necessary with regard to error probabilities. At first glance, it appears that the TFR gives a loss "of just 3 db" in performance at $|r(T)| = .35$, since its performance at $|r(T)| = .35$ is equal to that of an interference-free receiver operating with a d of 5. In many problems a depreciation in performance of 3 db in some sense is negligible. On the other hand, in communications systems such as the one considered here "just 3 db" may be a large factor. For example, suppose the binary simplex system is used to transmit 5-bit teletype characters. If the bit probability of error P_e is .00078 then the probability of a character error is .0039. If the performance of system is degraded by "just 3 db" the probability of a character error becomes .0614. Thus a "db down from ideal" measure of system performance is a crude measure for teletype systems.

3.3. Optimized Linear Filter Receivers

In Section 3.1 the canonical form of all admissible receivers was developed. For each set of tap weights C_j, a different admissible receiver is obtained using this canonical form. A very natural approach to the receiver design problem is to determine a set of C_j's which gives the smallest probability of error. The resulting receiver

would then be the optimum linear filter receiver.* Since the number of symbols in the transmission, m+1 , is normally very large, it is not practical to use the m + 1 tap delay line of the canonical receiver. Instead, it is necessary to constrain the problem by limiting the number of taps the receiver is allowed to use. The receivers resulting from such constrained optimization are called optimized linear filter receivers and are studied below.

Probability of Error

Consider the admissible linear filter receiver with $2q+1$ taps shown in Fig. 3.10. Let the weighting coefficients of the taps be $w_{-q} \cdots w_0 \cdots w_{+q}$ where w_{-q} is the weight of the tap representing the longest time delay. To avoid realizability difficulties, the time origin for the output of the adder is taken qT seconds after the time origin of the input. The system impulse response is then given by

$$h = \sum_{i=-q}^{+q} w_i \tilde{\rho}^i \tag{3.62}$$

where $\tilde{\rho}^i = \rho(iT - t)$ and the probability of error can be determined from Equation 3.14.

*Here we have made the assumption that the optimum linear filter receiver is an admissible receiver. Since the probability of error for any non-admissible receiver (with $\tilde{h}^k \cdot \rho^k > 0$) can be reduced by setting $|\tilde{h}_2^k| = 0$ this is a very reasonable assumption.

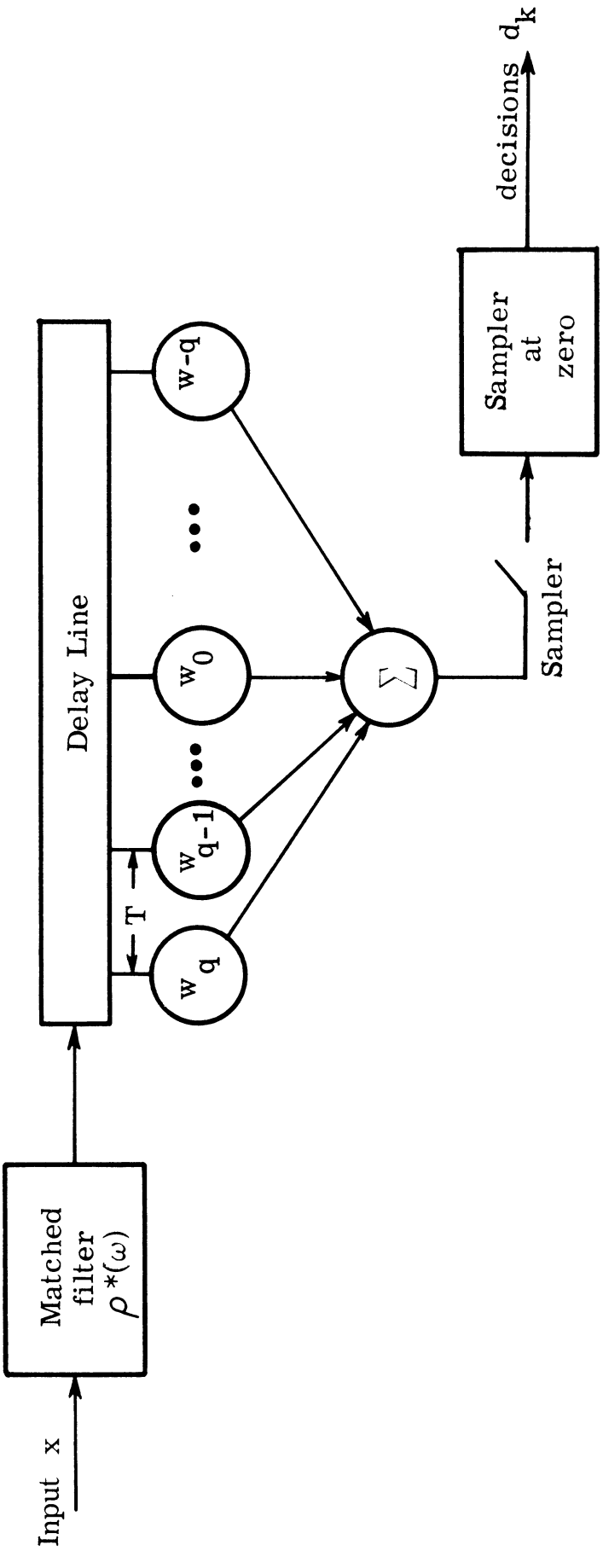

Fig. 3.10. Canonical admissible receiver with 2q+1 taps

Let

$$\overset{\sim k}{h} = \sum_{i=-q}^{+q} w_i \rho^{i+k} \tag{3.63}$$

then

$$\left| \overset{\sim k}{h} \right|^2 = \sum_{i=-q}^{+q} \sum_{j=-q}^{+q} w_i w_j \rho^{i+k} \cdot \rho^{j+k} \tag{3.64}$$

$$= |\rho|^2 \sum_{i=-q}^{+q} w_i^2 + 2\rho_0^k \cdot \rho_1^{k-1} \sum_{i=-q}^{q-1} w_i w_{i+1} \tag{3.65}$$

because of the phase equalization and M=1 assumptions, we have

$$\rho^k \cdot \rho^{k+i} = |\rho|^2 \text{ if } i=0 \tag{3.66}$$

$$\rho^k \cdot \rho^{k+i} = \rho_0^k \circ \rho_1^{k-1} \text{ if } i = \pm 1 \tag{3.67}$$

$$\rho^k \cdot \rho^{k+i} = 0 \qquad \text{otherwise} \tag{3.68}$$

from the preceding section. Let $\bar{b} = (b_{k-q-1} \cdots b_{k+q+1})$ and $\bar{w} = (w_{-q} \cdots w_{+q})$ then one can show by a similar procedure

$$\tilde{h}^{k} \cdot \rho^{k} + \sum_{i \neq k} b_i \rho^{i+k} \cdot \tilde{h}^{k} = |\rho|^2 Z_1(\bar{b}, \bar{w}) + \rho_0 \cdot \rho_1 Z_2(\bar{b}, \bar{w}) \tag{3.69}$$

where

$$Z_1(\bar{b}, \bar{w}) = w_0 + \sum_{i \neq k} b_i w_i \tag{3.70}$$

$$Z_2(\bar{b}, \bar{w}) = b_{-q-1} w_{-q} + b_{-q} w_{-q+1} + \sum_{i=-1}^{i=-q+1} b_i (w_{i-1} w_{i+1}) + w_{-1}$$

$$+ w_{+1} + \sum_{i=+1}^{i=q-1} b_i (w_{i-1} w_{i+1}) + b_q w_{q-1} + b_{q+1} w_q \tag{3.71}$$

Substituting Equations 3.64 and 3.69 into Equation 3.14 and converting to the real world parameters d and r(T) yields the probability of error for the receiver with the tap weights given by $\bar{w}$, $P_e(\bar{w})$

$$P_e(\bar{w}) = \frac{1}{2^{2q+1}} \sum_{\text{all } \bar{b}} \Phi \left[- \sqrt{d} \left\{ \frac{Z_1(\bar{b}, \bar{w}) + r(T) Z_2(\bar{b}, \bar{w})}{\sum_{-q}^{+q} w_i^2 + 2r(T) \sum_{i=-q}^{q-1} w_i w_{i+1}} \right\} \right] \tag{3.72}$$

When $r(T)$ is zero and $w_i = 0$ for $i \neq 0$, the above equation gives the probability of error for an interference-free matched filter receiver as one would expect.

The optimized $2q+1$ tap linear filter receiver, $OLFR_{2q+1}$, is defined as the canonical receiver having $2q+1$ taps with tap weights given by $\bar{w}^*$ which minimizes $P_e(\bar{w})$.* We note in passing that the MFR can be considered to be the $OLFR_1$, the simplest admissible receiver possible.

Determination of Tap Coefficients

In order to construct and evaluate the $OLFR_{2q+1}$ the optimum tap weights $\bar{w}^*$ must be determined as a function of both d and $r(T)$. Equation 3.72 is sufficiently intractable to preclude useful analytic expression for $\bar{w}^*$. Both Aein and Hancock (Ref. 2) and Aaron and Tufts (Ref. 3) have used the calculus of variations to derive the necessary coefficients for their analogous equations. Unfortunately, in both cases, their approaches produced equations as horrendous as Equation 3.72 and they resorted to numerical search techniques. We have therefore approached the problem directly by using a trial-and-error search technique to determine $\bar{w}^*$.

Several simple observations make the direct search for $\bar{w}^*$ easier. A convenient normalization is to take $w_0 = 1$. Because the

---

*The implicit assumption that there is a unique $\bar{w}^*$ is borne out by the work of Aaron and Tufts, Ref. 3.

received symbols are symmetric due to phase equalization and their values b_k are independent, the effects of b_{k+i} and b_{k-i} on the k^{th} symbol decision d_k are the same. Hence the tap coefficients are symmetric, that is, $w_i = w_{-i}$. If the weights $w_{\pm 1}$ are to help eliminate the interfering components of $b_{k \pm 1}$, the weights must be negative, or they will actually increase the intersymbol interference. Proceeding in this manner indicates that the tap weights $w_{\pm i}$ must alternate in sign. Because the output of the tap corresponding to w_0 represents a direct indication of the value of b_k, whereas the other taps serve to eliminate intersymbol interference, one would expect the magnitudes of $w_i (i \neq 0)$ to be less than $w_0 = 1$. These observations have been borne out by numerical analysis of Equation 3.72 and serve to reduce the search space to a unit cube in q-dimensional space.

Figure 3.11 depicts the optimum tap weights for $OLFR_3$, $OLFR_5$, and $OLFR_7$ as a function of $|r(T)|$ for a d of 10. These weights were obtained by searching over the unit cube with an effective resolution of .025, that is, the coefficients are within .025 of their true value. This resolution is considered sufficient because of the smooth variation of $P_e(\overline{w})$ with $\overline{w}$ and more elaborate techniques, such as the steepest descent technique do not appear necessary.

Performance

In Fig. 3.12, the probability of error for the $OLFR_1$, $OLFR_3$, $OLFR_5$, and $OLFR_7$ receivers is shown as a function of $|r(T)|$ for a

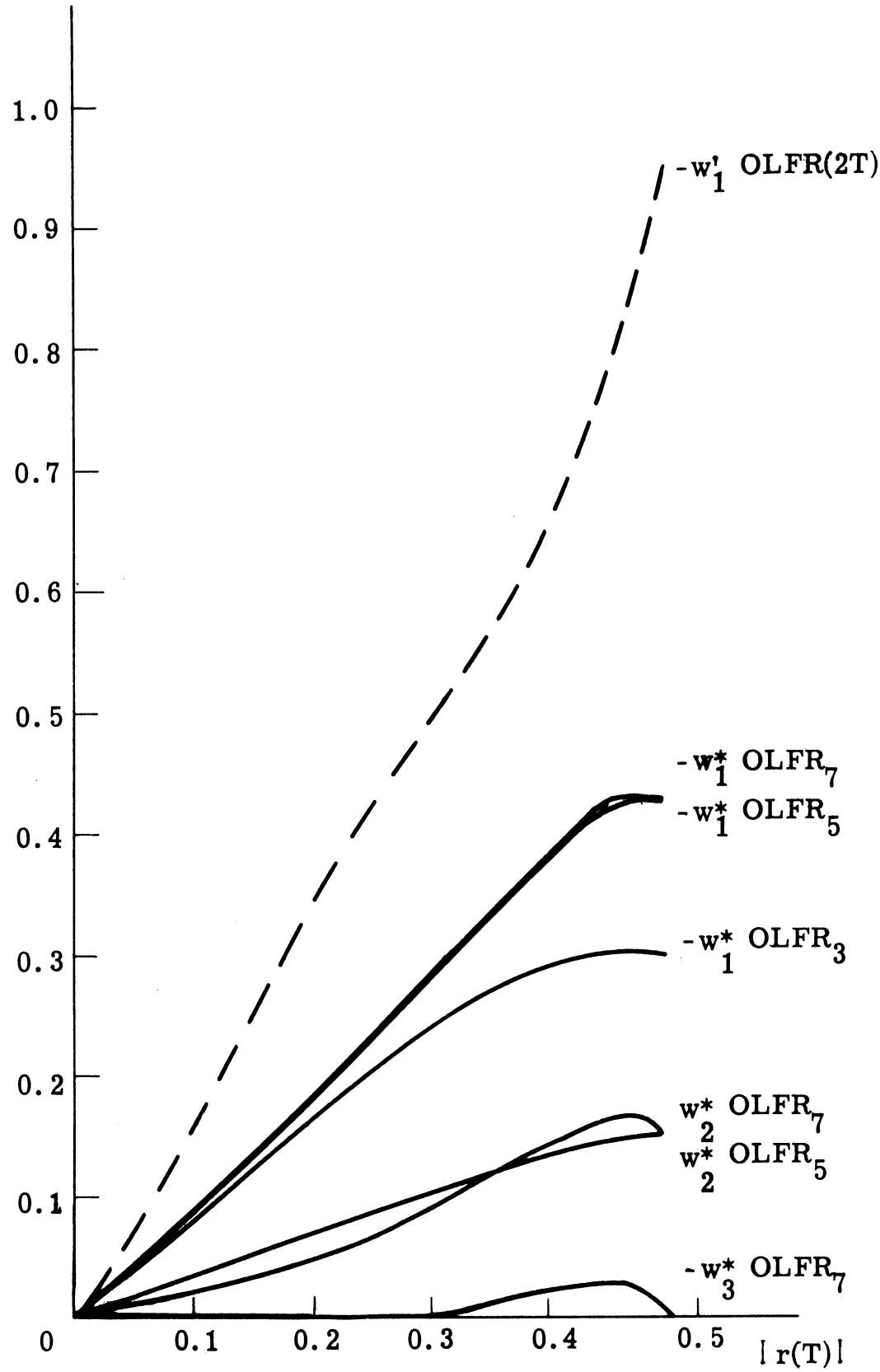

Fig. 3.11. Optimum tap weights for $OLFR_3$, $OLFR_5$, $OLFR_7$ d = 10

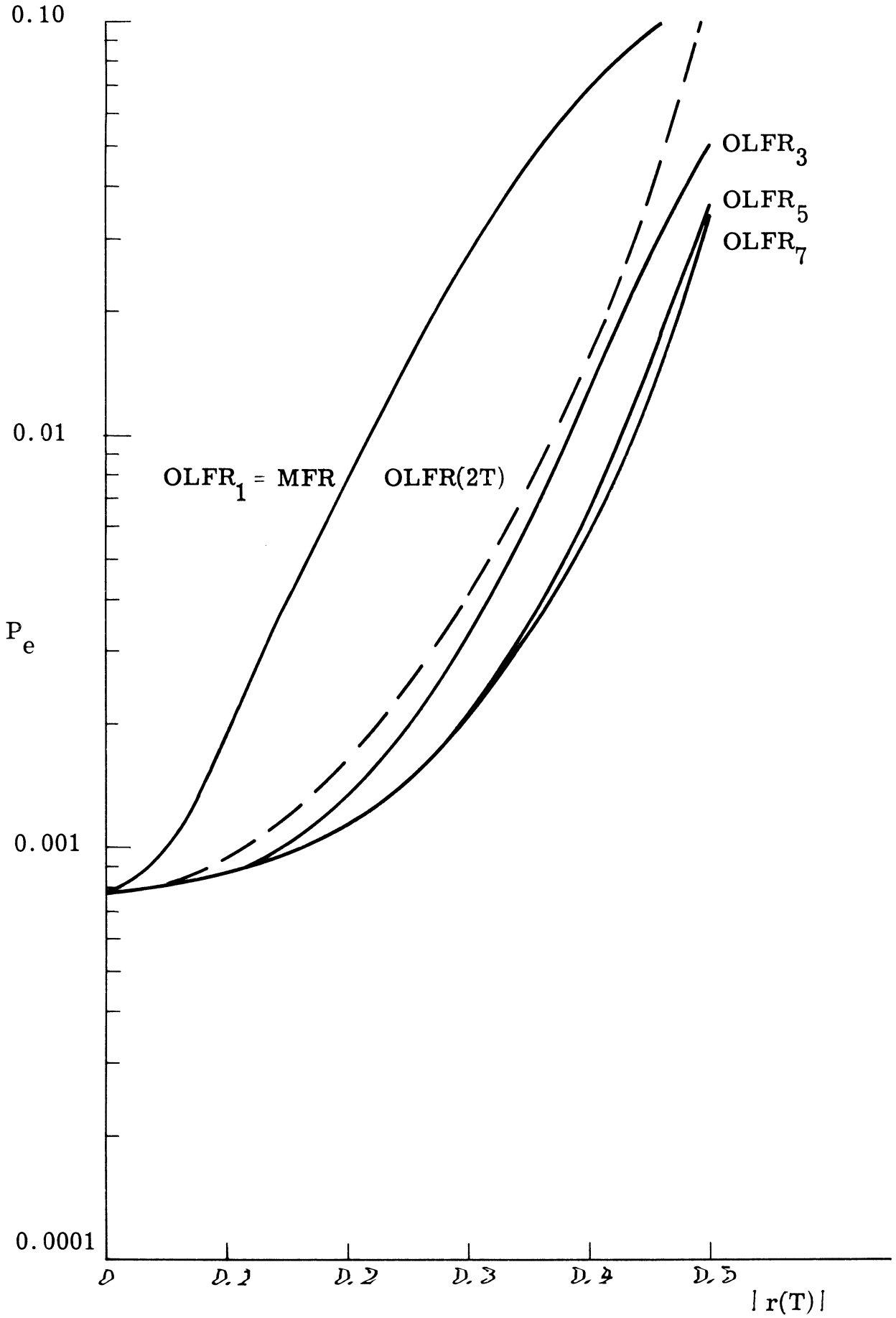

Fig. 3.12. Probability of Error for $OLFR_1$, $OLFR_3$, $OLFR_5$, $OLFR_7$ d = 10

d of 10. This figure shows that a very significant improvement in error performance is obtained in going from one tap (MFR) to 3 or more. There is little improvement between the 5- and 7-tap receivers, however.

Another Constraint

Another way of constraining the optimization is to limit the duration of the filter impulse response to some specified amount. This constraint may be a reasonable one in implementations of the linear filter which correlate a stored reference, $\tilde{h}^{k}$, with the reception. Receivers evolving from this constraint will not be admissible receivers but will have performances intermediate between that of the longest OLFR having an impulse response duration less than the constraint duration and the OLFR having two additional taps. We consider only the case in which the impulse response is limited to $2T$.

Let $\tilde{h}^{k}$ be of duration $2T$ and of the form*

$$\tilde{h}^{k} = w'_{-1}\rho_{1}^{k-1} + \rho^{k} + w'_{+1}\rho_{0}^{k+1} \qquad (3.73)$$

We wish to determine the constants $w'_{\pm 1}$ which minimize the probability of error. From symmetry arguments similar to the ones given earlier, $w'_{+1} = w'_{-1}$, and $-1 \leq w'_{\pm 1} \leq 0$. The optimum value of $w'_{\pm 1}$ is shown as function of $|r(T)|$ is shown as a dotted line for $d=10$ in

---

* One can show that $\tilde{h}^{k}$ should have this form from arguments analogous to those for admissible receivers.

Fig. 3.11. The error performance of this receiver, known as the optimized linear filter receiver over a time duration $2T$, OLFR(2T), is shown as a dotted line in Fig. 3.12. As expected, its performance lies between that of $OLFR_1$ and $OLFR_3$.

A major advantage to considering the OLFR(2T) is the insight it provides concerning the MFR and TFR. Since $\tilde{h}^k$ is of duration $2T$, the decision plane of the OLFR(2T) can be completely represented in the 3-space shown in Figs. 3.7 and 3.8. Figure 3.13 depicts the decision plane for these three receivers. The intermediate position of the decision plane of the OLFR(2T) between those of the MFR and TFR, indicates the trade-off between intersymbol interference elimination by the TFR and good noise performance by the MFR.

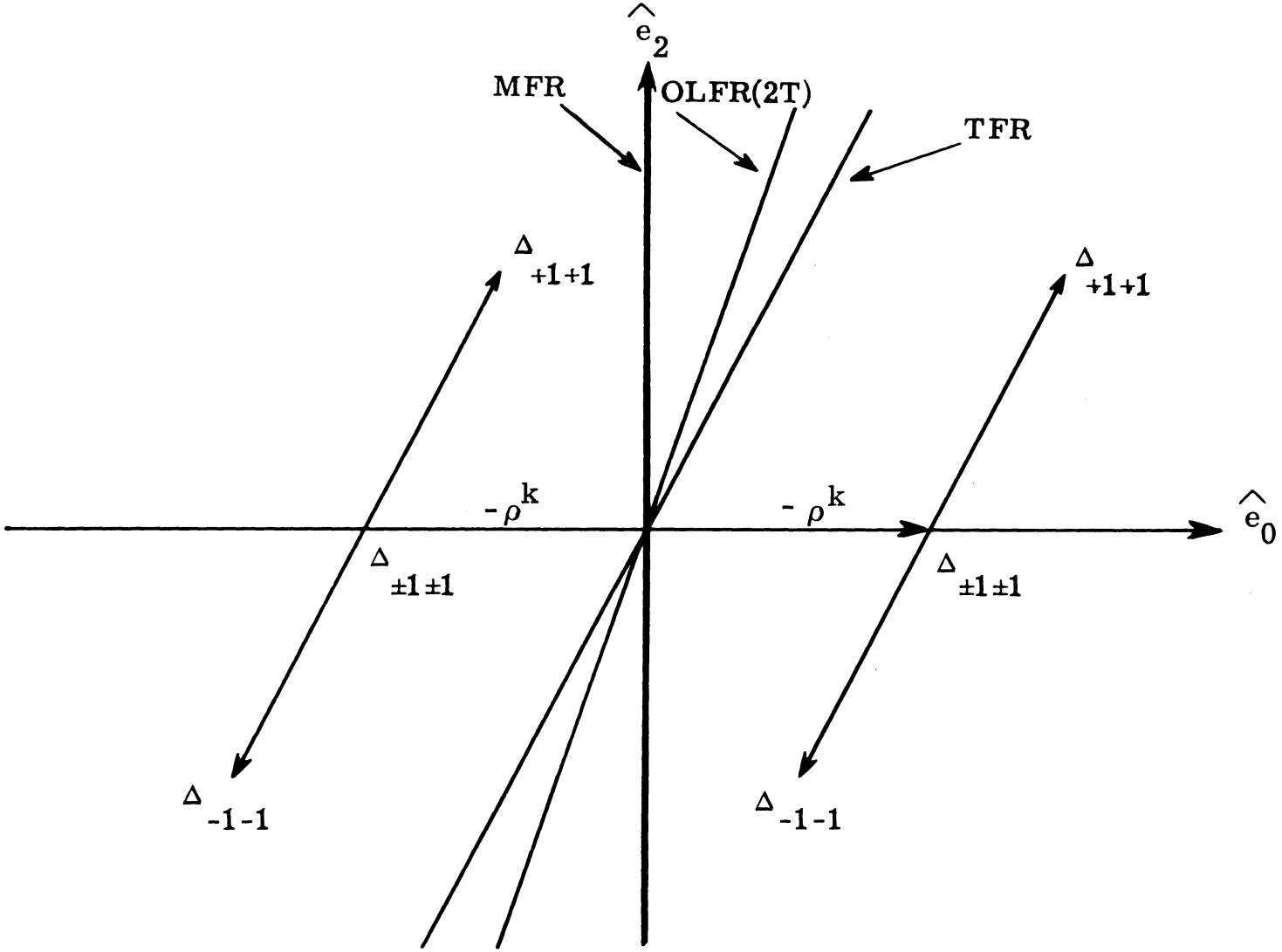

Fig. 3.13. Decision planes for the MFR, TFR, and OLFR(2T)

CHAPTER IV

TWO SIMPLE NONLINEAR RECEIVERS

The two receivers considered in this chapter are nonlinear receivers because their decision variable L_k is not a linear function of the reception. There are many possible nonlinear receivers which could be studied. The two receivers studied here, the switched-mode receiver and the iterated switched-mode receiver, are important because of their ease of implementation and comparatively good performance (relative to the optimized linear filter receivers). The first of these receivers, the switched-mode receiver, is a direct extension of a receiver of the same name proposed by Aein and Hancock (Ref. 2).* The second receiver, the iterated switched-mode receiver, is described for the first time here. Chapter V will show that the optimum (likelihood ratio) receiver is a nonlinear receiver and thus these receivers belong to a promising class of receivers.

The underlying principle of both the switched-mode receiver and the iterated switched-mode receiver is very simple. Suppose that the receiver is to make a decision on the k^{th} symbol. Then if the values of the interfering symbols b_{k-1} , b_{k+1} were known their

---

*Aein and Hancock (Ref. 2) appear to have been the first to make the important observation that a simple nonlinear receiver can perform better than a complicated optimized linear filter receiver.

"interference" could be subtracted out to give an interference free k^{th} symbol. Since the objective of the receiver is to produce decisions $d_0 \ldots d_m$ which are equal to the transmitted symbol values $b_0 \ldots b_m$, it seems reasonable to use symbol decisions to subtract out the interference to make even better symbol decisions. This sort of "boot strap" technique is the essence of both receivers.

4.1. The Switched-Mode Receiver

The switched-mode receiver (SMR) represents an elementary receiver using decisions to subtract out interference. Consider the receiver shown in Fig. 4.1 which uses a matched filter, $\rho^*(\omega)$,

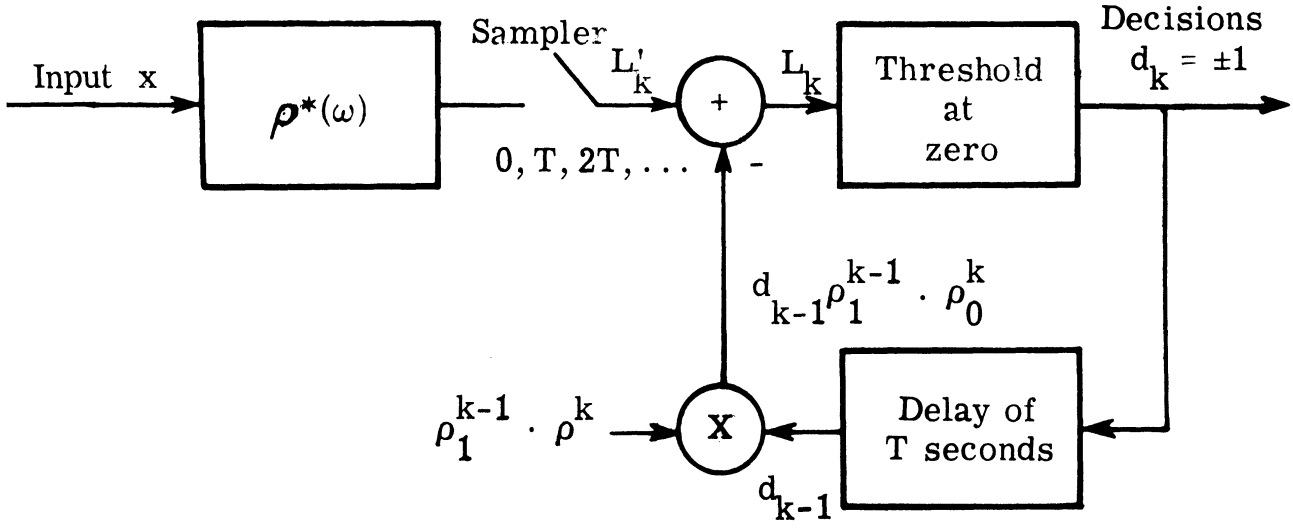

Fig. 4.1. Heuristic implementation of the switched-mode receiver

and a decision circuit containing memory. At time kT , the sampled output, L_k' , of the matched filter is

$$L_k' = b_{k-1}\rho_1^{k-1} \cdot \rho^k + b_k|\rho^k|^2 + b_{k+1}\rho_0^{k+1} \cdot \rho^k + n \cdot \rho^k \tag{4.1}$$

where we have used the notation introduced in Chapter III. The first and third terms in Equation 4.1 represent the intersymbol interference due to the $k\text{-}1^{th}$ and $k\text{+}1^{th}$ symbols; if they could be eliminated, the receiver performance would be that of an interference-free receiver.

Suppose that at time kT , the receiver has already made a decision d_{k-1} on the $(k\text{-}1)^{th}$ symbol. Form a new decision variable L_k , which is dependent on the previous decision d_{k-1} .

$$L_k = L_k' - d_{k-1}\rho_1^{k-1} \cdot \rho^k \tag{4.2}$$

$$= (b_{k-1} - d_{k-1})\rho_1^{k-1} \cdot \rho + b_k|\rho^k|^2 + b_{k+1}\rho_0^{k+1} \cdot \rho + n \cdot \rho^k \tag{4.3}$$

If the system is working with a low probability of error the first term in Equation 4.3 will be zero most of the time. Thus we have succeeded in forming a decision variable L_k in which there is less intersymbol interference than in L_k' . A receiver whose decision variable L_k is formed according to Equation 4.2, such as the receiver in Fig. 4.1 , is called

a switched-mode receiver (SMR). We note in passing that since $d_{k-1} = \pm 1$, L_k is not a linear function of the reception and, hence, the receiver is nonlinear.

The evaluation of the SMR's performance is straightforward. Let P_0 be the probability of error for the k^{th} symbol given that decision d_{k-1} is correct and let P_1 be the probability of error for the k^{th} symbol given that d_{k-1} is incorrect. Further let $P_e(k)$ be the probability of error for the k^{th} symbol. Then

$$P_e(k) = P_1 P_e(k - 1) + P_0(1 - P_e(k-1)) \tag{4.4}$$

If the k^{th} symbol is in the center of a long sequence of transmitted symbols, $P_e(k)$ is the average probability of error, P_e, for the system. Using

$$P_e(k) = P_e(k-1) = P_e \tag{4.5}$$

Equation 4.4 can then be solved for P_e

$$P_e = \frac{P_0}{1 - (P_1 - P_0)} \tag{4.6}$$

If there were no intersymbol interference, P_1 and P_0 would be equal and Equation 4.7 gives the probability of error for the optimum, interference free receiver. On the other hand, if intersymbol interference is severe, P_1 becomes much larger than P_0 and P_e increases

considerably over P_0.

We proceed in a general manner to compute the probabilities P_0 and P_1. Suppose that L_k is the output of the matched filter $\rho^*(\omega)$ with a constant term of the form $\alpha \rho_1^{k-1} \cdot \rho^k + \beta \rho^k \cdot \rho_0^{k+1}$ added.

$$L_k = \alpha \rho_1^{k-1} \cdot \rho^k + b_k \left|\rho^k\right|^2 + \beta \rho^k \cdot \rho_0^{k+1} + n \cdot \rho^k \qquad (4.7)$$

The distribution of L_k, $f(L_k \mid b_k, \alpha, \beta)$ is Gaussian since L_k consists of a zero mean Gaussian random variable, $n \cdot \rho^k$, plus a constant.

$$f(L_k \mid b_k, \alpha, \beta) = \phi\left[\frac{L_k - \left(\alpha \rho_1^{k-1} \cdot \rho^k + b_k \left|\rho^k\right|^2 + \beta \rho^k \cdot \rho_0^{k+1}\right)}{\left|\rho^k\right| \sqrt{N_0 / 2}}\right] \qquad (4.8)$$

Suppose that decisions are based on a comparison of L_k with zero in the usual manner. Then the probability of error $P_e(\alpha, \beta)$ is given by

$$P_e(\alpha, \beta) = \Phi\left[-\frac{\left|\rho^k\right|^2 + \alpha \rho_1^{k-1} \cdot \rho^k + \beta \rho_0^{k+1} \cdot \rho^k}{\left|\rho^k\right| \sqrt{N_0 / 2}}\right] \qquad (4.9)$$

Equation 4.9 can be written very simply in terms of the parameters d and r(T) introduced in the preceding chapter.

$$P_e(\alpha, \beta) = \Phi\left[-\sqrt{d}\left(1 + (\alpha + \beta) r(T)\right)\right] \qquad (4.10)$$

To determine P_0, the probability of error for the k^{th} symbol given that the decision d_{k-1} was correct, we use Equation 4.3

$$L_k = b_k \left|\rho^k\right|^2 + b_{k+1}\rho_0^{k+1} \cdot \rho^k + n \cdot \rho^k \qquad (4.11)$$

and

$$P_0 = \sum_{b_{k+1}=\pm 1} P(b_{k+1})\, P_e(b_{k+1}) \qquad (4.12)$$

$$P_0 = 1/2\ \Phi\left(-\sqrt{d}\,(1+r(T))\right) + 1/2\ \Phi\left(-\sqrt{d}\,(1-r(T))\right) \qquad (4.13)$$

Similarly, P_1, the probability of error for the k^{th} symbol given that the decision d_{k-1} was incorrect can be found. Under the condition that d_{k-1} is incorrect, L_k is given by

$$L_k = 2b_{k-1}\rho_1^{k-1} \cdot \rho^k + b_k\left|\rho^k\right|^2 + b_{k+1}\rho^k \cdot \rho_0^{k+1} + n \cdot \rho^k \qquad (4.14)$$

and

$$P_1 = \sum_{b_{k-1}b_{k+1}=\pm 1} P(b_{k-1}, b_{k+1})\, P_e(2b_{k-1}, b_{k+1}) \qquad (4.15)$$

$$P_1 = 1/4\left\{\Phi\left(-\sqrt{d}\left(1+3r(T)\right)\right) + \Phi\left(-\sqrt{d}\left(1+r(T)\right)\right)\right.$$
$$\left. + \Phi\left(-\sqrt{d}\left(1-r(T)\right)\right) + \Phi\left(-\sqrt{d}\left(1-3r(T)\right)\right)\right\} \tag{4.16}$$

As noted earlier as the intersymbol interference is reduced $(r(T) \to 0)$, P_1 approaches P_0; P_0 in turn approaches the probability of error for an interference free receiver.

The third section of this chapter compares the performance of the SMR with the various linear filter receivers.

The implementation of the SMR shown in Fig. 4.1 is certainly not the easiest one. Since the effect of the decision circuit is simply to bias L_k' one way or the other, the system is equivalent to one which has a variable threshold $\Gamma(d_{k-1})$ at time kT where

$$\Gamma(d_{k-1}) = d_{k-1}\rho_1^{k-1} \cdot \rho^k \tag{4.17}$$

$$= d_{k-1}R(T) \tag{4.18}$$

If a receiver gives a decision $d_k = +1$ if $L_k' \geq \Gamma(d_{k-1})$ and a decision $d_k = -1$ if $L_k' < \Gamma(d_{k-1})$, the decisions will be exactly the same as those of the SMR shown in Fig. 4.1. Figure 4.2 shows the simplified SMR. The fact that the threshold is switched by the preceding symbol decision in this realization gives the receiver its name.

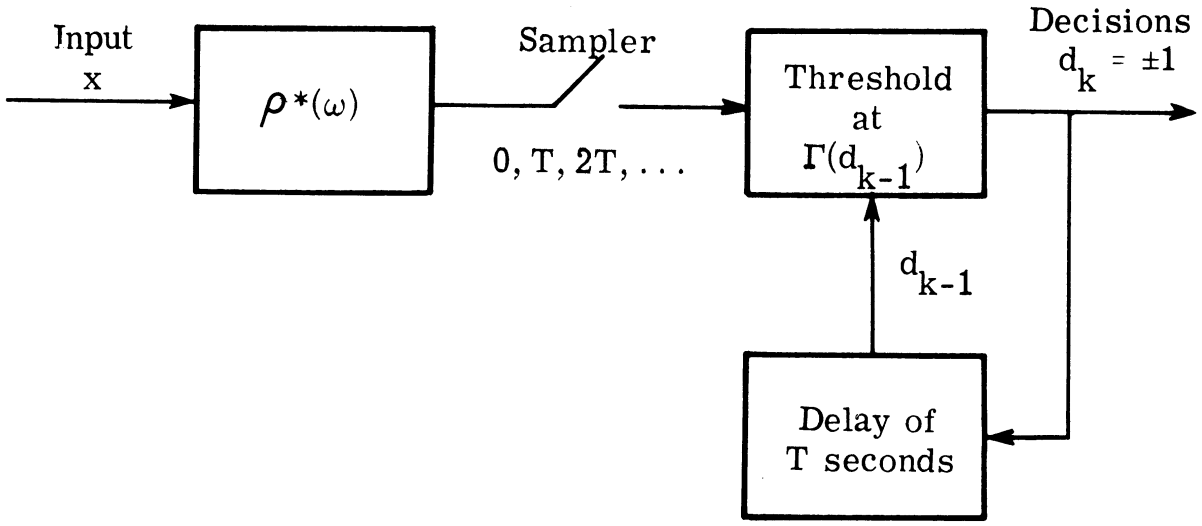

Fig. 4.2. Simplified implementation of the switched-mode receiver

4.2. Iterated Switched-Mode Receiver

Although the SMR discussed in Section 4.1 uses earlier decisions to try to eliminate the intersymbol interference of the preceding symbol it does nothing to eliminate the interference due to the subsequent symbol. At first this seems like an inherent limitation on a decision oriented receiver, since the decision on the $(k+1)^{th}$ symbol is to be made after the decision on the k^{th} symbol. This limitation is circumvented by making two decisions on each symbol: a "first guess" decision and a final decision. This idea of a double decision process is the foundation of the iterated switched-mode receiver (ISMR).

It is helpful to temporarily consider a complicated realization of the receiver before developing a simpler implementation. Suppose that the output L_k' of a matched filter, $\rho^*(\omega)$, is stored for all values of k, $0 \leq k \leq m$ during a transmission. Then for each k, L_k' is given by Equation 4.1. Let the "first guess" decisions d_k^o be made on the basis of a comparison of L_k' with a zero threshold in the usual manner. The decisions d_k^o are identical to those that would be made by a MFR under the same conditions. From Equation 3.46 the probability of error for the decisions d_k^o is

$$P_e^o = 1/4\ \Phi\left[-\sqrt{d}\left(1+2r(T)\right)\right] + 1/2\,\Phi(-\sqrt{d}) + 1/4\ \Phi\left[-\sqrt{d}\left(1-2r(T)\right)\right] \tag{4.19}$$

Given the stored matched filter outputs L_k' and the stored decisions d_k^o, subtract the interference from L_k' in a manner analogous to the SMR. Let

$$L_k = L_k' - d_{k-1}^o \rho_1^{k-1} \cdot \rho^k - d_{k+1}^o \rho_0^{k+1} \cdot \rho^k \tag{4.20}$$

$$= (b_{k-1} - d_{k-1}^o)\rho_1^{k-1} \cdot \rho^k + b_k \left|\rho^k\right|^2 + (b_{k+1} - d_{k+1}^o)\rho_0^{k+1} \cdot \rho^k + \rho^k \cdot n \tag{4.21}$$

If the decisions d_k^o have a low probability of error, the first and third terms in Equation 4.18 are zero most of the time and intersymbol

interference is eliminated from L_k. The final decisions d_k^1 of the ISMR are made by comparing L_k to zero. Since L_k is not a linear function of the reception, the ISMR is a nonlinear receiver.

We can determine the probability of error for the ISMR's final decisions easily. Let P_{00} be the probability that d_k^1 is in error given d_{k-1}^o and d_{k+1}^o are correct and let P_{11} be the probability that d_k^1 is in error given that d_{k+1}^o and d_{k-1}^o are incorrect. Further, let P_{01} be the probability that d_k^1 is in error given that exactly one of d_{k-1}^o, d_{k+1}^o is incorrect. Then the probability of error P_e^1 for decision d_k^1 is simply

$$P_e^1 = P_{00} P\left[d_{k-1}^o, d_{k+1}^o \text{ both correct}\right] + P_{01} P\left[\text{one of } d_{k-1}^o, d_{k+1}^o \text{ correct}\right] + P_{11} P\left[\text{both of } d_{k-1}^o, d_{k+1}^o \text{ incorrect}\right] \tag{4.22}$$

Decisions d_{k-1}^o and d_{k+1}^o are independent of each other since they are based on L'_{k-1} and L'_{k+1} which, in turn, correspond to disjoint time intervals. Thus Equation 4.22 can be written in terms of the "first guess" probability of error P_e^o as follows

$$P_e^1 = P_{00}(1-P_e^o)^2 + 2P_{01}(1-P_e^o)P_e^o + P_{11}(P_e^o)^2 \tag{4.23}$$

The probabilities P_{00}, P_{01}, and P_{11} are easily computed from Equation 4.21 under the appropriate condition and $P_e(\alpha, \beta)$ given by

Equation 4. 10.

$$P_{00} = P_e(0, 0) \tag{4.24}$$

$$= \Phi(-\sqrt{d}) \tag{4.25}$$

$$P_{01} = \sum_{b_{k+1} = \pm 1} P\left[b_{k+1}\right] P_e(0, 2b_{k+1}) \tag{4.26}$$

$$= 1/2\,\Phi\left(-\sqrt{d}\,(1+2r(T))\right) + 1/2\,\Phi\left(-\sqrt{d}\,(1-2r(T))\right) \tag{4.27}$$

$$P_{11} = \sum_{b_{k-1}, b_{k+1} = \pm 1} P\left[b_{k-1}, b_{k+1}\right] P_e(2b_{k-1}, 2b_{k+1}) \tag{4.28}$$

$$= 1/4\,\Phi\left(-\sqrt{d}\,(1+4r(T))\right) + 1/2\Phi(-\sqrt{d}) + 1/4\,\Phi\left(-\sqrt{d}\,(1-4r(T))\right) \tag{4.29}$$

The above probabilities can be substituted into Equation 4. 23 to give the probability of error for the ISMR.

The implementation suggested by the above discussion is unnecessarily complicated for practical applications. Just as in the SMR, the receiver can be considerably simplified by using a variable threshold $\Gamma(d^o_{k-1}, d^o_{k+1})$. Let

$$\Gamma(d^o_{k-1}, d^o_{k+1}) = d^o_{k-1}\rho_0^k \cdot \rho_1^{k-1} + d^o_{k+1}\rho_1^k \cdot \rho_0^{k-1} \qquad (4.30)$$

$$= R(T)\left[d^o_{k-1} + d^o_{k+1}\right] \qquad (4.31)$$

Then a receiver which compares L'_k to $\Gamma(d^o_{k-1}, d^o_{k+1})$ makes exactly the same decisions as the complicated implementation given earlier. Note that there are actually only 3 distinct values for $\Gamma(d^o_{k-1}, d^o_{k+1})$: $\pm$ 2R(T) and zero. Figure 4.3 depicts a possible implementation of the ISMR.

Before continuing to the comparison of the ISMR with other receivers in the next section, a word of caution about the ISMR is necessary. From the preceding discussion of the ISMR it seems reasonable to consider a multi-decision process in which an entire sequence of decisions $d^o_k \ldots d^i_k$ is made on each symbol in a logical extension of the ISMR procedure. The hope of such a procedure would be that the final probability of error P^i_e is reduced by making more preliminary decisions. Unfortunately this is not the case, as the interdependence of errors produced by more than two decisions in each symbol leads to an actual increase in error probability over that of the ISMR. Thus this logical extension of the ISMR procedure is of no avail.

4.3. Comparison with Linear Filter Receivers

This section compares the nonlinear SMR and ISMR with the linear filter receivers discussed in the preceding chapter. The

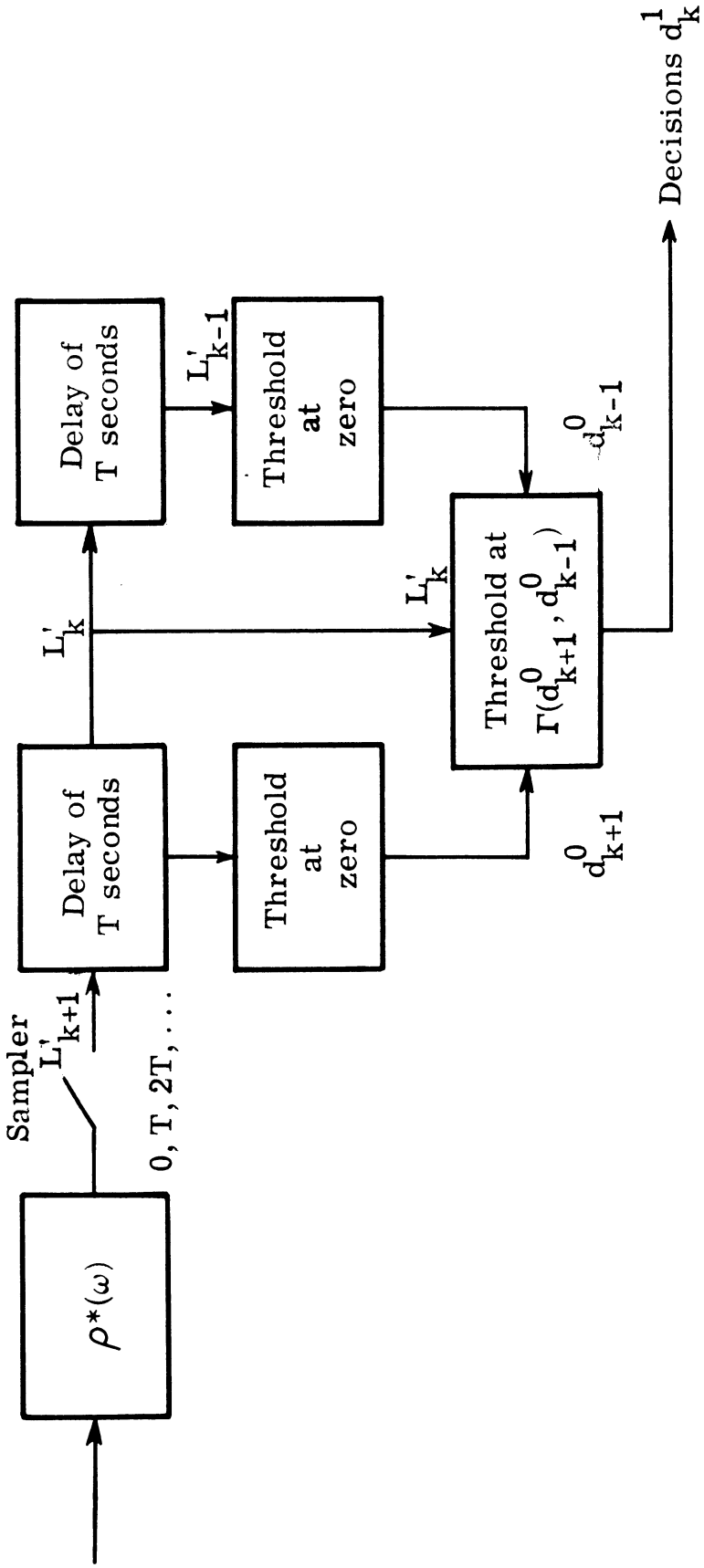

Fig. 4.3. An implementation of the ISMR

comparison is made taking into account the ease with which a receiver may be implemented.

Switched-Mode Receiver

Figure 4.4 depicts the probability of error for the SMR and the MFR, TFR and OLFR of the preceding section. In terms of error performance, the SMR is superior to the MFR for all $|r(T)|$ and is roughly comparable to the TFR and $OLFR_3$. The $OLFR_5$, the next more complicated optimized linear filter receiver, is noticeably superior to the SMR.

The SMR offers several distinct hardware advantages. First, the SMR requires only a single digital delay; i.e., a flip-flop, to remember d_{k-1}, whereas the TFR and OLFR receivers require an analog delay of at least $2T$ seconds. Second, the SMR has only a single variable, $\Gamma(d_{k-1})$ which must be adjusted whereas both the TFR and OLFR receivers require the adjustment of 2 or more tap coefficients. Finally, the single variable $\Gamma(d_{k-1})$ of the SMR is simply the autocorrelation of $\rho(t)$ evaluated at $t=T$. Both the TFR and OLFR require weighting coefficients which are relatively difficult to obtain.

From the above considerations, the SMR may be an acceptable substitute for either the TFR or $OLFR_3$ because of its ease of implementation. On the other hand, the SMR performance is noticeably worse than that of the more complicated $OLFR_5$. The SMR does appear to be an improvement over the simple MFR.

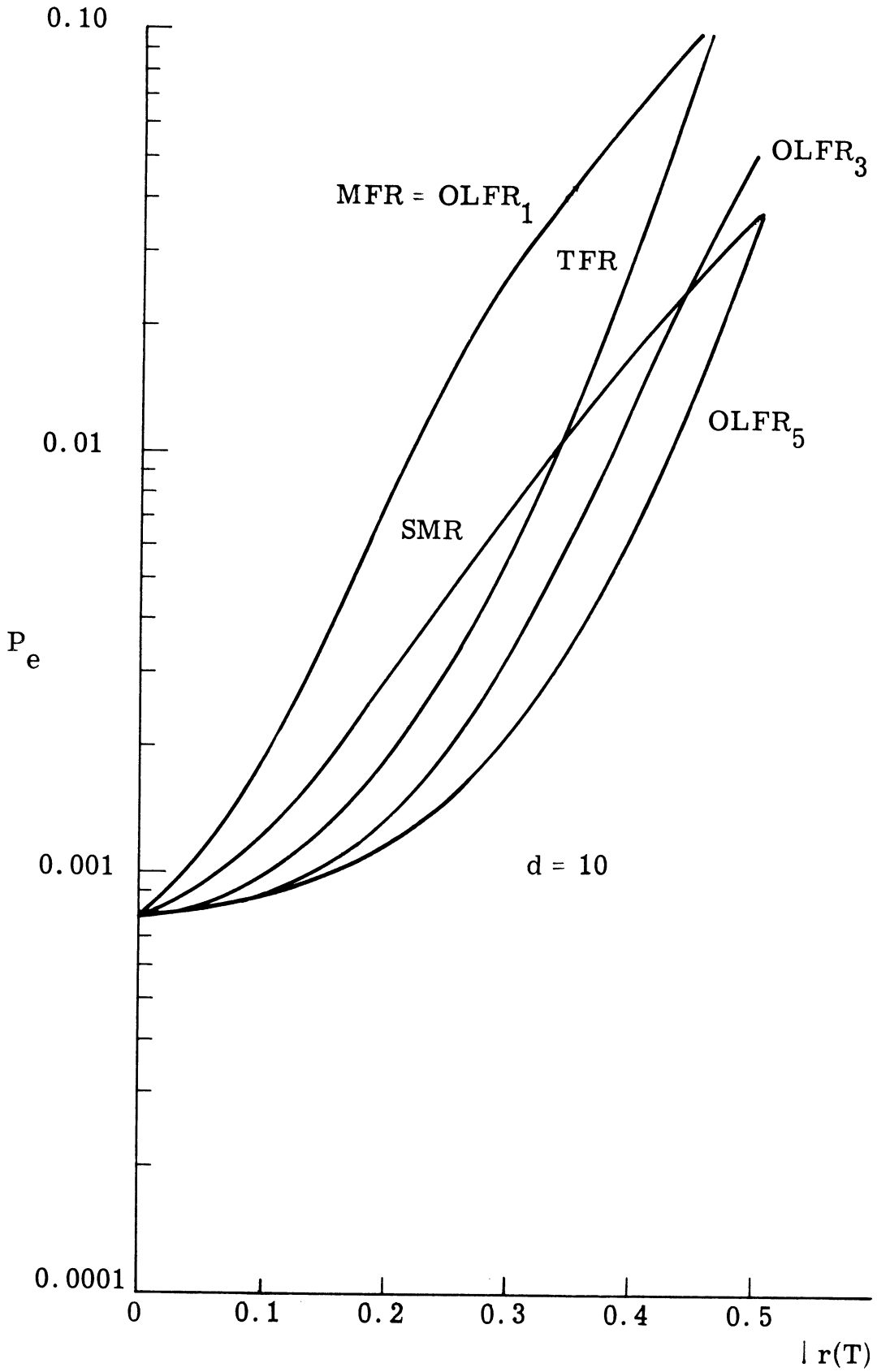

Fig. 4.4. Comparison of SMR with MFR, TFR, and $OLFR_{3,5}$

Iterated Switched-Mode Receiver

Figure 4.5 depicts the probability of error for the ISMR and the MFR, TFR and OLFR. The outstanding feature of this figure is that for $|r(T)| \leq .25$, the ISMR performs better than any linear receiver. For $|r(T)| > .25$, the ISMR performance is nearly that of the $OLFR_3$. By comparing Figs. 4.4 and 4.5, we see that the ISMR performance is superior to that of the SMR for $|r(T)| < .4$. Thus the ISMR is an excellent performer in moderate intersymbol interference and an acceptable performer under more severe conditions.

The ISMR shares with the SMR a significant ease of implementation. The ISMR can be implemented using one digital delay (i.e., flip-flop) and one analog delay of T seconds, which is easier to obtain than the long analog delays required by the TFR and OLFR. As with the SMR, only a single variable $\Gamma(d_{k-1}, d_{k+1})$ must be changed as $\rho(t)$ changes and this variable is easily computed from $\rho(t)$. The ISMR represents an increase in complexity over the SMR.

If a communication system is designed so that on the average, the intersymbol interference is only moderate, i.e., $|r(T)| \leq .25$, the ISMR is an excellent choice of receiver. Since larger amounts of intersymbol interference lead to considerable increases in the probability of error for any receiver, one might use $|r(T)| \leq .25$ as a reasonable restriction. Thus the ISMR is an important receiver in communications systems with intersymbol interference and noise.

As a final comparison, consider a system for the Mimi channel

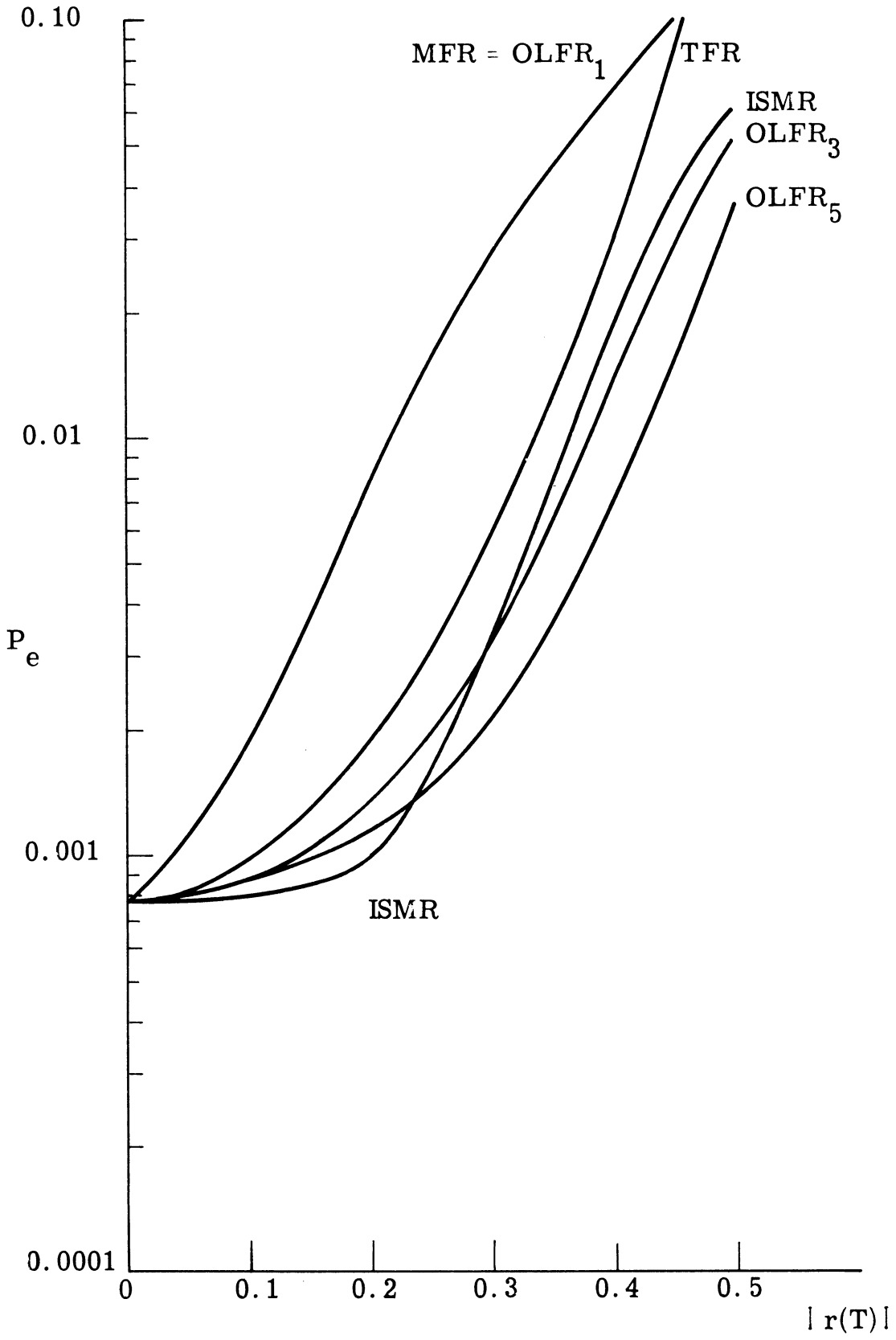

Fig. 4.5. Comparison of ISMR with MFR, TFR, and $OLFR_{3,5}$

shown in Figs. 1.2 and 1.3 which uses the 60-ms perfect word symbol shown in Figs. 2.10 and 2.11. When this symbol is transmitted through the Mimi channel, approximately 94% of the signal energy is within 2T = 120 ms for the phase-equalized received symbol, and hence the M = 1 assumption is valid. The value of r(T) found from the auto-correlation function of the received symbol is found to be -.2 .

Assuming a d of 10, which corresponds to a received S/N of approximately 3 in a 50 Hz band (+4.0 db), the probability of error for an interference-free receiver is .00078. For a simple MFR the probability of error is .0076, approximately 10 times that of the interference-free receiver; for a traditional TFR, the probability of error is .0019 or about two and a half times that of the interference-free receiver. In the same conditions the ISMR has a probability of error of only .00099. Table 4.1 gives these results.

Receiver	P_e	% increase in number of errors over interference free receiver
Interference Free	.000783	0
MFR	.007615	870
TFR	.001876	140
OLFR (3 tap)	.001332	70
(5 tap)	.001191	53
SMR	.002962	280
ISMR	.000993	27

Table 4.1. Results for system using Mimi channel (Fig. 1.2) and a 60 ms perfect word symbol (Fig. 2.10), d=10, r(t) = -.2

CHAPTER V

THE OPTIMUM (LIKELIHOOD RATIO) RECEIVER

Up to this point we have considered receivers which either represented reasonable approaches to the problem, such as the TFR or ISMR, or gave optimum system performance over a specified class, such as the OLFR. In so doing, we have neglected a well-known result from decision theory that states that optimum binary decisions (under any reasonable criteria) should be based on likelihood ratio. None of the receivers discussed so far base their decisions on likelihood ratio and, consequently, they are suboptimum in the absolute sense.*

The reason for the neglect of likelihood ratio in earlier receivers for the intersymbol interference in noise problem stems from the inherent difficulties of the general problem. By imposing the requirement of phase equalization and a unit degree of intersymbol interference ($M = 1$) analysis and evaluation are possible. Operating equations for the optimum receiver with $M > 1$ have been derived; however, the equations are quite complicated and offer no hope of evaluation. As mentioned in Chapter II, for reasonable signalling rates, the $M = 1$ assumption is acceptable and hence the results presented here have practical

---

*If there is no intersymbol interference ($|r(t)| = 0$), any of the linear filter receivers bases its decisions on likelihood ratio, as can be seen from classical detection theory.

importance.

Because of the difficulties inherent in implementing the optimum receiver, even for $M = 1$, the subsequent analysis is, in a sense, a mathematical exercise. Only in the most critical applications could the complexity of the optimum receiver be justified. The major benefit obtained from the analysis is the absolute bound on system performance which it gives and the method of operation it suggests. The lower bound on probability of error derived shows to what extent intersymbol interference is a fundamental problem and the optimum receiver's method of operation provides guidelines for the development of practical suboptimum receivers.

The following section reviews the concept of likelihood ratio and derives the operating equations for the optimum receiver. In the second section, the time symmetry produced by phase equalization is used to evaluate the receiver performance in a relatively simple manner. Finally the performance and operation of the optimum receiver is compared to the performance and operation of the receivers studied earlier.

5.1. Operation of the Receiver

This section reviews the basic concept of likelihood ratio which provides the basis for the optimum receiver's design. A convenient transformation of the likelihood ratio is introduced which allows sequential operation and analysis of the receiver. Using this transformation,

the operating equations for the receiver are derived.

Likelihood Ratio

Let x be the total reception, a waveform of duration $(m+2)T$ and let b_k be the value of the k^{th} symbol in x. In the reception x there are components of other symbols whose values are independent of b_k, and added white, Gaussian noise. The likelihood ratio of the reception x for the k^{th} symbol $l_k(x)$ is defined by

$$l_k(x) = \frac{p(x \mid b_k = +1)}{p(x \mid b_k = -1)} \tag{5.1}$$

where $p(x \mid b_k = \pm 1)$ is the conditional probability (or probability density) of the waveform x given that the k^{th} symbol has the specified value.* A major result from binary decision theory states that the likelihood ratio $l_k(x)$ (or any monotone function of it) is the best possible indication of the value of the k^{th} symbol. For the case in which the symbol values $b_k = \pm 1$ are equiprobable and in which both types of error are equally costly, as they are here, the classical theory requires that $l_k(x)$ be compared to a threshold of one. If $l_k(x)$ is greater than or equal to one, a $d_k = +1$ decision is made, if $l_k(x)$ is less than one, a $d_k = -1$ decision is made.**

*More elegant definitions of likelihood ratio are available but unnecessary for our analysis.

**The decision when $l_k(x)$ is equal to one is arbitrary, the decision indicated here is simply a convention.

The above results completely specify the optimum receiver, and from one theoretical point of view, the problem is solved. To provide useful results, however, a method of determining $l_k(x)$ from the reception x must be found. To do this conveniently, a sequential form of Equation 5.1 and the log odds ratio transformation will be introduced.

Let x_j be the portion of the reception in the time interval $(jT, (j+1)T)$ and let X_j be the portion of the reception in the interval $(0, jT)$. Note that $X_{m+2} = x$. Then from two forms of $P(b_k, x_j \mid X_j)$ we have

$$P(b_k \mid (X_j, x_j) = X_{j+1}) p(x_j \mid X_j) = P(b_k \mid X_j) p(x_j \mid b_k, X_j) \qquad (5.2)$$

Dividing Equation 5.2 with $b_k = +1$ by Equation 5.2 with $b_k = -1$ we obtain

$$\frac{P(b_k = +1 \mid X_{j+1})}{P(b_k = -1 \mid X_{j+1})} = \frac{P(b_k = +1 \mid X_j)}{P(b_k = -1 \mid X_j)} \frac{p(x_j \mid b_k = +1, X_j)}{p(x_j \mid b_k = -1, X_j)} \qquad (5.3)$$

Define the log odds ratio of the k^{th} symbol given X_j, L_k^j as

$$L_k^j = \ln \frac{P(b_k = +1 \mid X_j)}{P(b_k = -1 \mid X_j)} \qquad (5.4)$$

and the log likelihood ratio of x_j for the k^{th} symbol, as

$$\text{lnl}_k(x_j) = \ln \frac{p(x_j \mid b_k = +1, X_j)}{p(x_j \mid b_k = -1, X_j)} \tag{5.5}$$

Then Equation 5.3 becomes simply

$$L_k^j = L_k^{j-1} + \text{lnl}_k(x_j) \tag{5.6}$$

That is, the log odds ratio at time $j-1$ is updated to give the log odds ratio at time j using the log likelihood ratio. Figure 5.1 is helpful in visualizing the above results.

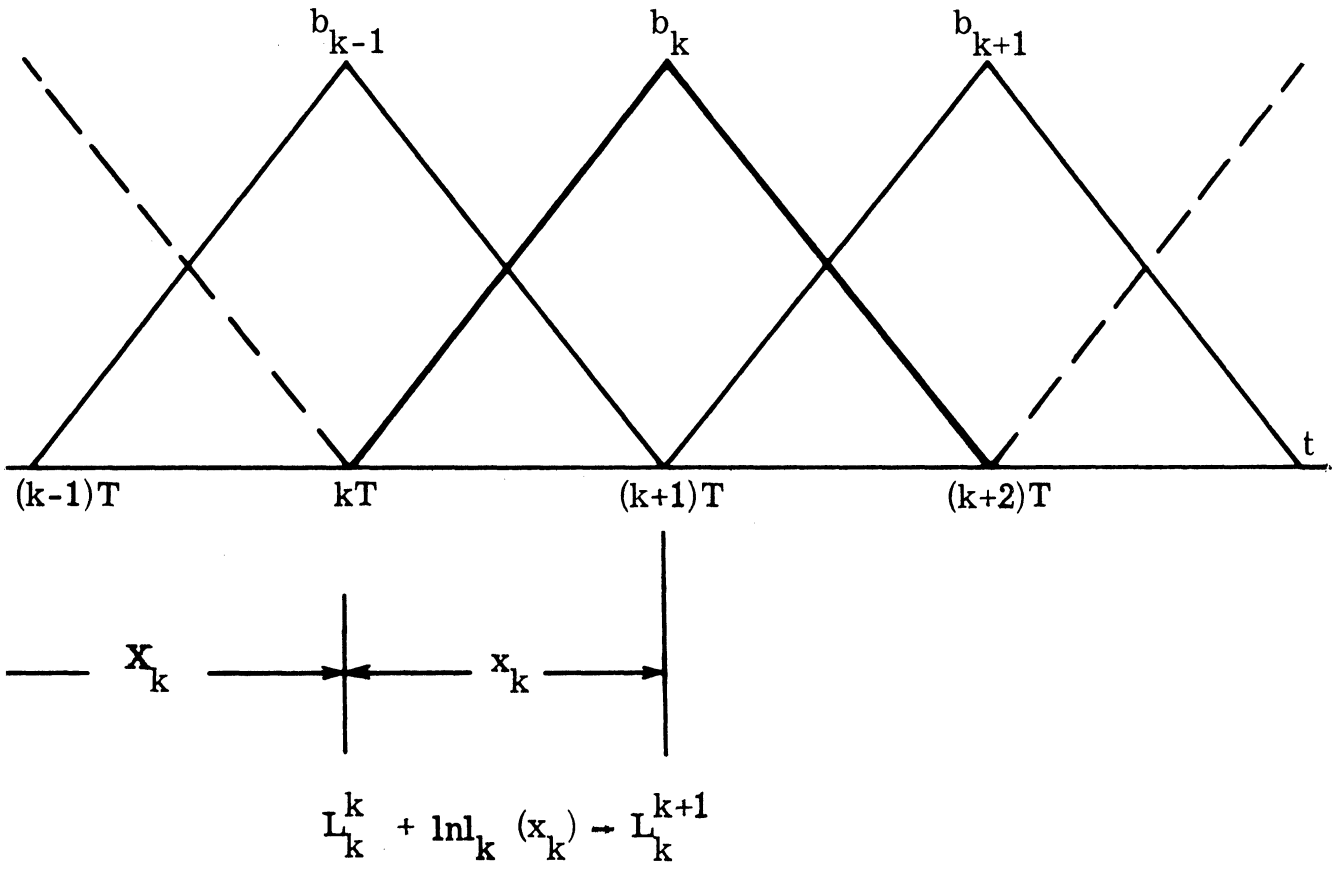

Fig. 5.1. Updating the log odds ratio L_k^j

We now show that for equiprobable symbols the log odds ratio after the entire transmission has been received, L_k^{m+2}, is identical with the log of the likelihood ratio of the observation $l_k(x)$. From two forms of $P(b_k, X_{m+2})$

$$P(b_k = \pm 1 \mid X_{m+2})p(X_{m+2}) = p(X_{m+2} \mid b_k = \pm 1)P(b_k = \pm 1) \qquad (5.7)$$

Divide Equation 5.7 with $b_k = +1$ by Equation 5.7 with $b_k = -1$ and take the logarithm

$$L_k^{m+2} = \ln l_k(x) + \ln \frac{P(b_k = +1)}{P(b_k = -1)} \qquad (5.8)$$

The last term is zero since the symbols are equiprobable. Thus in our work the log odds ratio L_k^j and the log likelihood ratio $\ln l_k(X_j)$ are the same. Since the log odds ratio is a monotone function of the likelihood ratio, we will base decisions directly on log odds ratio. It is easy to see that comparing the log odds ratio to zero (deciding $d_k = +1$ if $L_k^{m+2} \geq 0$ and $d_k = 1$ if $L_k^{m+2} < 0$) is equivalent to comparing the likelihood ratio to one in the manner described earlier.

It is easy to determine the probability of b_k given X_j from the log odds ratio L_k^j

$$P(b_k \mid X_j) = \frac{e^{.5(b_k+1)L_k^j}}{1+e^{L_k^j}} \qquad (5.9)$$

In subsequent work it will be convenient to use the symbols $L_k^j = \pm \infty$ to indicate that $P(b_k \mid X_j)$ takes on a value of one or zero; $L_k^j = +\infty$ signifies that $P(b_k = +1 \mid X_j) = 1$ and $P(b_k = -1 \mid X_j) = 0$.

Derivation of the Log Likelihood Ratio $lnl_k(x_j)$

The derivation of the log likelihood ratio $lnl_k(x_j)$ is quite tedious and the resulting equations are discouraging at best. Inspection of these equations indicates the enormous difficulty involved in implementing the optimum (likelihood ratio) receiver and, at first, evaluation of receiver performance seems impossible. As we will see in the second section of the chapter, evaluation of receiver performance is actually not too difficult. Thus the equations derived here are important not because one would try to implement them, but because they provide a basis for the evaluation of the optimum receiver's performance.

With the above comments well in mind, let us derive the equations for $lnl_k(x_j)$. As a convenience we consider four separate cases, $j < k$, $j = k$, $j = k+1$, $j > k+1$. The first case, with $j < k$ is the easiest since there is no energy corresponding to k^{th} symbol in either X_j or in x_j for $j < k$. Thus

$$lnl_k(x_j) = 0. \quad (j < k) \tag{5.10}$$

For the cases where $j \geq k$ expand $p(x_j \mid b_k = \pm 1, X_j)$ in terms of the four possible signals, determined by b_{j-1}, b_j, which are present

in the reception x_j. Let $b = (b_{j-1}, b_j)$, then

$$p(x_j \mid b_k, X_j) = \sum_{b_{j-1} b_j} P(b \mid b_k = \pm 1, X_j)\, p(x_j \mid b, b_k, X_j) \qquad (5.11)$$

Since the symbol values b_{j-1}, b_j are independent, the first factor in each term of Equation 5.11 can be written as a product. Further, $p(x_j \mid b, b_k = \pm 1\, X_j)$ is completely specified by b so that the last two conditions are superfluous. Then from Equations 5.5 and 5.11

$$\operatorname{lnl}_k(x_j) = \ln \frac{\sum_{b_{j-1} b_j} P(b_{j-1} \mid b_k = +1, X_j)\, P(b_j \mid b_k = +1, X_j)\, p(x_j \mid b)}{\sum_{b_{j-1} b_j} P(b_{j-1} \mid b_k = -1, X_j)\, P(b_j \mid b_k = -1, X_j)\, p(x_j \mid b)} \qquad (j \geq k) \qquad (5.12)$$

If $j = k \neq 0$, Equation 5.12 simplifies considerably since $P(b_j \mid b_k, X_j)$ is either one or zero and $P(b_{j-1} \mid b_k, X_j)$ is independent of b_k. The case where $j = k = 0$ will be treated later.

$$\operatorname{lnl}_k(x_j) = \ln \frac{\sum_{b_{j-1}} P(b_{j-1} \mid X_j)\, p(x_j \mid b_{j-1}, b_j = +1)}{\sum_{b_{j-1}} P(b_{j-1} \mid X_j)\, p(x_j \mid b_{j-1}, b_j = -1)} \qquad (j = k \neq 0) \qquad (5.13)$$

For $j > k$, Equation 5.12 also can be simplified. Since there is no energy corresponding to the j^{th} symbol in X_j, we have $p(b_j \mid b_k, X_j) = .5$. For $j = k+1$

$$\ln l_k(x_j) = \ln \frac{.5 \sum_{b_j} p(x_j \mid b_{j-1} = +1, b_j)}{.5 \sum_{b_j} p(x_j \mid b_{j-1} = -1, b_j)} \qquad (j = k+1) \qquad (5.14)$$

For $j > k + 1$, Equation 5.12 reduces to

$$\ln l_k(x_j) = \ln \frac{.5 \sum_{b_{j-1}} P(b_{j-1} \mid b_k = +1, X_j) \left\{ p(x_j \mid b_{j-1}, b_j = +1) + p(x_j \mid b_{j-1}, b_j = -1) \right\}}{.5 \sum_{b_{j-1}} P(b_{j-1} \mid b_k = -1, X_j) \left\{ p(x_j \mid b_{j-1}, b_j = +1) + p(x_j \mid b_{j-1}, b_j = -1) \right\}}$$

$$(j > k+1) \qquad (5.15)$$

Equations 5.10, 5.13, 5.14 and 5.15 give the equation for the log likelihood ratio in each of the four possible cases. We must now write the probabilities in these equations in terms of the reception, x_j.

The determination of the probabilities $p(x_j \mid b)$ in the preceding equations leads to some deep mathematical questions. These questions concern the representation of a waveform by a finite dimensional vector having independent components (Ref. 12). We avoid a lengthy discussion of this well-studied problem and merely state its result. That is,

$$p(x_j \mid b_{j-1}b_j) = Ke^{-\frac{1}{N_0}\left\{|x_j|^2 - 2x_j \cdot s_b + |s_b|^2\right\}} \tag{5.16}$$

where

$$s_b = b_{j-1}\rho_1^{j-1} + b_j\rho_0^j \tag{5.17}$$

and the dot product is the L^2 inner product used in Chapter III. The constant K is the normalizing constant. The result given by Equation 5.16 is valid under what is essentially a bandwidth limitation.*

Before proceeding further, we will normalize all waveforms in the problem by dividing by $\sqrt{N_0/2}$. Under this convention, Equation 5.16 becomes

$$p(x_j \mid b) = Ke^{-.5(|x_j|^2 - 2x_j \cdot s_b + |s_b|^2)} \tag{5.18}$$

which is a unit variance Gaussian density.

We can now determine the log likelihood ratio for each of the three remaining cases, through the use of Equations 5.9 and 5.18 and much manipulation. From Equation 5.13, we have for $j = k \neq 0$,**

---

*Equation 5.16 does not, however, require a Fourier series bandlimited assumption and hence does not lead to paradoxical results.

**Equation 5.19 is derived in Appendix B.

$$\ln l_k(x_j) = 2x_j \cdot \rho_0^j + \ln \frac{\cosh\left(\frac{L_{k-1}^k}{2} + \rho_1^{j-1} \cdot (x_j - \rho_0^j)\right)}{\cosh\left(\frac{L_{k-1}^k}{2} + \rho_1^{j-1} \cdot (x_j + \rho_0^j)\right)} \qquad (j=k\neq 0)$$

(5.19)

$$\triangleq G_0(x_j, L_{k-1}^k) \qquad (j=k\neq 0) \qquad (5.20)$$

Equation 5.19 can be checked very simply. Suppose that the value of the $k\text{-}1^{th}$ symbol is almost certain to be $b_{k-1} = +1, (-1)$ then L_{k-1}^k is of large magnitude and positive (negative) and the cosh functions approach an exponential. As the cosh functions approach exponential, the terms common to both their arguments cancel and we have

$$\lim_{L_{k-1}^k \to \pm\infty} \ln l_k(x_k) = 2\rho_0^j(x_j \mp \rho_1^{j-1}) \qquad (j=k\neq 0) \qquad (5.21)$$

This limiting form of $\ln l_k(x_k)$ is the same as if b_{k-1} were known exactly and the interference component $b_{k-1}\rho_1^{j-1}$ subtracted from x_j. The interference free difference is then correlated with the signal ρ_o^j as one would expect.

After some manipulation the log likelihood ratio for $j=k+1$ can

be found from Equation 5.14*

$$\ln l_k(x_j) = 2x_j \cdot \rho_1^{j-1} + \ln \frac{\cosh\left(\rho_0^j (x_j - \rho_1^{j-1})\right)}{\cosh\left(\rho_0^j (x_j + \rho_1^{j-1})\right)} \qquad (j=k+1) \qquad (5.22)$$

$$\triangleq G_1(x_j) \qquad (j=k+1) \qquad (5.23)$$

Equation 5.22 can also be readily checked. Suppose that $b_j = +1(-1)$ and that the component of x_j in the ρ_0^j direction is large and positive (negative). This is equivalent to saying that the symbol value b_j is pretty well known. Then Equation 5.22 becomes

$$\lim_{\rho_0^j \cdot x_j \to \pm\infty} \ln l_k(x_j) = 2\rho_1^{j-1}(x_j \mp \rho_0^j) \qquad (j=k+1) \qquad (5.24)$$

Thus the limiting form of $\ln l_k(x_{k+1})$ corresponds to the correlation of ρ_1^{j-1} with the reception x minus the "known" interference.

For $j > k+1$, no particularly convenient simplification of Equation 5.15 is possible. Define the conditional log odds ratio $L_{j-1}^{j}(b_k)$ as**

---

*Equation 5.22 is derived in Appendix B.

**Note that the symbol for the conditional log odds ratio $L_{j-1}^{j}(b_k)$ always has the condition in parenthesis, whereas the symbol for the (unconditional) log odds ratio L_{j-1}^{j} never contains parenthesis.

$$L_{j-1}^{j}(b_k) = \ln \frac{P(b_{j-1} = +1 \mid X_j, b_k)}{P(b_{j-1} = -1 \mid X_j, b_k)} \qquad (5.25)$$

Then Equation 5.15 becomes*

$$\text{lnl}_k(x_j) = .5\left(L_{j-1}^{j}(+1) - L_{j-1}^{j}(-1)\right) + \ln \frac{1+e^{L_{j-1}^{j}(-1)}}{1+e^{L_{j-1}^{j}(+1)}}$$

$$+ \ln \frac{e^{.5\left\{L_{j-1}^{j}(+1) + 2x_j \cdot \rho_0^j\right\}} \cosh(\rho_1^{j-1} \cdot (x_j - \rho_0^j)) + e^{-.5\left\{L_{j-1}^{j}(+1) + 2x_j \cdot \rho_0^j\right\}} \cosh(\rho_1^{j-1} \cdot (x_j + \rho_0^j))}{e^{.5\left\{L_{j-1}^{j}(-1) + 2x_j \cdot \rho_0^j\right\}} \cosh(\rho_1^{j-1} \cdot (x_j - \rho_0^j)) + e^{-.5\left\{L_{j-1}^{j}(-1) + 2x_j \cdot \rho_0^j\right\}} \cosh(\rho_1^{j-1} \cdot (x_j + \rho_0^j))}$$

$$(j > k+1) \qquad (5.26)$$

For convenience write

$$\text{lnl}_k(x_j) \triangleq G_2\left(x_j, L_{j-1}^{j}(+1), L_{j-1}^{j}(-1)\right) \qquad (j > k+1) \qquad (5.27)$$

We note in passing that $\text{lnl}_k(x_j)$ is zero for $j > k+1$ only if $L_{j-1}^{j}(+1) = L_{j-1}^{j}(-1)$. This means that $\text{lnl}_k(x_j)$ is zero only when a knowledge of

*Equation 5.26 is derived in Appendix B.

the k^{th} symbol would not affect the decision on $j\text{-}1^{th}$ symbol. One would expect as symbols $j-1$ and k are separated by increasing time amounts, $\text{lnl}_k(x_j)$ would become small.

Although Equations 5.10, 5.19, 5.22, and 5.26 give $\text{lnl}_k(x_j)$ for all four possible cases, in Equation 5.26 a new variable, the conditional log odds ratio was introduced. In order to determine $\text{lnl}_k(x_j)$ for $j > k+1$ we must also be able to determine $L^j_{j-1}(b_k)$. In a manner analogous to that used in deriving Equation 5.6

$$L^j_{j-1}(b_k) = L^{j-1}_{j-1}(b_k) + \text{lnl}_{j-1}(x_{j-1} \mid b_k) \tag{5.28}$$

where the conditional log likelihood ratio $\text{lnl}_{j-1}(x_{j-1} \mid b_k)$ is given by

$$\text{lnl}_{j-1}(x_{j-1} \mid b_k) = \ln \frac{p(x_{j-1} \mid b_{j-1} = +1, X_{j-1}, b_k)}{p(x_{j-1} \mid b_{j-1} = -1, X_{j-1}, b_k)} \tag{5.29}$$

Because no energy corresponding to the $j\text{-}1^{th}$ symbol is contained in X_{j-1}, $L^{j-1}_{j-1}(b_k)$ is always zero. Hence $L^j_{j-1}(b_k) = \text{lnl}_{j-1}(x_{j-1} \mid b_k)$.

The conditional log likelihood ratio $\text{lnl}_{j-1}(x_{j-1} \mid b_k)$ is derived in essentially the same manner as the unconditional log likelihood ratio given in Equation 5.19. We have

$$\text{lnl}_{j-1}(x_{j-1} \mid b_k) = G_0\left(x_{j-1}, L^{j-1}_{j-2}(b_k)\right) \quad (j \geq k+2) \tag{5.30}$$

If $j=k+2$, we interpret $L_{j-2}^{j-1}(b_k) = L_k^{k+1}(b_k)$ as having the singular value $b_k\infty$, that is, of very large magnitude and of the same sign as b_k. Thus we have from Equation 5.19

$$L_k^{k+1}(b_k = \pm 1) = 2\rho_0^{k+1}\cdot(x - b_k\rho_1^k) \tag{5.31}$$

Using the above equation as the starting point, we can derive $L_{j-1}^{j}(b_k)$ for all $j > k+1$ as required by Equation 5.26.

One small problem must be cleared up before discussing the operation of the receiver. This problem occurs at the very start of the decision process when $j=k=0$. Since there is no preceding symbol, we have

$$\ln l_0(x_0) = \ln \frac{p(x_0 \mid b_0 = +1)}{p(x_0 \mid b_0 = -1)} \qquad (j=k=0) \tag{5.32}$$

$$= 2x_0 \cdot \rho_0^0 \qquad (j=k=0) \tag{5.33}$$

$$\triangleq G_0'(x_0) \qquad (j=k=0) \tag{5.34}$$

which is the log likelihood ratio for an interference free reception, as x_0 certainly is.

The foregoing results are summarized in Table 5.1.

j	$\ln l_k(x_j)$	equation
$j < k$	0	5.10
$j = k = 0$	$G_0'(x_0)$	5.34
$j = k \neq 0$	$G_0(x_j, L_{k-1}^k)$	5.20
$j = k+1$	$G_1(x_j)$	5.23
$j > k+1$	$G_2\left(x_j, L_{j-1}^j(b_k = 1),\ L_{j-1}^j(b_k = -1)\right)$ where	5.27
$j = k+2, k+3, \ldots$	$L_{j-1}^j(b_k) = G_0\left(x_{j-1}, L_{j-2}^{j-1}(b_k)\right)$ $L_k^{k+1}(b_k) = b_k \infty$	5.30

Table 5.1. Equations for the log likelihood ratio $\ln l_k(x_j)$

Operation of the Receiver

The operation of the receiver is best understood by considering the operation relative to a single symbol, b_k, in the interior of the transmission. To go from this single symbol operation to a receiver which updates L_k^j for all symbols simultaneously is not difficult. Later we discuss the memory requirements for such a receiver.

Since L_k^j is zero for $j \leq k$

$$L_k^{k+1} = \text{lnl}_k(x_k) \tag{5.35}$$

$$= G_0(x_k, L_{k-1}^k) \tag{5.36}$$

The quantity L_{k-1}^k is required to perform this computation. The log odds ratio L_{k-1}^k can be computed inductively with

$$L_0^1 = G_0'(x_0) \tag{5.37}$$

$$L_i^{i+1} = G_0(x_i, L_{i-i}^i) \quad i = 1, 2, \ldots k-1 \tag{5.38}$$

From Equations 5.36 and 5.38 we note that L_{k-1}^k is dependent on X_k, the entire reception up to time kT.

Given L_k^{k+1} compute L_k^{k+2} by adding the log likelihood ratio $\text{lnl}_k(x_{k+1})$ to L_k^{k+1}.

$$L_k^{k+2} = L_k^{k+1} + G_1(x_{k+1}) \tag{5.39}$$

Then given L_k^{k+2} compute L_k^j for $j = k+3, k+4, \ldots m+2$ inductively

$$L_k^j = L_k^{j-1} + G_2\left(x_{j-1}, L_{j-2}^{j-1}(+1), L_{j-2}^{j-1}(-1)\right) \tag{5.40}$$

where

$$L_{j-2}^{j-1}(b_k) = G_0\left(x_{j-2}, L_{j-3}^{j-2}(b_k)\right) \tag{5.41}$$

$$L_k^{k+1}(b_k) = b_k \infty \tag{5.42}$$

Figure 5.2 depicts the process used to determine L_k^j. The decision d_k on the k^{th} symbol is made by comparing the log odds ratio L_k^{m+2} to zero in the usual way.

By operating in parallel many single symbol receivers of the form described above, decisions can be made for all of the transmitted symbols. It is easy to see that the memory requirements of such a receiver are enormous. At each stage j, the receiver must have in memory the updated log odds ratios $L_0^j \ldots L_{j-1}^j$ for the symbols which have been received up to this time. Furthermore, the receiver must also retain in memory the conditional log odds ratios $L_{j-1}^j(b_0) \ldots L_{j-1}^j(b_{j-2})$ so that the total memory requirement at time jT is $3j-2$ memory variables. This memory requirement and the great amounts of computation required, make this implementation of the optimum receiver economically infeasible (in 1968) for transmission lengths encountered in communications.

A natural compromise is to base decisions on only a portion of the reception. That is, to base the decision d_k on L_k^{k+q} $(q << m+1-k)$ instead of on L_k^{m+2}. Such an implementation requires $3q-2$ memory

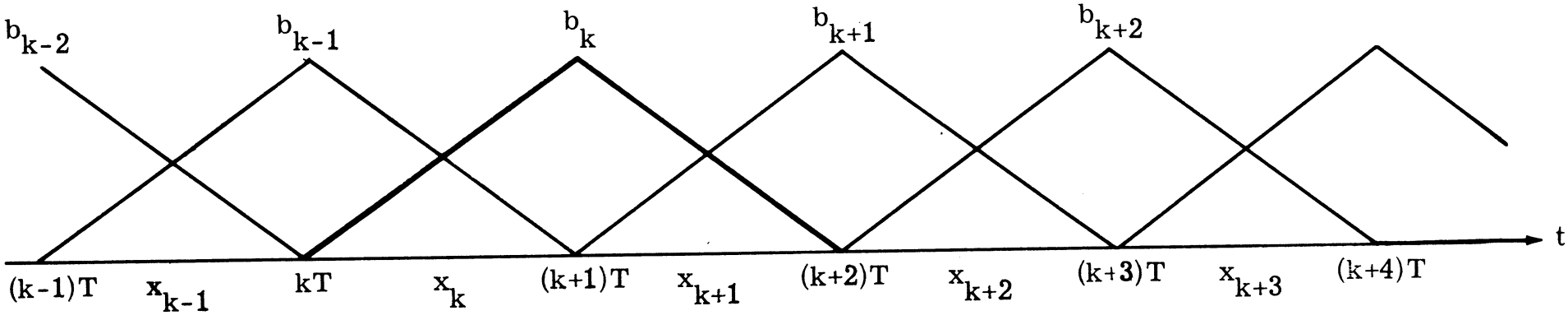

L_{k-1}^{k}

Log odds ratio $L_k^k = 0 \xrightarrow{G_0} L_k^{k+1} \xrightarrow{G_1} L_k^{k+2} \xrightarrow{G_2} L_k^{k+3} \xrightarrow{G_2} L_k^{k+4}$

$L_k^{k+1}(b_k = 1) \xrightarrow{G_0} L_{k+1}^{k+2}(b_k = +1) \xrightarrow{G_0} L_{k+2}^{k+3}(b_k = -1) \xrightarrow{G_0} L_{k+3}^{k+4}(b_k = +1)$

$= +\infty$

Conditional Log odds ratios $L_k^{k+1}(b_k = -1) \xrightarrow{G_0} L_{k+1}^{k+2}(b_k = -1) \xrightarrow{G_0} L_{k+2}^{k+3}(b_k = -1) \xrightarrow{G_0} L_{k+3}^{k+4}(b_k = -1)$

$= -\infty$

Fig. 5.2. Procedure used to determine L_k^J during observation

locations to process a reception of any length and gives the optimum decisions based on the truncated reception X_{k+q}. Receivers of this type are called truncated observation optimum receivers (TOOR). Figure 5.3 depicts the operation of a TOOR with $q=3$. The author expects that the difference in performance between the optimum receiver and a TOOR with $q \sim 3$ would be very slight. Even with the reduced memory requirement, implementation of a TOOR would be justified only in very critical applications because of the computations needed.

In Section 5.2 one method of operation for the optimum (likelihood ratio) receiver in which the number of computations is greatly reduced will be described. Unfortunately, this method has an even greater memory requirement than the optimum receiver described above.

We note in passing that each computation of $\ln l_k(x_j)$ requires the quantities $x_j \cdot \rho_1^{j-1}$ and $x_j \cdot \rho_0^j$. These quantities can be obtained as the output of filters matched to ρ_1^{j-1} and ρ_0^j respectively. Because the optimum receiver does not correlate the reception with the noise-free symbol ρ^j, it is essential that the optimum receiver be preceded by a phase-equalizing filter in order for the above results to be valid. This is in contrast with linear filter receivers in which the first element in the canonical form is a filter matched to ρ^j, making previous phase equalization unnecessary. Thus the optimum receiver has the additional disadvantage of requiring a separate phase-equalizing filter.

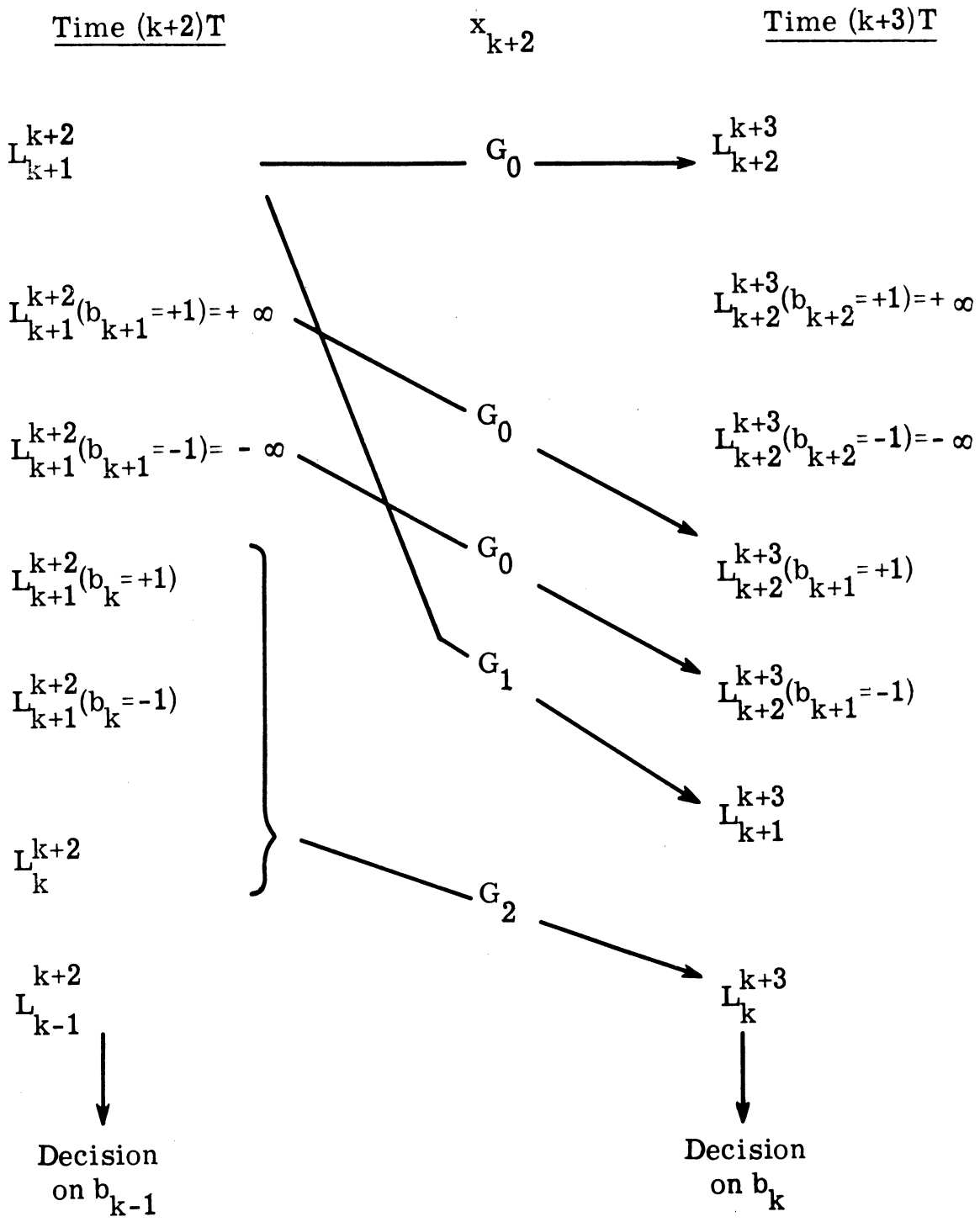

Fig. 5.3. Updating process used by TOOR (q = 3)

Insights

The notation associated with the operating equations given above obscures the basic nature of the receiver's operation. To better understand what the receiver really does consider the following explicit equation for L_k^{m+2} .

$$L_k^{m+2} = \ln \left\{ \frac{\cosh\left(\frac{L_{k-1}^{k}}{2} + \rho_1^{k-1} \cdot (x_k - \rho_0^k)\right)}{\cosh\left(\frac{L_{k-1}^{k}}{2} + \rho_1^{k-1} \cdot (x_k + \rho_0^k)\right)} \right\} \qquad \text{Term A}$$

$$+ 2x_k \cdot \rho_0^k + 2x_{k+1}\rho_1^k \qquad \text{Term B}$$

$$+ \ln \left\{ \frac{\cosh\left(\rho_0^{k+1} \cdot (x_{k+1} - \rho_1^k)\right)}{\cosh\left(\rho_0^{k+1} \cdot (x_{k+1} + \rho_1^k)\right)} \right\} + \sum_{j=k+2}^{j=m+1} \ln l_k(x_j) \qquad \text{Term C}$$

(5.43)

Term B in the above equation is recognized as simply the correlation of the reception (x_k, x_{k+1}) containing k^{th} symbol with the noise-free symbol ρ^k . In the absence of intersymbol interference, the log odds ratio from classical detection theory is given by Term B.

The effects of Terms A and C can best be understood by considering their limiting values as L_{k-1} and $\rho_0^{k+1} \cdot x_{k+1}$ become large in magnitude. Neglecting the second term in Term C, we have from Equations 5.21 and 5.24

$$\lim_{\substack{L_{k-1}^{k} \to b_{k-1}\infty \\ \rho_0^{k+1} \cdot x_{k+1} \to b_{k+1}\infty}} L_k^{m+2} = 2\rho_0^k \cdot (x - b_{k-1}\rho_1^{k-1}) + 2\rho_1^k \cdot (x - b_{k+1}\rho_0^{k+1}) \tag{5.44}$$

As the value of b_{k-1} becomes better known, $\left|L_{k-1}^{k}\right| \to \infty$, and as the component of x_{k+1} in the ρ_0^{k+1} direction becomes large, the receiver subtracts the "known" interference from the reception and correlates the result with the noise-free received symbol. Terms A and C serve to subtract components due to the interfering symbols from the decision variable L_k^{m+2}.

The notion of "subtracting out" interference components is, of course, the fundamental idea behind the nonlinear ISMR. In the ISMR, however, the amount subtracted can take on only one of three possible values. The optimum receiver, on the other hand, subtracts a continuous valued amount which depends, in a nonlinear manner, on the entire reception. Except for this difference, the operations of the optimum receiver and the ISMR are similar.

5.2. Evaluation of the Optimum Receiver

At first glance, evaluation of the optimum receiver's performance appears virtually impossible. By looking at the problem in a different way, however, the evaluation can be done quite easily. This section describes a method of evaluating the receiver's performance exactly on a digital computer. This method of evaluation also provides insight into the operation of the optimum receiver and suggests another possible implementation.

The objective of evaluation is to determine the probability of error for a single symbol located interior to a long sequence of transmitted symbols. If the number of transmitted symbols, $m+1$, is very large, as we have assumed, this probability of error will be the system probability of error P_e. Since the decision d_k is based on L_k^{m+2} we must determine

$$P_e = P(L_k^{m+2} < 0 \mid b_k = +1) \tag{5.45}$$

$$= \int_{-\infty}^{0} p(L_k^{m+2} \mid b_k = +1)\, dL_k^{m+2} \tag{5.46}$$

The major problem of evaluation is to determine the density function $p(L_k^{m+2} \mid b_k = +1)$ of the decision variable L_k^{m+2} when $b_k = +1$.

Determination of $p(L_k^{m+2} \mid b_k = +1)$

The preceding section gave a sequential method of computing

L_k^{m+2} starting with x_0 and working along in time until time $(m+2)T$. The computation of L_k^{m+2} is not dependent on which direction in time the sequential operation proceeds. It is also possible to start with x_{m+1} and work backwards in time until time 0.

Let $\tilde{X}_j$ be the portion of the reception in the interval $(jT,(m+2)T)$. The total reception x is equivalent to the pair $\tilde{X}_j$ and X_j as shown in Fig. 5.4. Define the reverse log odds ratio $\tilde{L}_k^j$ as simply

$$\tilde{L}_k^j = \ln \frac{P(b_k = +1 \mid \tilde{X}_j)}{P(b_k = -1 \mid \tilde{X}_j)} \tag{5.47}$$

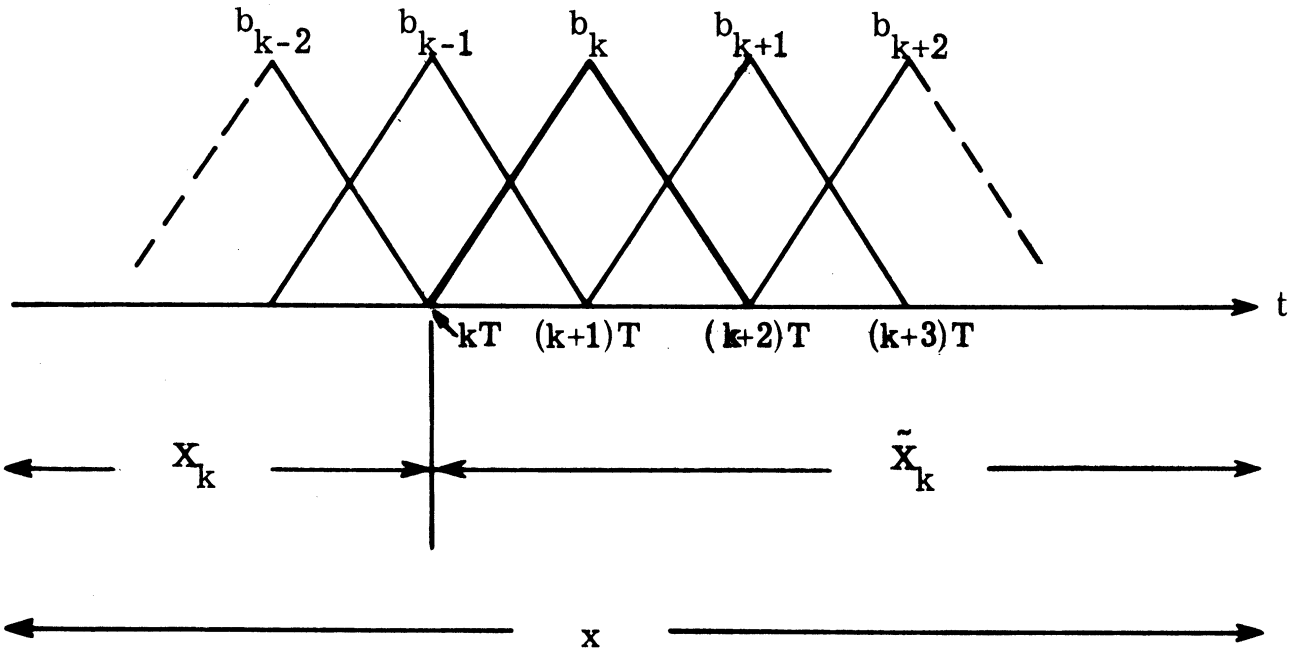

Fig. 5.4. Division of the reception x into X_k and $\tilde{X}_k$

From the discussion of the preceding paragraph,

$$L_k^{m+2} = \tilde{L}_k^0 \tag{5.48}$$

Reiterating, the log odds ratio for the k^{th} symbol given the entire reception does not depend on whether it was obtained by a forward operating receiver or a backward operating receiver.

Suppose that we conceptually "burn the candle at both ends" by operating in the forward direction to obtain L_k^{k+1} and then operating in the reverse direction to obtain $\tilde{L}_k^{k+1}$. We will now show that

$$L_k^{m+2} = L_k^{k+1} + \tilde{L}_k^{k+1} \tag{5.49}$$

and that given the value of b_k, L_k^{k+1} and $\tilde{L}_k^{k+1}$ are independent random variables.

From Equation 5.8,

$$L_k^{m+2} = \ln \frac{P(x \mid b_k = +1)}{P(x \mid b_k = -1)} \tag{5.50}$$

$$= \ln \frac{p(X_{k+1} \mid b_k = +1)\, p(\tilde{X}_{k+1} \mid X_{k+1}, b_k = +1)}{p(X_{k+1} \mid b_k = -1)\, p(\tilde{X}_{k+1} \mid X_{k+1}, b_k = -1)} \tag{5.51}$$

The only component that X_{k+1} and $\tilde{X}_{k+1}$ have in common is the waveform due to the k^{th} symbol, since the noise is independent from interval

to interval. Hence the condition on b_k makes the condition X_{k+1} unnecessary,

$$p(\tilde{X}_{k+1} | X_{k+1}, b_k) = p(\tilde{X}_{k+1} | b_k) \tag{5.52}$$

Substituting Equation 5.52 into Equation 5.51

$$L_k^{m+2} = \ln \frac{p(X_{k+1} | b_k = +1)}{p(X_{k+1} | b_k = -1)} + \ln \frac{p(\tilde{X}_{k+1} | b_k = +1)}{p(\tilde{X}_{k+1} | b_k = -1)} \tag{5.53}$$

$$= L_k^{k+1} + \tilde{L}_k^{k+1} \tag{5.54}$$

Whenever the value b_k of the k^{th} symbol is given L_k^{k+1} and $\tilde{L}_k^{k+1}$ are statistically independent since their only common component is specified.

Let us now continue our effort to determine $p(L_k^{m+2} | b_k = +1)$. Under the condition that $b_k = +1$, L_k^{k+1} and $\tilde{L}_k^{k+1}$ are independent random variables. Since L_k^{m+2} is the sum of two independent random variables, L_k^{k+1} and $\tilde{L}_k^{k+1}$, the desired density function of L_k^{m+2} is the convolution of the densities $p(L_k^{k+1} | b_k = +1)$ and $p(\tilde{L}_k^{k+1} | b_k = +1)$

$$p(L_k^{m+2} | b_k = +1) = p(L_k^{k+1} | b_k = +1) \circledast p(\tilde{L}_k^{k+1} | b_k = +1) \tag{5.55}$$

We can go another step further. If the k^{th} symbol is located in the

interior of a long sequence of symbols, the densities $p(L_k^{k+1} \mid b_k = +1)$ and $p(\tilde{L}_k^{k+1} \mid b_k = +1)$ will be the same because of the time symmetry (about time $(k+1)T$) produced by phase equalization.* That is,

$$p(L_k^{k+1} \mid b_k = +1) = p(\tilde{L}_k^{k+1} \mid b_k = +1) \tag{5.56}$$

and thus Equation 5.55 can be written

$$p(L_k^{m+2} \mid b_k = +1) = p(L_k^{k+1} \mid b_k = +1) \circledast p(L_k^{k+1} \mid b_k = +1) \tag{5.57}$$

The distribution $p(L_k^{k+1} \mid b_k = +1)$ is relatively easy to obtain, as we shall see.

From Equation 5.20,

$$L_k^{k+1} = G_0(x_k, L_{k-1}^k) \tag{5.58}$$

which is a mapping from the random variables representing the reception, $x \cdot \rho_1^{k-1}$ and $x \cdot \rho_0^k$ and the random variable L_{k-1}^k into a new random variable L_k^{k+1}. Let us suppose that the distribution of L_k^{k+1} conditional to L_{k-1}^k, $p(L_k^{k+1} \mid L_{k-1}^k, b_k = +1)$, is known. Later in this section we will derive an equation for this distribution.

$$p(L_k^{k+1} \mid b_k = +1) = \int_{-\infty}^{+\infty} p(L_k^{k+1} \mid L_{k-1}^k, b_k = +1)\, p(L_{k-1}^k \mid b_k = +1)\, d\, L_{k-1}^k \tag{5.59}$$

---

*Of course, the random variables L_k^{k+1} and $\tilde{L}_k^{k+1}$ themselves will generally be different.

Since there is no energy corresponding to the k^{th} symbol in the portion of the reception from which L_{k-1}^{k} is computed

$$p(L_{k-1}^{k} \mid b_k = +1) = p(L_{k-1}^{k}) \tag{5.60}$$

$$= \frac{1}{2}\left\{ p(L_{k-1}^{k} \mid b_{k-1} = +1) + p(L_{k-1}^{k} \mid b_{k-1} = -1)\right\} \tag{5.61}$$

Because of the symmetry of the problem

$$p(L_{k-1}^{k} \mid b_{k-1} = -1) = p(-L_{k-1}^{k} \mid b_{k-1} = +1) \tag{5.62}$$

From Equations 5.60, 5.62 and 5.63,

$$p(L_{k}^{k+1} \mid b_k = +1) = \int_{-\infty}^{+\infty} p(L_{k}^{k+1} \mid L_{k-1}^{k},\ b_k = +1) \left\{ \frac{p(L_{k-1}^{k} \mid b_{k-1} = +1) + p(-L_{k-1}^{k} \mid b_{k-1} = +1)}{2} \right\} d\, L_{k-1}^{k} \tag{5.63}$$

From $p(L_0^1 \mid b_0 = +1)$ we can compute $p(L_k^{k+1} \mid b_k = +1)$ iteratively and then convolve $p(L_k^{k+1} \mid b_k = +1)$ with itself to obtain $p(L_k^{m+2} \mid b_k = +1)$. The system probability of error P_e can then be found from Equation 5.46.

Intuitively one would expect that for sufficiently large k, that

$p(L_k^{k+1} \mid b_k = +1)$ is stationary. That is,

$$p(L_k^{k+1} \mid b_k = +1) = p(L_{k-1}^{k} \mid b_{k-1} = +1) \tag{5.64}$$

Under this condition, then, Equation 5.63 becomes

$$p(L_k^{k+1} \mid b_k = +1) = \int_{-\infty}^{+\infty} p(L_k^{k+1} \mid L_{k-1}^{k}, b_k = +1) \left\{ \frac{p(L_k^{k+1} \mid b_k = +1) + p(-L_k^{k+1} \mid b_k = +1)}{2} \right\} d L_{k-1}^{k} \tag{5.65}$$

which can be reduced to a homogeneous Fredholm equation of the second kind. Although the integral equation for $p(L_k^{k+1} \mid b_k = +1)$ is interesting from a mathematical point of view, it is much easier to apply the inductive procedure on Equation 5.63 to obtain $p(L_k^{k+1} \mid b_k = +1)$. The result of this inductive procedure is the solution to the above integral equation and the solution is obtained with 2 or 3 iterations.

To initialize the induction process $p(L_0^1 \mid b_0 = +1)$ is needed. From Equation 5.33,

$$L_0^1 = 2x_0 \cdot \rho_0^0 \tag{5.66}$$

L_0^1 is the output of a linear filter matched to ρ_0. From either the discussion of Section 3.1 or classical detection theory

$$p(L_0^1 \mid b_k = +1) = \phi(L_0^1 - \sqrt{d/2^1}) \tag{5.67}$$

where $\phi(u)$ is the zero mean, unit variance Gaussian density function. This is the initializing distribution $p(L_0^1 \mid b_k = +1)$ for Equation 5.63 .

Determination of $p(L_k^{k+1} \mid L_{k-1}^k, b_k = +1)$

Let us now determine the conditional density function, $p(L_k^{k+1} \mid L_{k-1}^k, b_k = +1)$. Although the derivation is long, it provides insight into the operation of the receiver.

Let the reception x_k be represented in terms of its components in the plane of the signal vectors ρ_0^k and ρ_1^{k-1} . Since $L_k^{k+1} = \ln l_k(x_k)$ depends only on the inner product of x_k with ρ_0^k and ρ_1^k this representation is adequate. Define the orthonormal axes $\hat{u}_0$ and $\hat{u}_1$ as

$$\hat{u}_0 = \rho_0^k / \lvert \rho_0^k \rvert \tag{5.68}$$

$$\hat{u}_1 = \frac{\rho_1^{k-1} - (\rho_1^{k-1} \cdot \hat{u}_0)\hat{u}_0}{\left| \rho_1^{k-1} - (\rho_1^{k-1} \cdot \hat{u}_0)\hat{u}_0 \right|} \tag{5.69}$$

and let

$$\rho'_{ij} = \rho_i^{k-i} \cdot \hat{u}_j \qquad \begin{matrix} i = 0, 1 \\ j = 0, 1 \end{matrix} \tag{5.70}$$

be the component of the ρ_i^{k-i} signal vector in the $\hat{u}_j$ direction. Then we can represent the projection $\bar{x}_k$ of the reception x_k onto the plane defined by $\hat{u}_0$, $\hat{u}_1$. Let x_k^0 be the component of $\bar{x}_k$ in the u_0 direction and let x_k^1 be the component of $\bar{x}_k$ in the u_1 direction, so that

$$\bar{x}_k = x_k^0 \hat{u}_0 + x_k^1 \hat{u}_1 \tag{5.71}$$

Figure 5.5 depicts the above relations for $b_k = +1$.

In terms of the real world quantities d and r(T) from Chapter III,

$$\rho'_{00} = \sqrt{d/2} \tag{5.72}$$

$$= \rho'_{10}{}^2 + \rho'_{11}{}^2 \tag{5.73}$$

Similarly,

$$\rho_0^k \cdot \rho_1^{k-1} = \rho'_{00}\rho'_{10} \tag{5.74}$$

$$= r(T)\, d \tag{5.75}$$

Thus the signal components are completely specified by the quantities d and r(T) as in the receivers considered earlier.

We now determine $p(x_k^0, x_k^1 \mid L_{k-1}^k, b_k = +1)$. Given b_{k-1}, b_k the distribution of (x_k^0, x_k^1) is bivariate normal with unit variance (because of the normalization of all waveforms by dividing by $\sqrt{N_0/2}$) and

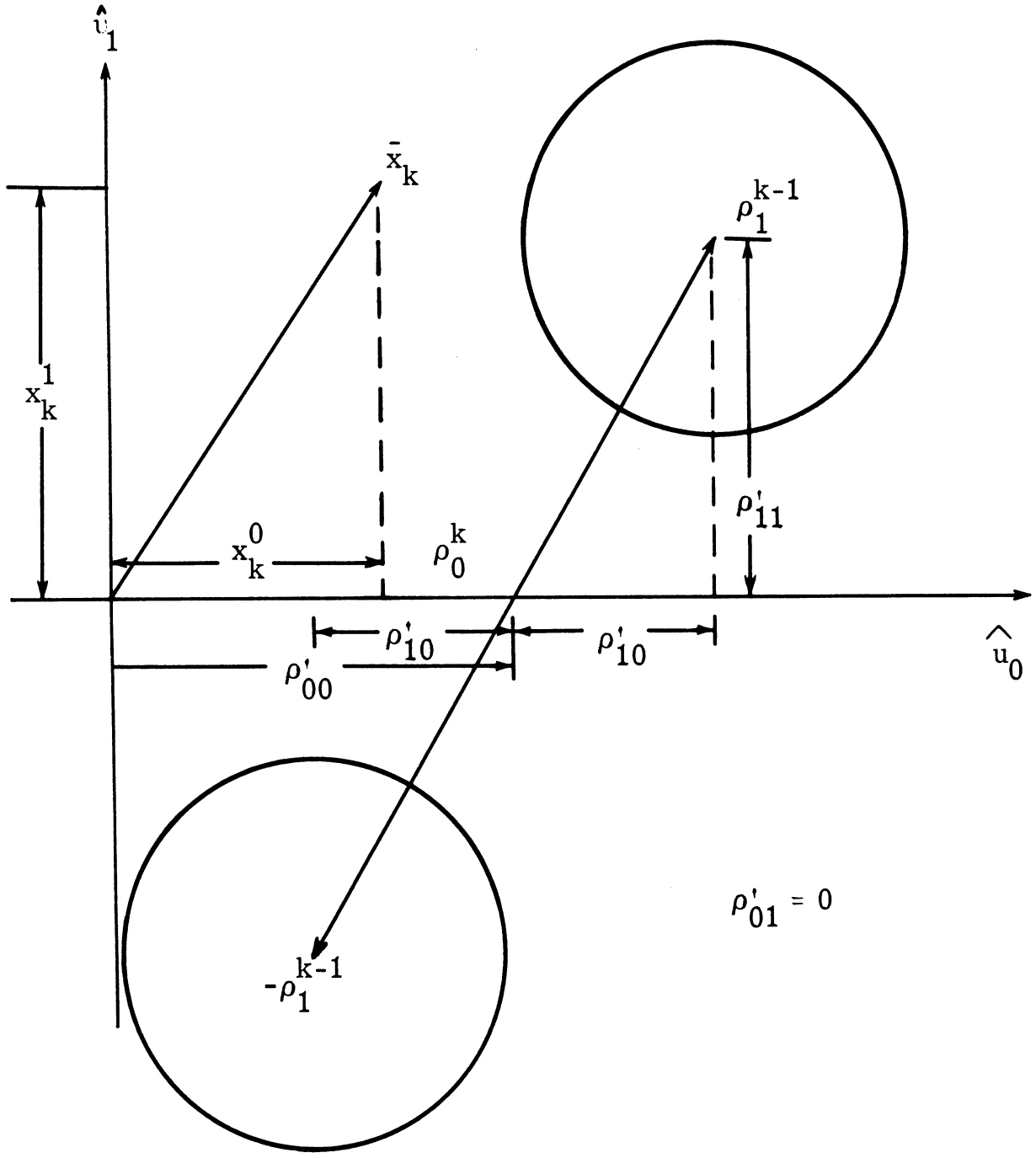

Fig. 5.5. Representation of x_k in the plane defined by $\hat{u}_0$, $\hat{u}_1$

mean $b_k \rho_0^k + b_{k-1} \rho_1^{k-1}$. Because the axes $\hat{u}_0$, $\hat{u}_1$ are orthogonal, the components of the reception x_k^0 , x_k^1 are independent and

$$p\left(\bar{x}_k = (x_k^0, x_k^1) \middle| b_{k-1}\, b_k\right) = \phi\left(x_k^0 - (b_k \rho'_{00} + b_{k-1} \rho'_{10})\right) \phi\left(x_k^1 - b_{k-1} \rho'_{11}\right) \tag{5.76}$$

The density $p(x_k^0, x_k^1 \,|\, L_{k-1}^k, b_k = +1)$ is then a weighted (by L_{k-1}^k) sum of the above densities. Using Equation 5.9, we have

$$p(\bar{x}_k \,|\, L_{k-1}^k, b_k = +1) = \sum_{b_{k-1}} P(b_{k-1} \,|\, L_{k-1}^k)\, p(\bar{x}_k \,|\, b_{k-1}, b_k = +1) \tag{5.77}$$

$$= \frac{1}{1 + e^{L_{k-1}^k}} \left\{ \phi\left(x_k^0 - (\rho'_{00} + \rho'_{10})\right) \phi\left(x_k^1 - \rho'_{11}\right) e^{L_{k-1}^k} \right.$$

$$\left. + \phi\left(x_k^0 - (\rho'_{00} - \rho'_{10})\right) \phi\left(x_k^1 + \rho'_{11}\right) \right\} \tag{5.78}$$

Thus the density function for the vector $\bar{x}_k$ consists of two bivariate Gaussian "hills" of generally unequal height as indicated by circles in Fig. 5.5.

From Equation 5.20,

$$L_k^{k+1} = G_0\left((x_k^0, x_k^1), L_{k-1}^k\right) \tag{5.79}$$

which, when L_{k-1}^{k} is fixed, is a mapping from the two random variables x_k^0, x_k^1 into a single random variable, L_k^{k+1}. Letting x_k^0 be the auxiliary variable, one can show by the usual procedure that

$$p(L_k^{k+1} \mid L_{k-1}^{k}, b_k = +1)$$

$$= \int \frac{p\left(x_k^0, x_k^1 = G_0^{-1}(x_k^0, L_{k-1}^{k}, L_k^{k+1}) \mid L_{k-1}^{k}, b_k = +1\right)}{J(x_k^0, x_k^1)} \, dx_k^0 \tag{5.80}$$

where G_0^{-1} is the inverse (given L_{k-1}^{k} and L_k^{k+1}) of the G_0 mapping and $J(x_k^0, x_k^1)$ is the Jacobian associated with G_0. The limits of the above integral can be found by inspection of the G_0^{-1} mapping, as will soon be seen.

By studying the function G_0^{-1} we can gain insight into the operation of the receiver. After considerable manipulation of Equation 5.19 we obtain*

$$G_0^{-1}(x_k^0, L_{k-1}^{k}, L_k^{k+1}) = \frac{1}{2\rho'_{11}} \left\{ - L_{k-1}^{k} - 2\rho'_{10} x_k^0 + \ln \frac{\sinh\left[\rho'_{00}\rho'_{10} - \frac{L_k^{k+1}}{2} - x_k^0 \rho'_{00}\right]}{\sinh\left[\rho'_{00}\rho'_{10} + \frac{L_k^{k+1}}{2} - x_k^0 \rho'_{00}\right]} \right\} \tag{5.81}$$

*Equation 5.81 is derived in Appendix B.

$$G_0^{-1}(x_k^0, L_{k-1}^k, L_k^{k+1}) = x_k^1 \tag{5.82}$$

One can show that x_k^1 is defined only in the interval $\frac{1}{\rho'_{00}}\left\{\frac{L_k^{k+1}}{2} - \rho'_{00}\rho'_{10}\right\} < x_k^0 < \frac{1}{\rho'_{00}}\left\{\frac{L_k^{k+1}}{2} + \rho'_{00}\,\rho'_{10}\right\}$ which are the limits of integration for the integral in Equation 5.80. Similarly, one can show that

$$\lim_{x_k^0 \to \frac{1}{\rho'_{00}}\left\{\frac{L_k^{k+1}}{2} \pm \rho'_{00}\,\rho'_{10}\right\}} x_k^1 = \pm\,\infty \tag{5.83}$$

The curve, $\gamma(L_{k-1}^k, L_k^{k+1})$, of x_k^1 versus x_k^0 for fixed L_{k-1}^k and L_k^{k+1} is S shaped and has an inflection point at

$x_k^0 = \frac{L_k^{k+1}}{2}$, $x_k^1 = \left(-L_{k-1}^k - L_k^{k+1}\,\rho'_{10}\right)$. Figure 5.6 depicts $\gamma(L_{k-1}^k, L_k^{k+1})$ for selected values of L_{k-1}^k, L_k^{k+1}.

One may interpret Equation 5.80 as the integral of the density function of $\bar{x}_k$ along the line $\gamma(L_{k-1}^k, L_k^{k+1})$. As L_{k-1}^k becomes large in magnitude and with sign given by b_{k-1}, $\gamma(L_{k-1}^k, L_k^{k+1})$ is effectively a vertical line at $x_k^0 = \left\{\frac{1}{\rho'_{00}}\left[\frac{L_k^{k+1}}{2} + b_{k-1}\,\rho'_{00}\,\rho'_{10}\right]\right\}$. Evaluating

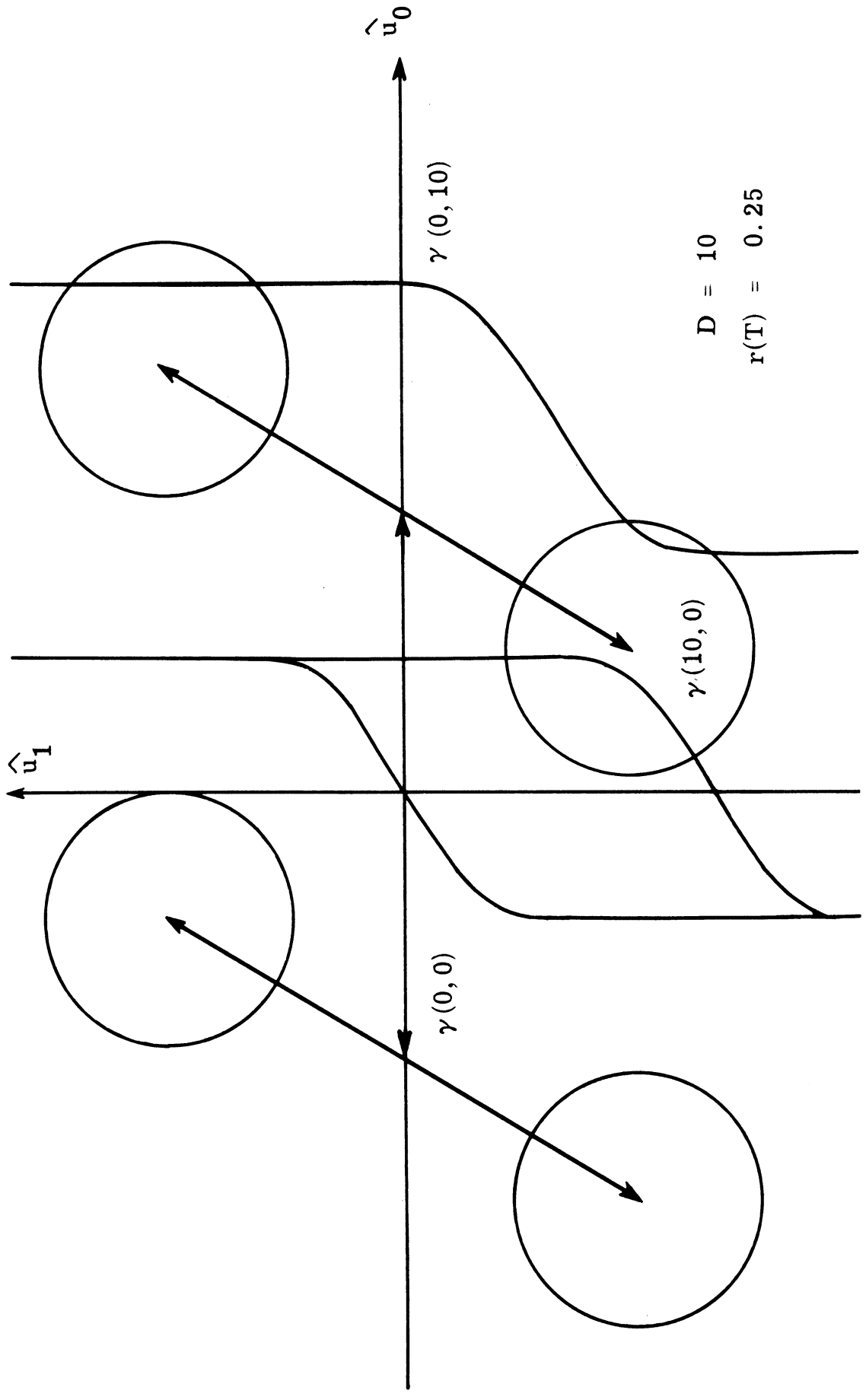

Fig. 5.6. Plot of $\gamma(L_{k-1}^{k}, L_{k}^{k+1})$ for r(T) = .25, d = 10

Equation 5.80 along this line gives

$$p(L_k^{k+1} \mid L_{k-1}^{k}, b_k = +1) \cong p\left(x_k^0 = \frac{1}{\rho'_{00}}\left\{\frac{L_k^{k+1}}{2} + b_{k-1}\rho'_{00}\rho'_{10}\right\} \mid b_{k-1}, b_k = +1\right)$$

$$* \int_{-\infty}^{+\infty} \frac{p(x_k^1 \mid b_{k-1}\, b_k = +1)}{J(x_k^0, x_k^1)} \left|\frac{d\, x_k^0}{d\, x_k^1}\right| d\, x_k^1$$

(5.84)

$$\cong p(L_k^{k+1} \mid b_{k-1}, b_k = +1) \qquad (5.85)$$

Thus as the magnitude of L_{k-1}^{k} becomes large, $p(L_k^{k+1} \mid L_{k-1}^{k}, b_k = +1)$ approaches the distribution on L_k^{k+1} which would be obtained if b_{k-1} were actually known.

Numerical Evaluation of the Optimum Receiver

The foregoing equations for the evaluation of the optimum receiver are readily implemented numerically. This subsection briefly summarizes the numerical methods used to obtain the results presented in the next section and gives selected examples of the density functions involved in the computations.

The conditional density function $p(L_k^{k+1} \mid L_{k-1}^{k}, b_k = +1)$ was

determined by performing the integration indicated in Equation 5.80. To speed up the integration process different techniques were used on the central and asymptotic portions of the $\gamma(L_{k-1}^{k}, L_{k}^{k+1})$ curve. In addition, the cases where $|r(T)| = 0$ or $|r(T)| > .49$ were treated separately due to the peculiar form of $\gamma(L_{k-1}^{k}, L_{k}^{k+1})$ involved in these cases. The resulting density functions resemble slightly distorted Gaussian densities as shown in Fig. 5.7 for $d = 10$, $|r(T)| = .5$.

To determine the density $p(L_k^{k+1} | b_k = +1)$, the initial density function $p(L_0^1 | b_k = +1)$ (Equation 5.67) was represented by its values taken at 40 equally spaced points on the real line. A matrix of 1600 entries corresponding to $p(L_k^{k+1} | L_{k-1}^{k}, b_k = +1)$ taken over the same points was computed. Then the iterative process given by Equation 5.63 was performed five times, with the density $p(L_k^{k+1} | b_k = +1)$ apparently converging to its stationary value, the solution of the integral Equation 5.65, in two or three iterations. Figure 5.8 depicts $p(L_k^{k+1} | b_k = +1)$ for $k=0, 1, 2, 3$ with $d=10$, $r(T) = .5$, a relatively slowly converging case.*

After the determination of $p(L_k | b_k = +1)$ by the above procedure, the density was convolved with itself to obtain $p(L_k^{m+2} | b_k = +1)$. Figure 5.9 depicts $p(L_k^{m+2} | b_k = +1)$ for $|r(T)| = .0, .1, .2, .3, .4, .5$, $d = 10$. A simple integration of $p(L_k^{m+2} | b_k = +1)$ according to

---

*The rapid convergence of $p(L_k | b_k = +1)$ suggests that the performance of a TOOR with $q = 3$ probably is very close to that of the optimum receiver.

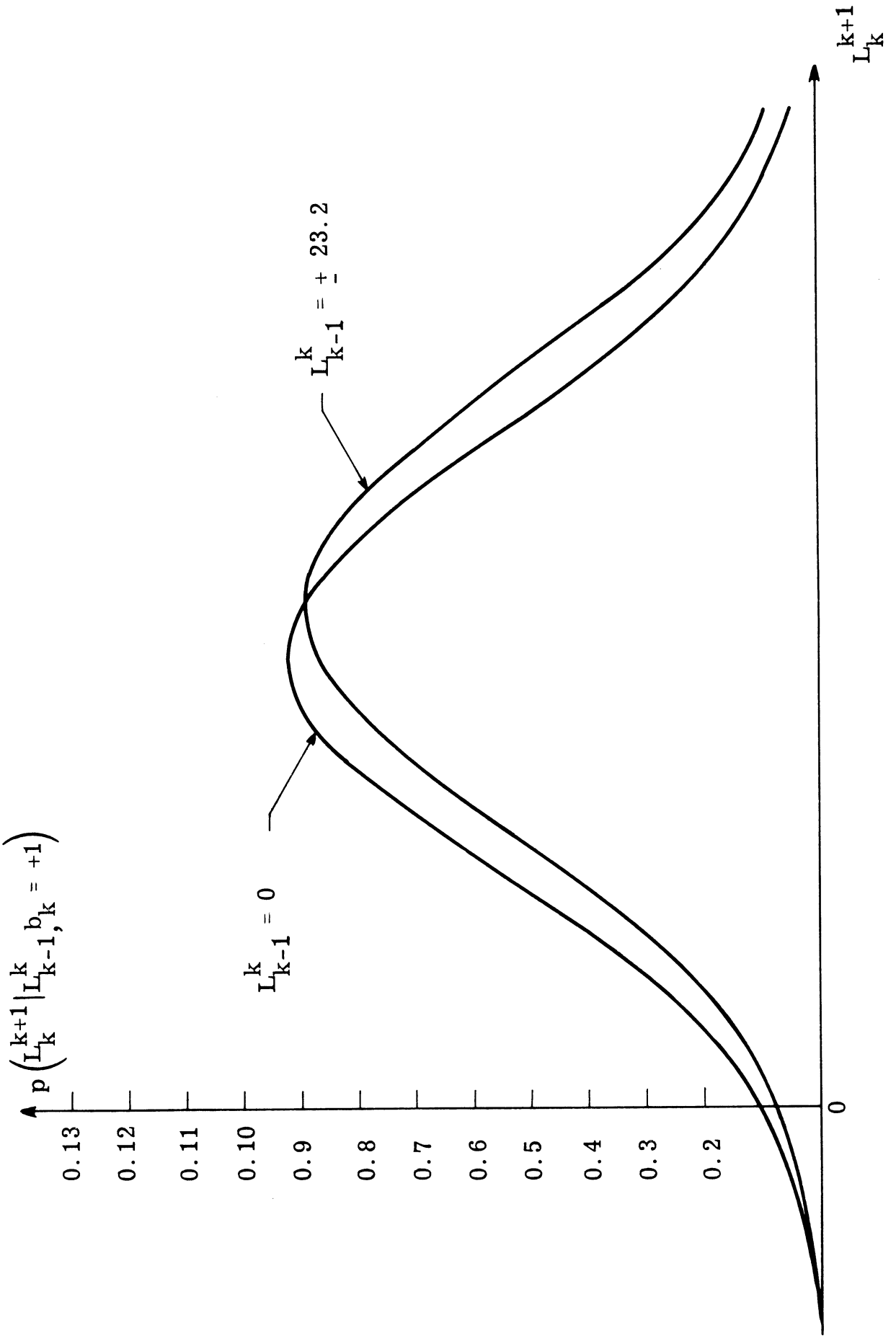

Fig. 5.7. Plot of $p(L_k^{k+1} | L_{k-1}^k b_k = +1)$ for $|r(T)| = .25$, d = 10

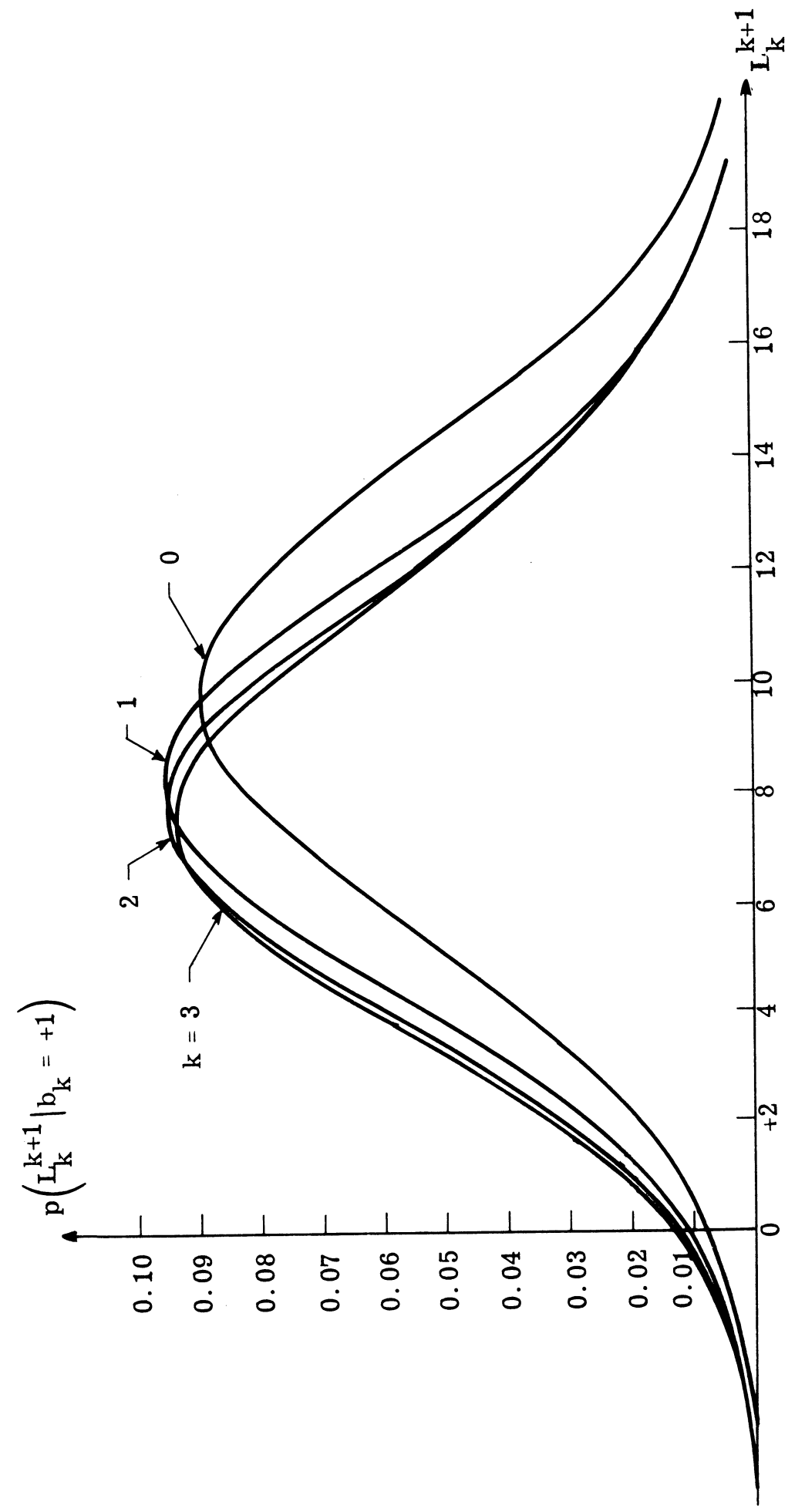

Fig. 5.8. Plot of $p(L_k^{k+1} \mid b_k = 1)$ $k = 0, 1, 2, 3$; $|r(T)| = .5$; $d = 10$

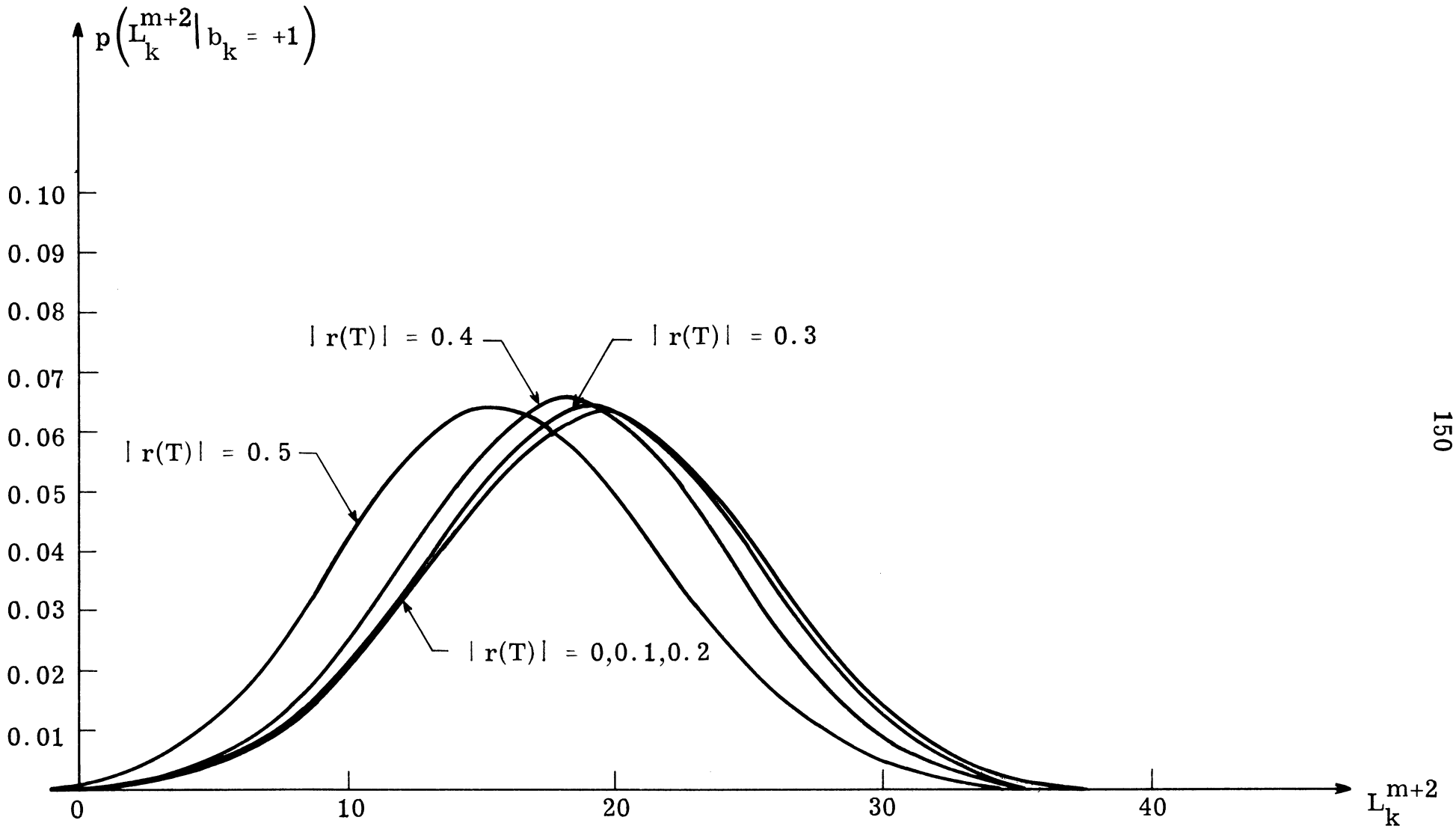

Fig. 5.9. Plot of $p(L_k^{m+2} \mid b_k = +1)$ for $|r(T)| = .0, .1, .2, .3, .4, .5$, $d = 10$

Equation 5.46 gives P_e. Representation of the density functions by 60 points instead of 40 showed no significant changes in any of the results. Because of the relatively small number of points used in the representation, no attempt to analyze receiver performance for values of d greater than 20 ($P_e < .000004$) has been made.

Two-Pass Implementation of the Optimum Receiver

The method of evaluation for the optimum receiver has the added advantage of suggesting what is perhaps the easiest implementation of the receiver. This implementation requires that the entire reception be stored and two separate analyses (passes) of the data are made. Although this implementation has a large memory requirement and does not allow real time analysis of the data, the operations performed by the receiver are relatively simple. The performance of this implementation is identical with that of the "one-pass" implementation given in Section 5.1.

Let us consider a heuristic implementation of the two-pass optimum receiver in which the reception x is stored on a long magnetic tape. On the first pass the receiver computes the log odds ratio L_k^{k+1} through Equation 5.19 and records the result on a separate channel of the magnetic tape. During the second pass the receiver computes the reverse log odds ratios $\tilde{L}_k^{k+1}$ using exactly the same procedure as used on the first pass and adds the result to the recorded value L_k^{k+1} to obtain L_k^{m+2}. The receiver's decision d_k is then based on L_k^{m+2}.

Figure 5.10 depicts this implementation of the two-pass processor.

5.3. Comparison of Optimum and Suboptimum Receivers

A major objective of the analysis and evaluation of the optimum (likelihood ratio) receiver was to provide an absolute basis for comparison for the suboptimum receivers. This section compares the error performance of four suboptimum receivers with the optimum receiver and each other.

For the sake of clarity only four of the suboptimum receivers have been selected for comparison: MFR, TFR, ISMR and $OLFR_7$. Each of these receivers is representative of one approach to the intersymbol interference in noise problem. The MFR and TFR were chosen because they represent the approaches which neglect either the intersymbol interference (MFR) or the noise (TFR). The $OLFR_7$ represents very closely the best possible linear filter receiver which could be used. The ISMR was selected as a good example of an easily implemented nonlinear receiver.

The results presented here are for values of signal detectability index d in the range from 5 to 15. The error probabilities for an ideal interference-free receiver operating with signal detectabilities in this range go from .012 to .00005. The lower limit was chosen because it corresponds to what seems to be the highest probability of error one might tolerate in a communication system. The upper limit was selected because it represents a high signal-to-noise ratio case and

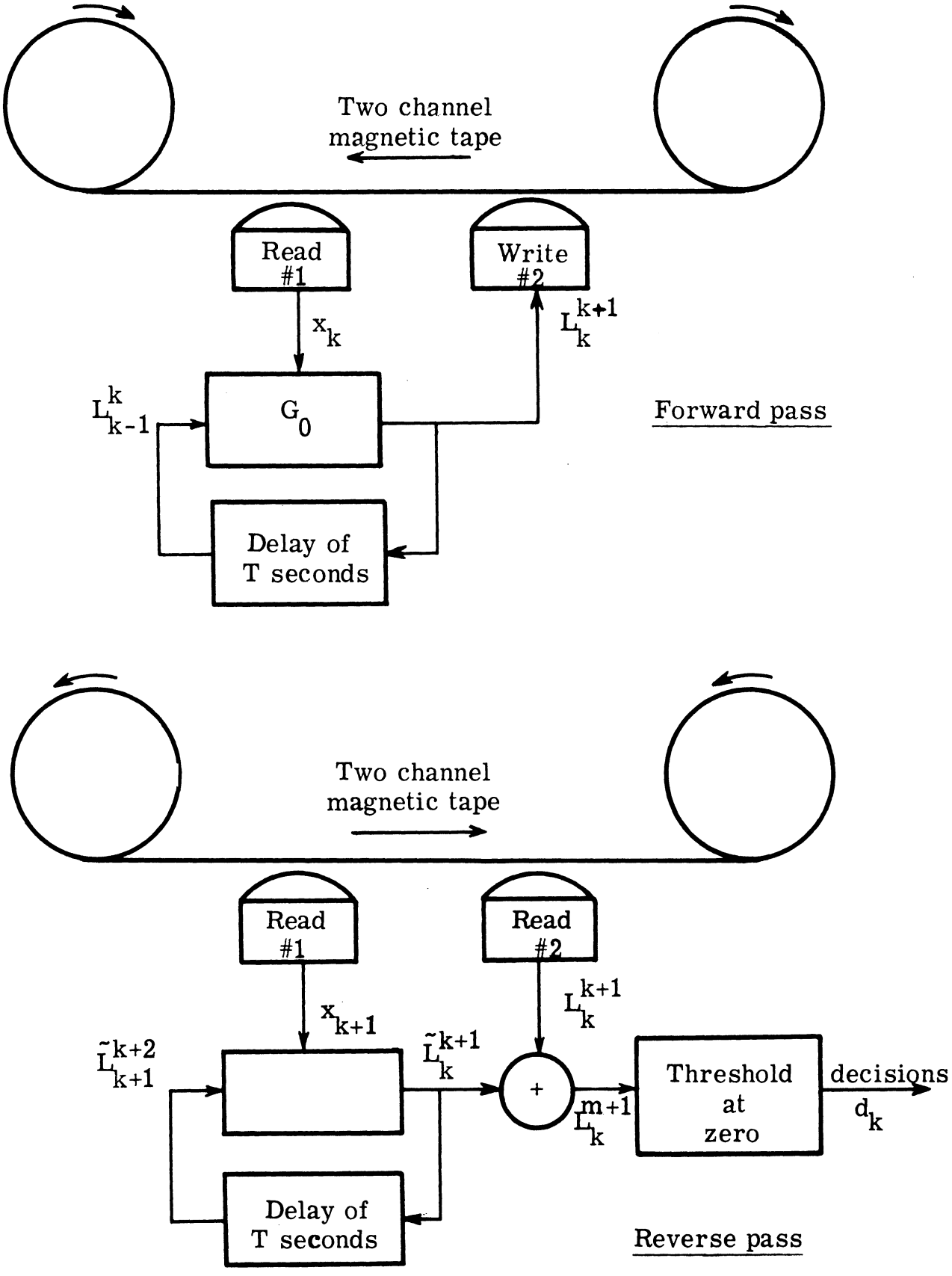

Fig. 5.10. Heuristic two-pass implementation of the optimum receiver

because the evaluation of the optimum receiver becomes difficult for higher values of d. We will later see that our results are easily extrapolated to other values of d.

In one sense, the result of our comparisons will be obvious--the optimum (likelihood ratio) receiver always yields the smallest error probability. The real objective, however, is to compare receiver performances taking into account the cost of implementation. Such a comparison requires much subjective judgment and a detailed knowledge of the particular problem at hand. The subsequent discussion is the author's personal view relative to current technology and the Mimi channel. The reader is free to draw his own inferences from the results presented.

Comparison for Constant d

Figures 5.11 through 5.15 depict the error probabilities of the four suboptimum receivers and the optimum receiver as a function of $|r(T)|$. This can be viewed as showing the effects of increased intersymbol interference for a fixed received signal-to-noise ratio. As suggested in Chapter II, increased intersymbol interference is caused by signalling too rapidly relative to the bandwidth of the channel.

The results show that the error probability for the simple MFR increases rapidly with $|r(T)|$. When intersymbol interference is moderate, the probability of error for the MFR is many times that of the other receivers. For example, if $|r(T)| = .25$ and $d = 10$, the probability of error for the MFR is about 15 times that of the optimum receiver, and

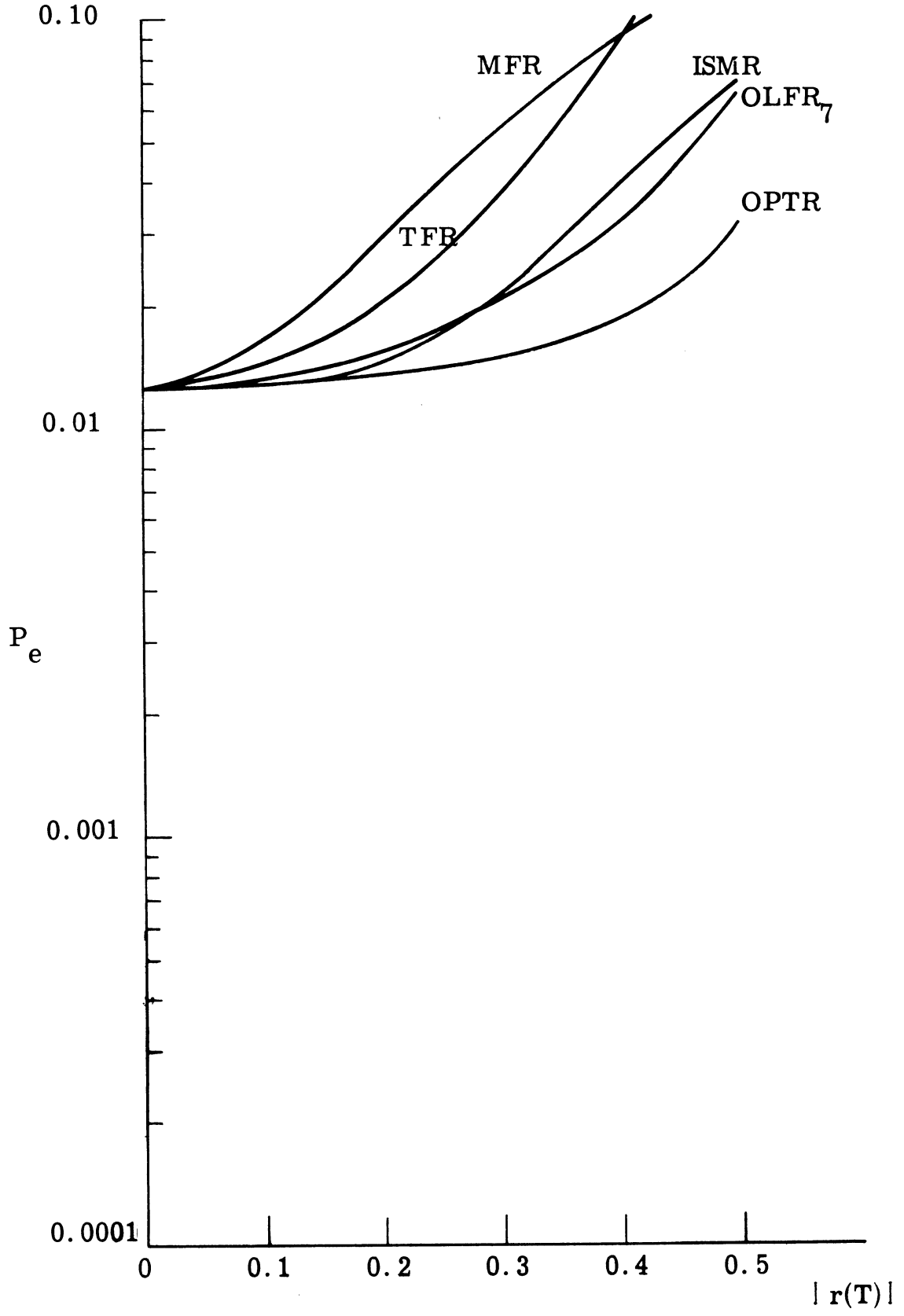

Fig. 5.11. Probability error P_e versus | r(T) | , d = 5

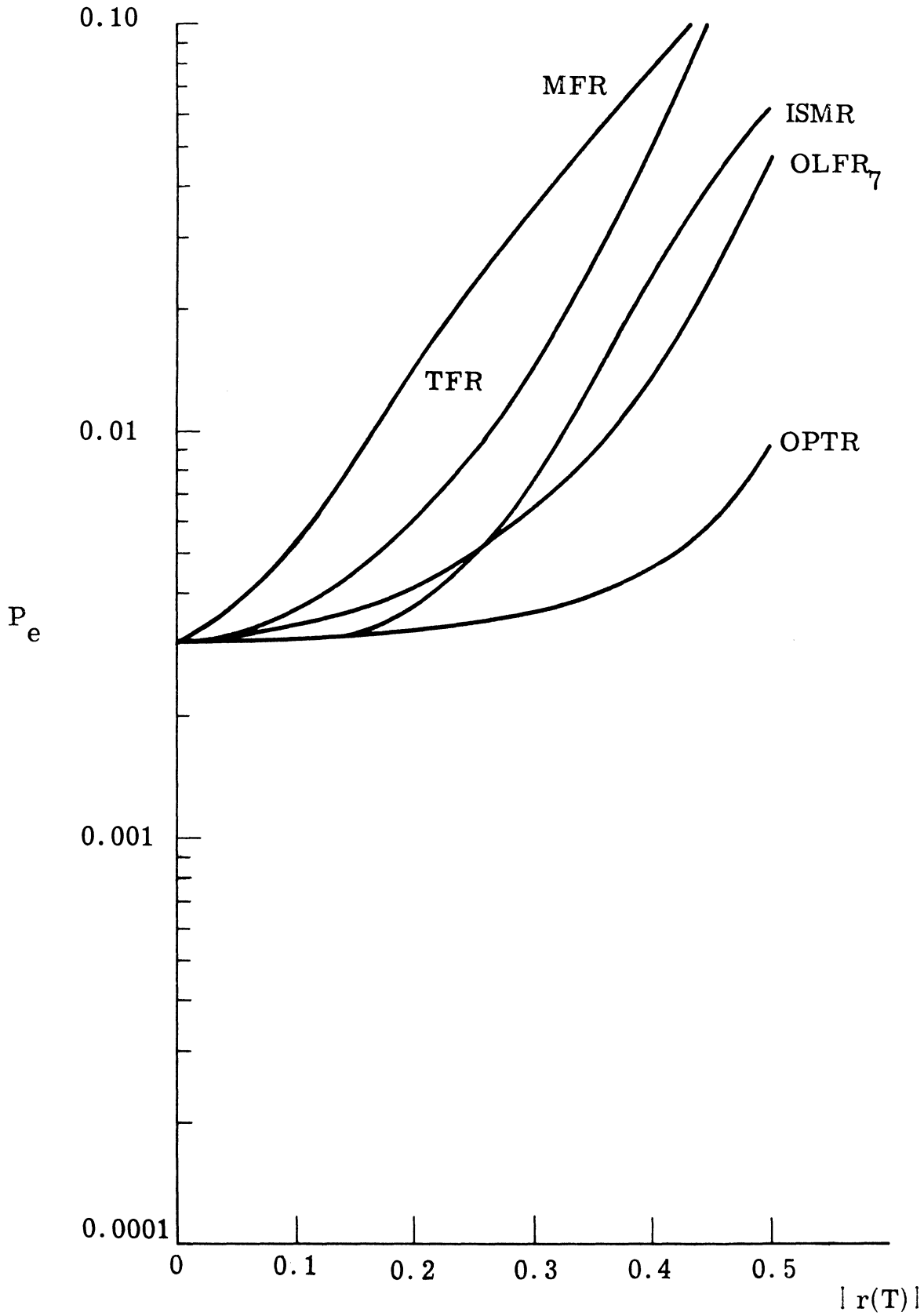

Fig. 5.12. Probability error P_e versus $|r(T)|$, d = 7.5

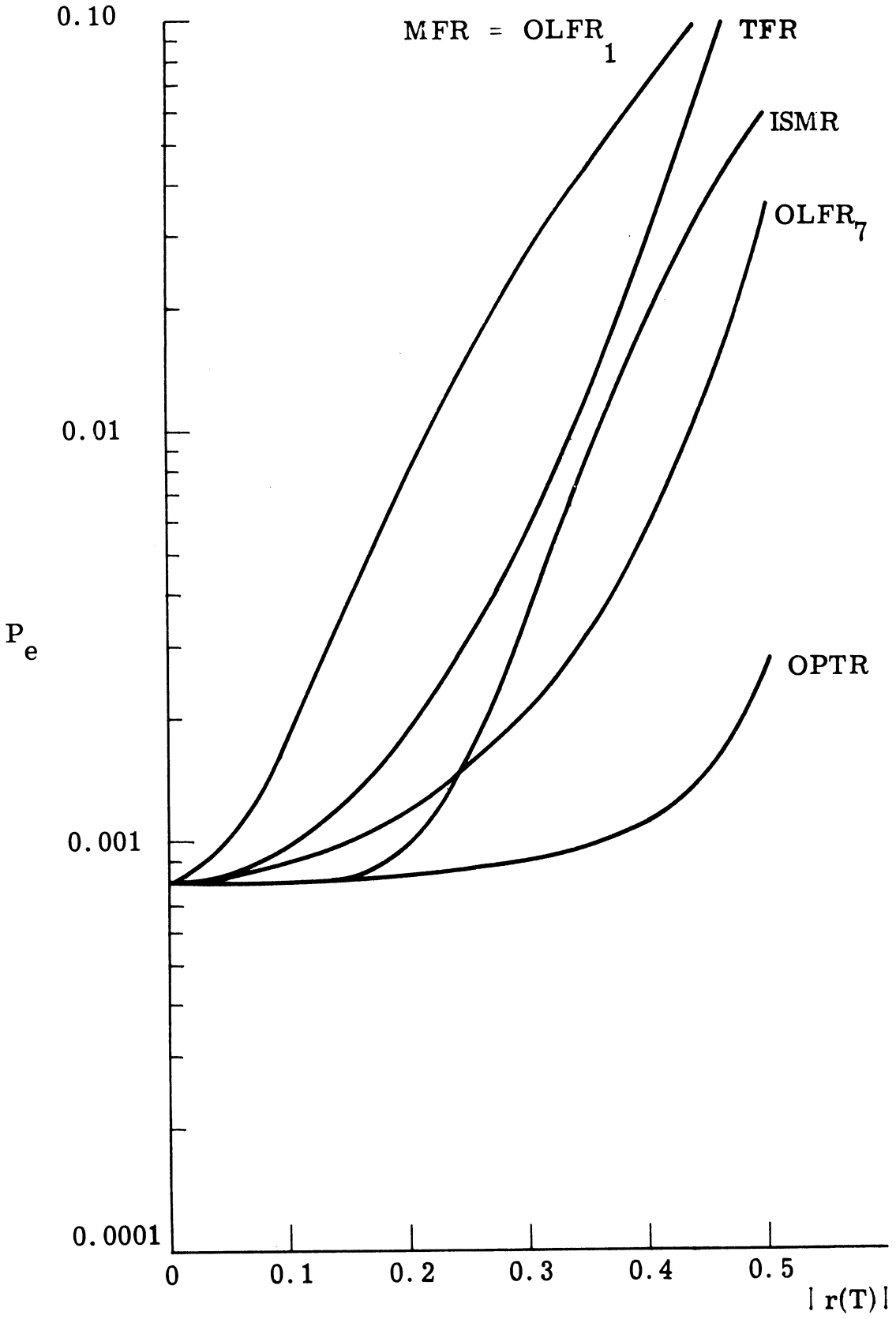

Fig. 5.13. Probability error P_e versus | r(T) | , d = 10

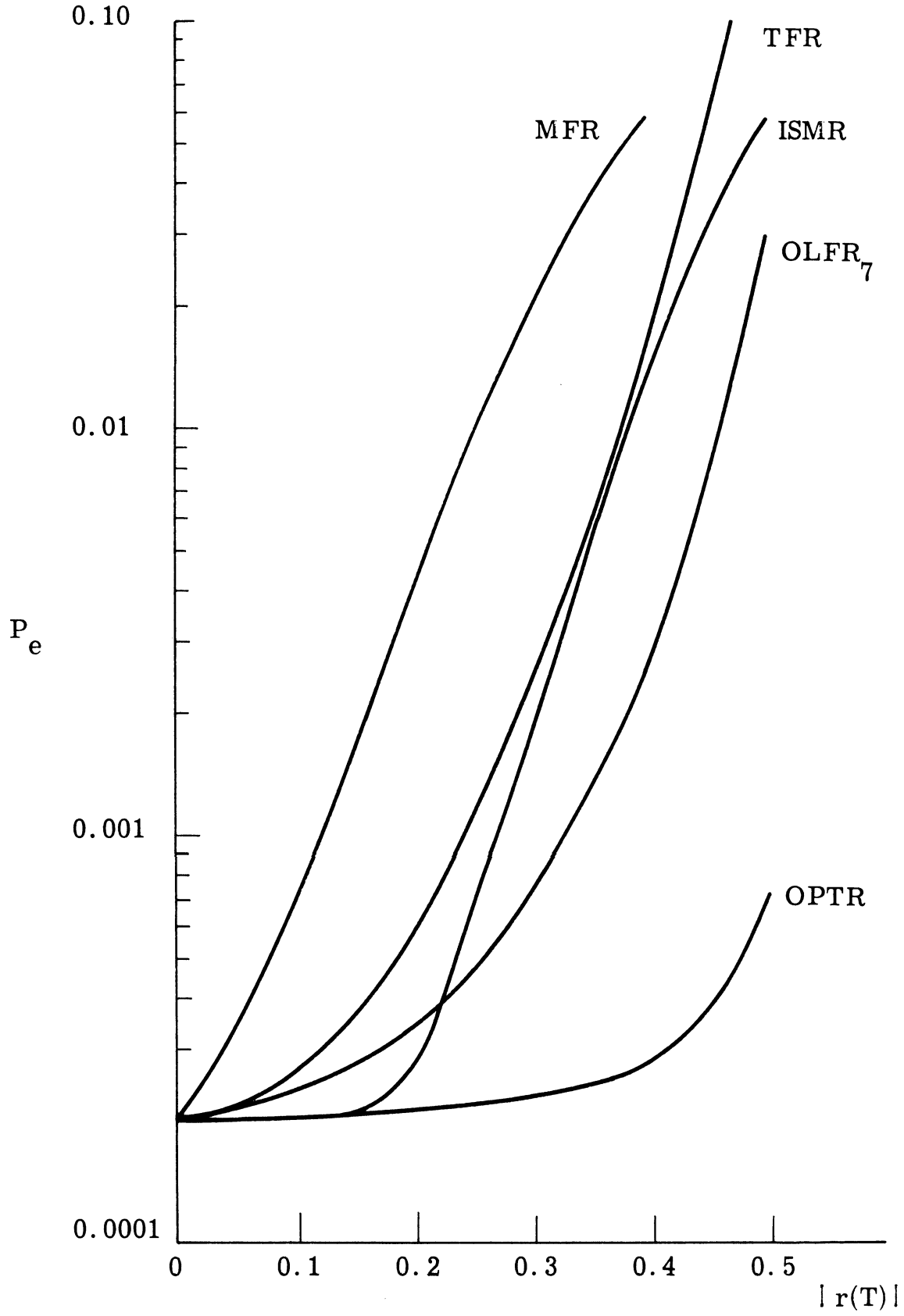

Fig. 5.14. Probability error P_e versus | r(T) | , d = 12.5

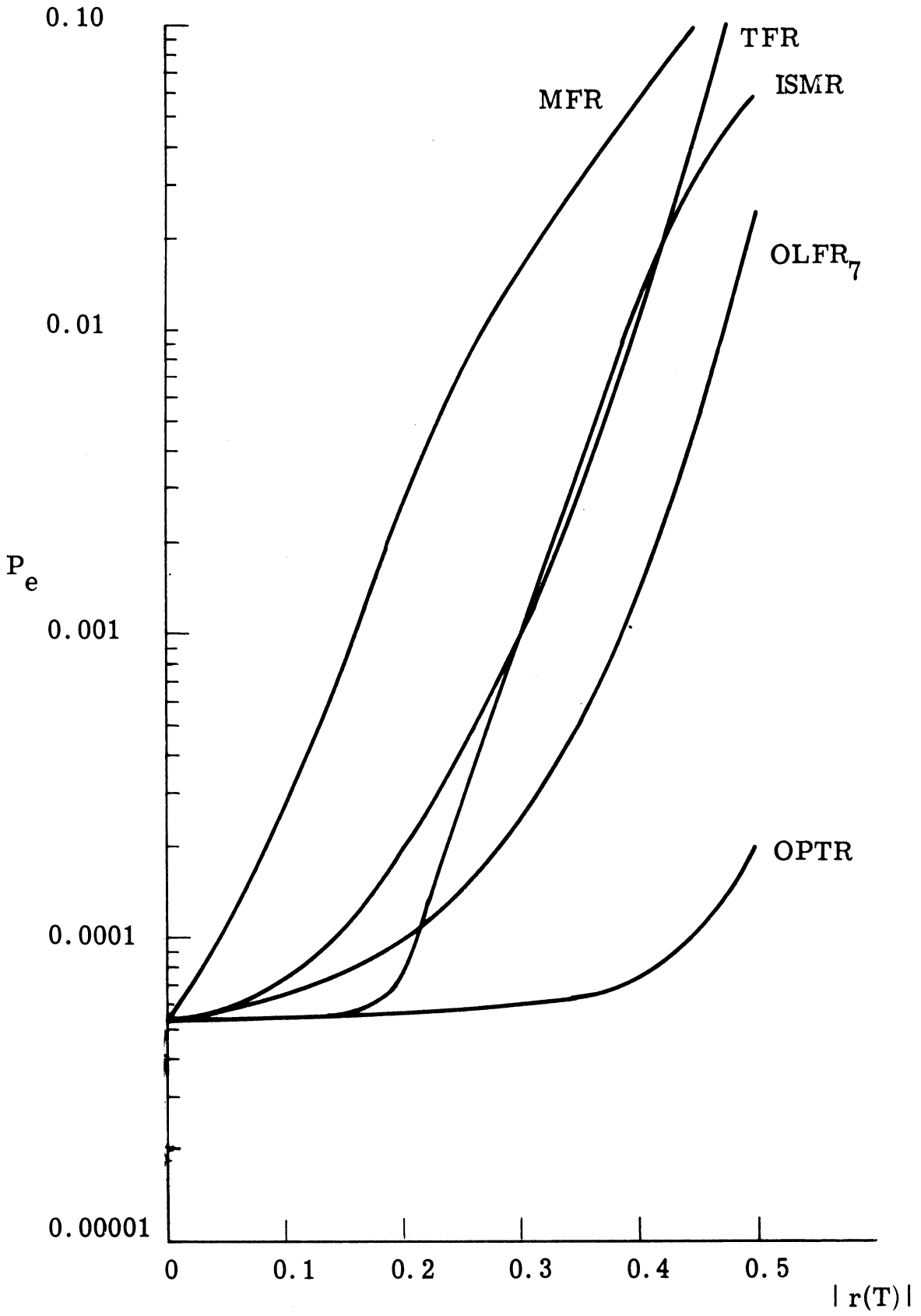

Fig. 5.15. Probability error P_e versus $|r(T)|$, d = 15

about 10 times that of the ISMR. Even if the intersymbol interference is very slight, i.e., $|r(T)| = .1$, the use of the MFR can lead to a twofold increase in the number of errors. I conclude, then, that a better receiver than the MFR is necessary even when intersymbol interference is not particularly severe.

The TFR, $OLFR_7$ and ISMR receivers offer improvement in performance with less complexity in implementation than that required by the optimum receiver. Among these three receivers, the relative error performance depends considerably on $|r(T)|$ and to a lesser extent, d. For $|r(T)| \leq .25$ the ISMR is generally slightly superior to the TFR and $OLFR_7$ in performance. On the other hand, if $|r(T)| > .25$ the $OLFR_7$ gives the best performance, the TFR and ISMR performances are roughly comparable. In terms of implementation, the ISMR is distinctly superior to both the TFR and the $OLFR_7$.

The optimum receiver performs significantly better than the suboptimum receivers such as the ISMR and $OLFR_7$ only when $|r(T)| > .25$. Even though a substantial reduction of the error probability is possible for $|r(T)| > .25$, the complexity of the optimum receiver makes its use impractical. A reduction in signalling rate to reduce $|r(T)|$ and allow the use of a simpler receiver such as the ISMR would be a wise alternative to implementing the optimum receiver.

Comparison for Constant $|r(T)|$

Let us now fix the amount of intersymbol interference, as given

by $|r(T)|$ and examine the receiver performances as a function of d. This is equivalent to fixing the channel spectrum and signalling rate and observing the effects of varying signal-to-noise ratio. Figures 5.16 through 5.20 give the performances of the four receivers as a function of d for $|r(T)| = .1, .2, .3, .4,$ and $.5$. The curve labeled IFR in each of these figures represents the performance of an interference-free receiver operating with the given value of d. The smoothness of the curves allows us to extrapolate our general results for values of d outside the range plotted.

Figures 5.16 through 5.20 show that the performance of the MFR relative to the interference-free receiver actually deteriorates as d increases. The MFR is relatively more successful (in its limited way) at low signal-to-noise ratios than at high signal-to-noise ratios. This can be attributed to the fact that as the signal-to-noise ratio increases, the error producing effect of intersymbol interference over-shadows the effects of the noise.

Because the TFR represents the optimum receiver in the absence of noise, one might hope that as d becomes large, the TFR performance would approach that of the optimum receiver. Figures 5.16 through 5.20 indicate that this does not happen even for the larger values of d considered here. This suggests that "neglecting noise" and using a "noise-free" receiver design is a poor approach.

For $|r(T)| > .25$ the performance of the ISMR relative to the

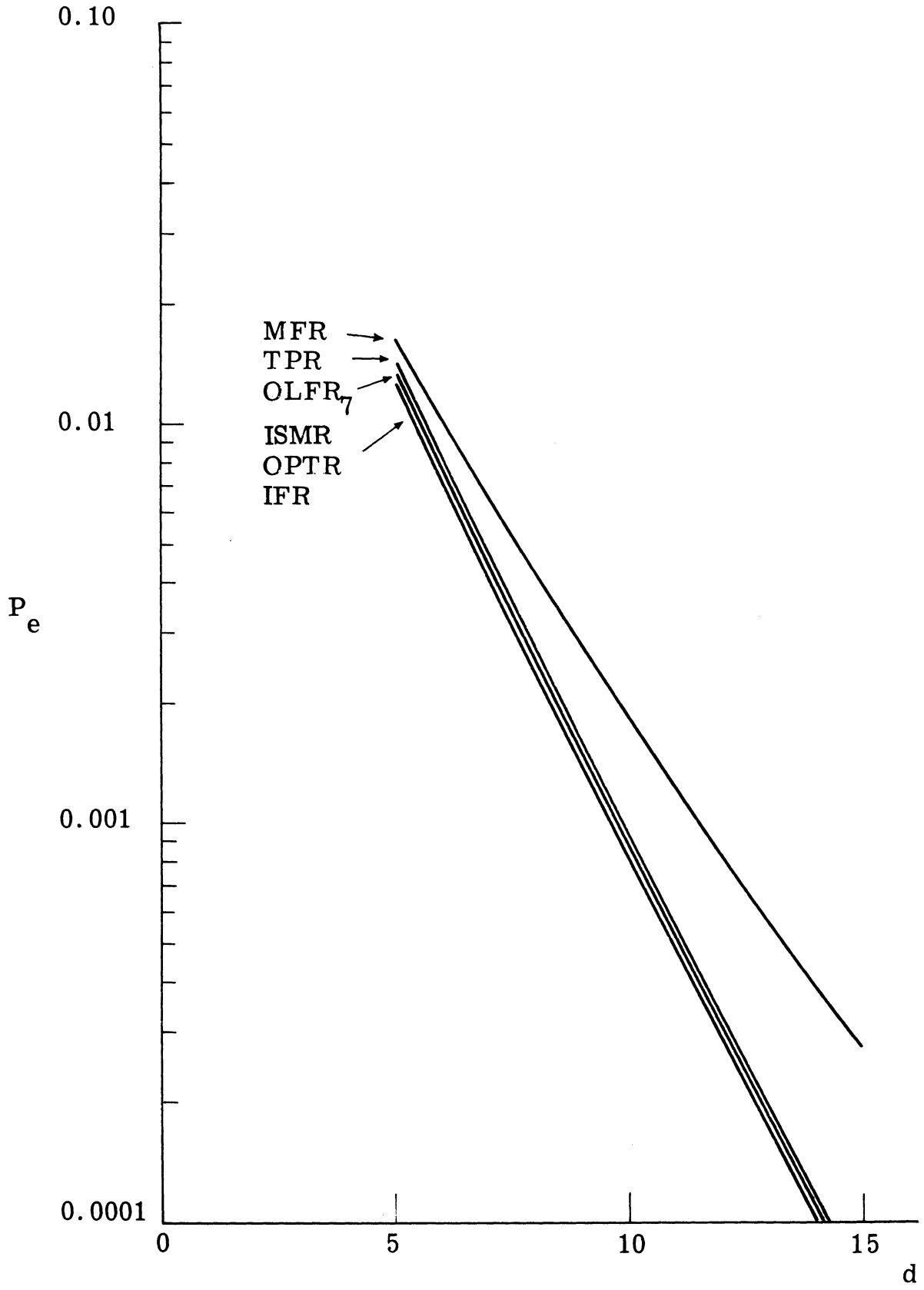

Fig. 5.16. Probability error P_e versus d, $|r(T)| = .1$

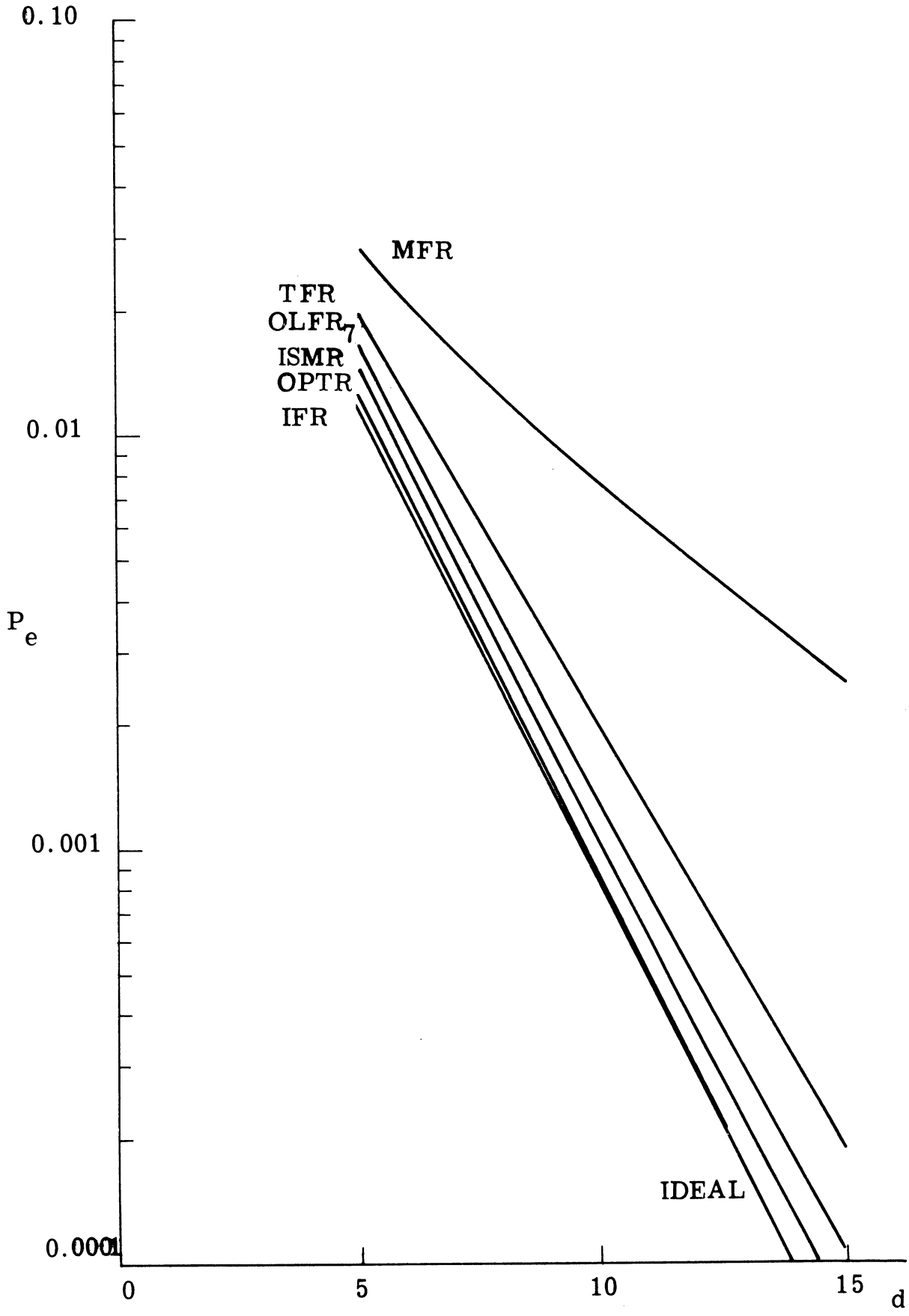

Fig. 5.17. Probability error P_e versus d, $|r(T)| = .2$

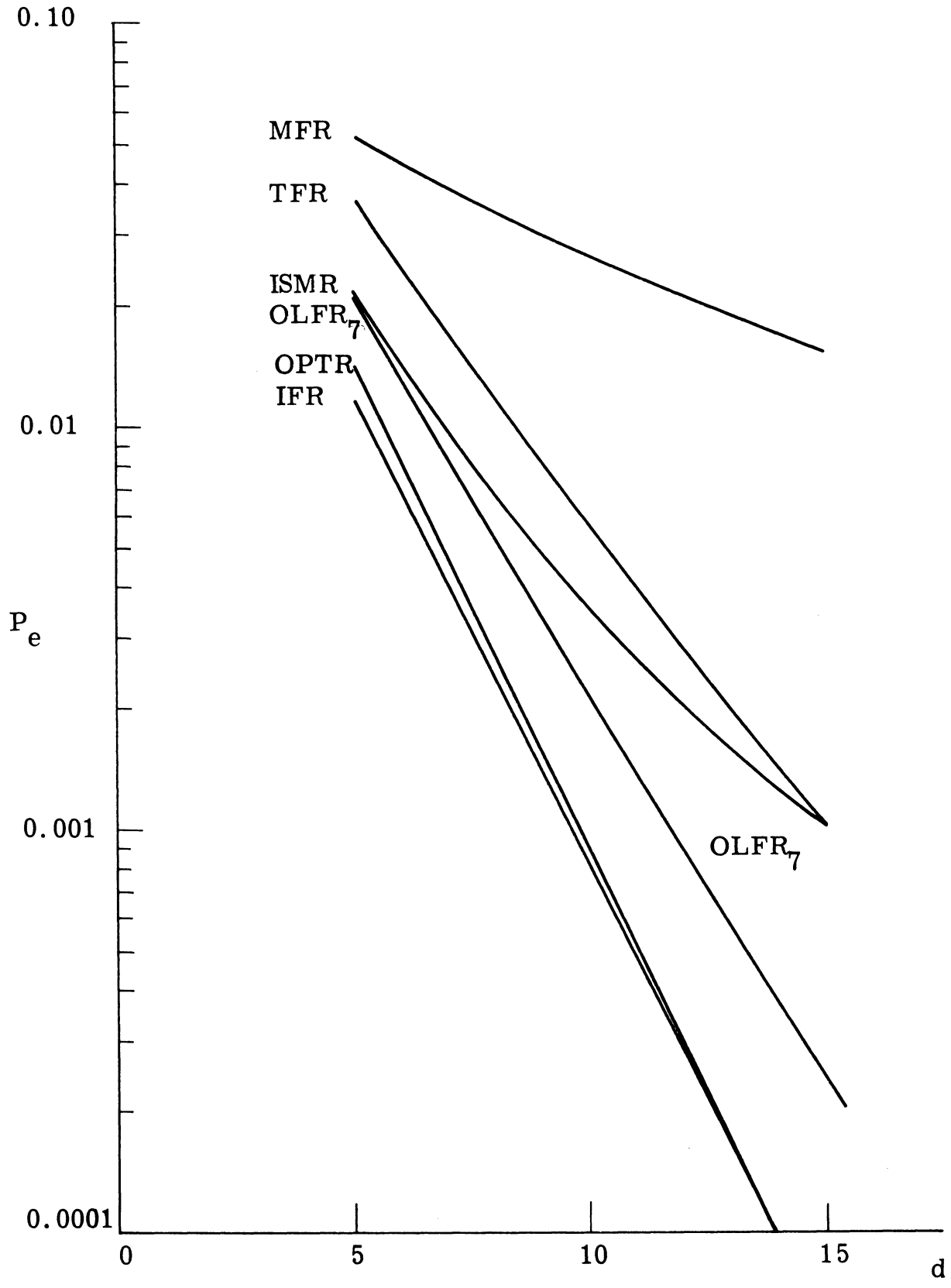

Fig. 5.18. Probability error P_e versus d, $|r(T)| = .3$

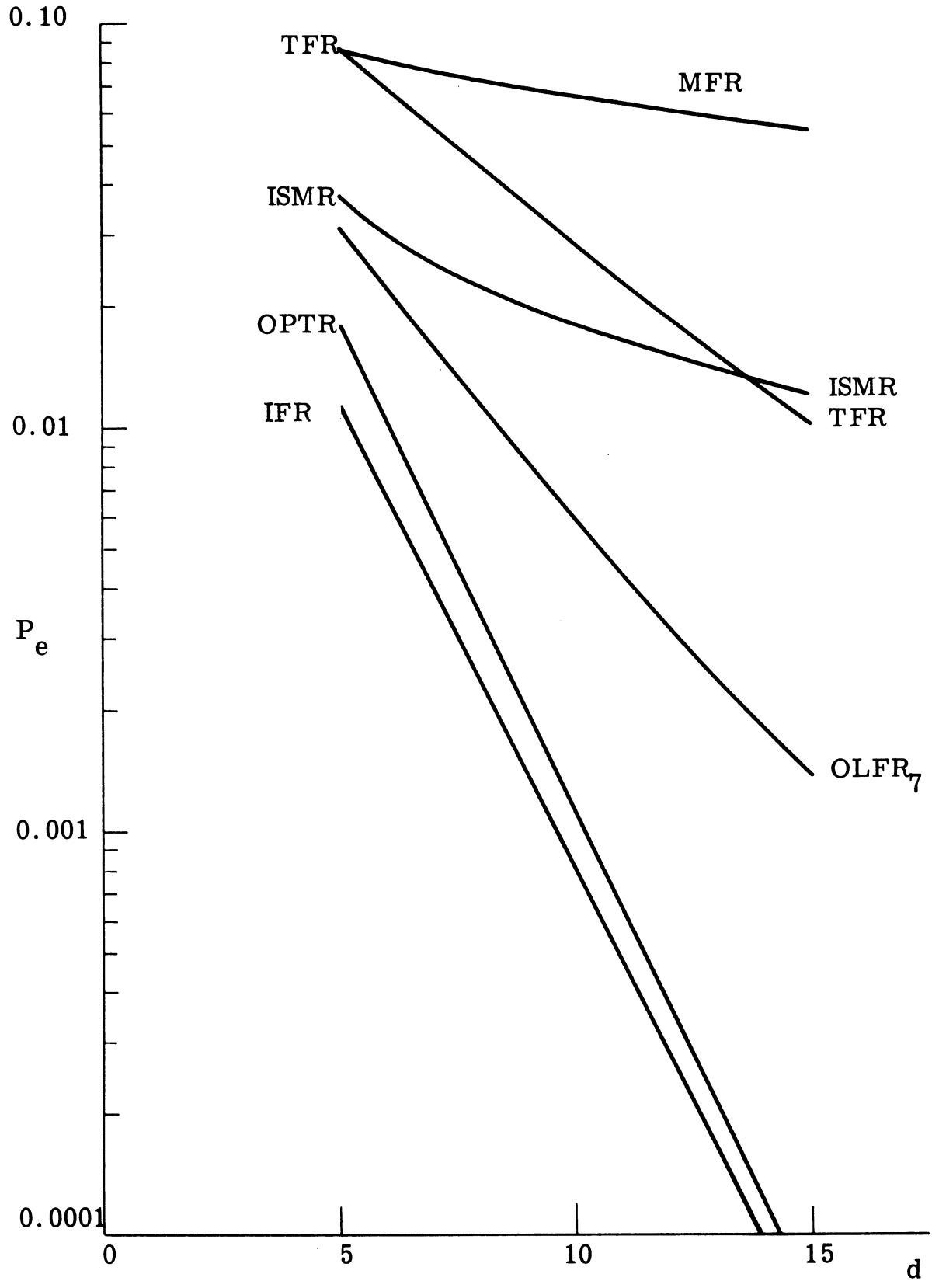

Fig. 5.19. Probability error P_e versus d, $|r(T)| = .4$

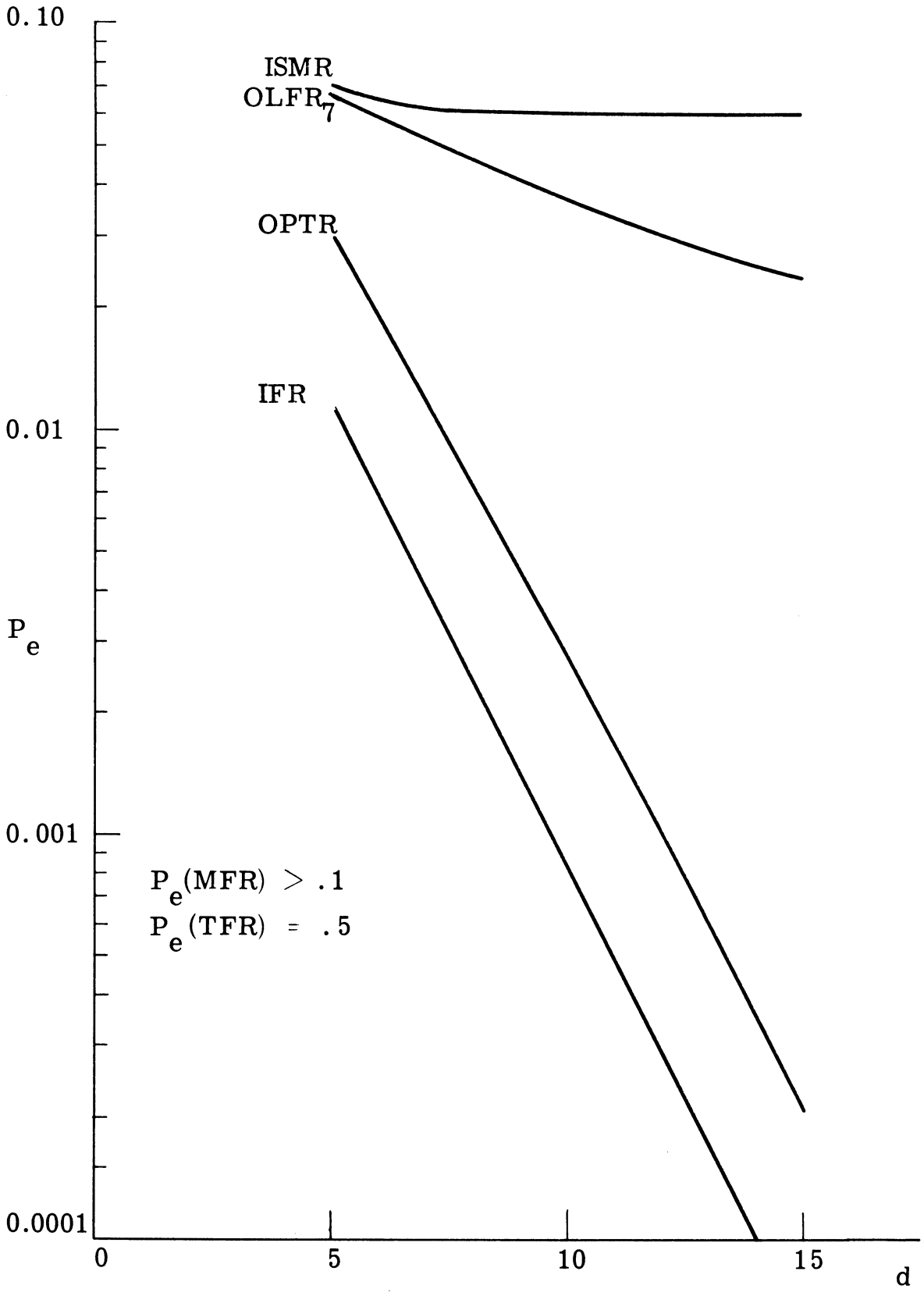

Fig. 5.20. Probability error P_e versus d, $|r(T)| = .5$

optimum receiver depreciates in essentially the same manner as the MFR as d increases. This can be attributed to poor "first guess" decisions used in the ISMR, which have the same probability of error as the MFR. Thus the ISMR is not a suitable receiver for problems with severe intersymbol interference and high signal-to-noise ratios. However, $|r(T)| \leq .25$ the ISMR is a good performer for all values of d.

The performance of the $OLFR_7$ depreciates slightly relative to the optimum receiver as d increases, with greater depreciation occurring when intersymbol interference is severe.

The performance of the optimum receiver, on the other hand, actually improves relative to the interference-free receiver performance as d increases. This can be attributed to the receiver's better knowledge of the interfering symbol values at high signal-to-noise ratios.

Conclusions

The above results show that the amount of intersymbol interference determines which is the best suboptimum receiver. If $|r(T)| \leq .25$, the ISMR is the best suboptimum receiver, both in error performance and in ease of implementation. Further, this remains true for all d. If $|r(T)| > .25$, however, the performance of the ISMR is inferior to that of the $OLFR_7$ and depreciates relative to the ideal receiver with increasing d. The actual choice between the TFR, $OLFR_7$ and ISMR

receivers for $|r(T)| > .25$ is a difficult one.

We can draw still another important conclusion from the results presented. Since the system designer can usually control $|r(T)|$ by varying the signalling rate, the above results suggest a good choice of signalling rate. When $|r(T)| > .25$, two undesirable things happen. First, the receiver required becomes more complex, such as the $OLFR_7$ or TFR. Secondly, the probability of error for this receiver is significantly larger than that for an interference-free situation. On the other hand, if the signalling rate is reduced so that $|r(T)| \leq .25$, the best practical receiver (ISMR) is easily implemented and gives near interference free performance. Furthermore, when $|r(T)| \leq .25$, the $M = 1$ assumption on which the foregoing work is based is more likely to be valid. Thus, I suggest as a general rule of thumb, the signalling rate for a binary communication system should be reduced to give $|r(T)| \leq .25$ in order to obtain both good error performance and a relatively simple receiver implementation.

The 60-ms perfect word symbol described in Chapter II for the Mimi channel of Fig. 1.2 provides an example of the application of this rule of thumb. For this symbol we have $|r(T)| = .2$. Table 5.2 below gives the performances of the five receivers for $d = 5$, 10 and 15 for this example. The ISMR gives excellent performance.

	d = 5		d = 10		d = 15	
Receiver	P_e	% Increase in Errors	P_e	% Increase in Errors	P_e	% Increase in Errors
IFR	.012675	0	.000783	0	.000054	0
OPTR	.013579	7	.000826	6	.000059	9
ISMR	.014580	15	.000993	27	.000101	87
$OLFR_7$	.015516	23	.001191	53	.000102	89
TFR	.020212	59	.001876	140	.000973	1700
MFR	.029020	129	.007615	870	.015194	2800

Table 5.2. Results for system using Mimi channel and a 60-ms perfect word symbol, $|r(T)| = .2$

Chapter VI

CONCLUSIONS AND FUTURE STUDIES

In this chapter we state the major conclusions of this paper and the future studies which they suggest.

6.1 Conclusions

Chapter II showed that the amount of intersymbol interference can be related to the power spectrum or, equivalently, on the auto-correlation function of the received symbol. This relationship was shown from the existence of a waveform of minimum RMS time duration which could be obtained through the use of a phase-equalizing filter. Ripples or notches in the power spectrum increased the RMS time duration of the received symbol and consequently increased intersymbol interference. Thus intersymbol interference could be viewed intuitively as a result of signalling too fast for the bandwidth of the channel.

The dependence of intersymbol interference on power spectrum is important because the usual (unequalized) channel symbol response often appears to indicate much more intersymbol interference than is actually present. The dependence on power spectrum also indicates that the linear variations of different slopes in the channel phase spectrum believed to be caused by multipath effects do not produce intersymbol interference. Instead, the notches in the

power spectrum caused by multipath effects (selective fading) are the source of intersymbol interference. By examining the actual channel power spectrum, an intuitive idea of a reasonable signalling rate can be obtained.

The optimum (likelihood ratio) receiver was derived and evaluated under the assumption of phase equalization and limited intersymbol interference. The results of this analysis are important not because we would ever implement the optimum receiver, but because of the insight into the design of suboptimum receivers which it provides. Since the optimum receiver is a nonlinear receiver, the receiver designer should look for good nonlinear suboptimum receivers instead of the best linear filter receiver. The performance of the optimum receiver also provides an important lower bound on the probability of error in a given situation.

Several common or proposed suboptimum receivers have been compared with the optimum receiver on the same frame of reference: phase equalization and limited intersymbol interference ($M = 1$). From this comparison the system designer can determine the relative merits of the various receivers for his particular problem.

The results of this comparison provide another important guideline to the system designer. If the received signal has $|r(T)| \leq .25$ then an easily implemented receiver (ISMR) can provide near ideal performance. On the other hand, if $|r(T)| > .25$ more

complicated receivers must be used and even with these receivers the probability of error is significantly increased. From a practical point of view, then it is very desirable to reduce the signalling rate so that $|r(T)| < .25$.

An easily implemented nonlinear receiver, the iterated switched-mode receiver (ISMR), which performs very well under the condition $|r(T)| \leq .25$, has been described for the first time. This receiver does not require the long tapped delay line of proposed linear filter receivers and does not require carefully computed tap coefficients in its operation. The ISMR represents an economical and flexible solution to the receiver design problem when intersymbol interference is not too severe.

6.2 Future Studies

At the conclusion of any theoretical study, the question arises as to whether to pursue the theory further, or to jump into the perilous experimental world for confirmation of the results. The most productive approach seems to be the latter. A carefully controlled implementation of a communication system through the Mimi channel would point out the truly significant problems of underwater communications and perhaps eliminate others from consideration.

Although actual implementation of a communication system through the Mimi channel is the next logical step, several theoretical problems are of particular interest. The problem of simultaneous

channel measurement to provide a receiver with an up-to-date replica of the noise-free symbol response is important. While transmitted reference techniques suggested in Section 1.2 can be used, a portion of the transmitted signal energy must be devoted to the reference. One could hope that if the probability of error is sufficiently low, a reference component could be reconstructed from a transmission consisting of only an information component. The development and analysis of such a technique would simplify both transmitter and receiver design.

Another subject for future study would be to consider non-binary communication systems such as M-ary signalling. By using a larger number of transmitted symbols, the transmitted symbol duration could be lengthened while maintaining the same data rate. Hopefully, the reduced symbol duration in such a system would reduce the effects of intersymbol interference.

From a purely theoretical point of view, it would be interesting to consider receiver designs when intersymbol interference is more severe; that is, when $M > 1$. The operating equations for the optimum receiver are known for such problems but offer no hope of evaluation. Development and analysis of a good suboptimum receiver, analogous to the ISMR would provide a reasonable approach to the problem.

APPENDIX A

PROOF OF THE DECREASE IN $P_e(k)$ WITH A DECREASE IN $|\tilde{h}_2^k|$

Proposition

If $h_1^k \cdot \rho^k > 0$ then the probability of error $P_e(k)$ for the canonical linear filter receiver is reduced by decreasing $|\tilde{h}_2^k|$ to zero.

Proof

Since $\tilde{h}_2^k$ is orthogonal to all of the ρ^i, $i = 0, \ldots, m$ Eq. 3.14 becomes

$$P_e(k) = \frac{1}{2^m} \sum \Phi \left[- \frac{\tilde{h}_1^k \cdot \rho^k + \sum_{i \neq k} b_i \rho^i \cdot \tilde{h}_1^k}{\sqrt{N_0(|\tilde{h}_1^k|^2 + |\tilde{h}_2^k|^2)/2}} \right] \qquad (A.1)$$

Let

$$y_1 = \tilde{h}_1^k \cdot \rho^k \qquad (A.2)$$

$$y_2(\bar{b}) = \sum_{i \neq k} b_i \rho^i \cdot \tilde{h}_1^k \qquad (A.3)$$

$$y_3 = 1/\sqrt{N_0(|\tilde{h}_1^k|^2 + |\tilde{h}_2^k|^2) / 2} \qquad (A.4)$$

then Eq. A.1 can be written as

$$P_e(k) = \frac{1}{2^m} \sum_{B_k} -y_3(y_1 + y_2(\bar{b})) \tag{A.5}$$

Let $\bar{b} = (b_0 \ldots b_i \ldots b_m)$ $i \neq k$, and let $-\bar{b} = (-b_0 \ldots -b_i \ldots -b_m)$, then

$$y_2(-\bar{b}) = -y_2(\bar{b}) \tag{A.6}$$

Define $|B_k|$ as any set of 2^m vectors $\bar{b} \in B_k$ such that if $\bar{b} \in |B_k|$, then $-\bar{b} \notin B_k$. Equation A.5 becomes

$$P_e(k) = \frac{1}{2^m} \sum_{|B_k|} \left\{ \Phi[-y_3(y_1 + y_2(\bar{b}))] + \Phi[-y_3(y_1 - y_2(\bar{b}))] \right\} \tag{A.7}$$

Differentiating Eq. A.7 with respect to y_3 we have

$$\frac{dP_e(k)}{dy_3} = -\frac{1}{2^m} \sum_{|B_k|} \left\{ (y_1 + y_2(\bar{b}))\, \phi[-y_3(y_1 + y_2(\bar{b}))] + (y_1 - y_2(\bar{b}))\, \phi[-y_3(y_1 - y_2(\bar{b}))] \right\} \tag{A.8}$$

Each term in the summation of equation A.8 is positive if $y_1 > 0$. This can be shown by considering the function $S(u_1, u_2)$

$$S(u_1, u_2) = u_1 \phi(u_1) + u_2 \phi(u_2) \tag{A.9}$$

which is strictly positive if $u_1 + u_2$ is positive. Let

$u_1 = y_3(y_1 + y_2(\bar{b}))$, $u_2 = y_3(y_1 - y_2(\bar{b}))$ then

$$u_1 + u_2 = y_1 y_3 > 0 \tag{A.10}$$

if $y_1 > 0$.

Since $y_1 > 0$ by hypothesis from equation A.8 we have that

$\frac{dP_e(k)}{dy_3}$ is negative, so that $P_e(k)$ is reduced by increasing

y_3. Since y_3 is increased by decreasing $|\tilde{h}_2^k|$, $P_e(k)$

is reduced by decreasing $|\tilde{h}_2^k|$.

APPENDIX B

DERIVATION OF EQUATIONS 5.19, 5.22, 5.26 AND 5.81

Derivation of Equation 5.19

Substituting Equations 5.9 and 5.18 into Equation 5.13 gives for $j=k\neq 0$

$$\ln l_k(x_j) =$$

$$\ln \frac{\dfrac{K}{1+e^{L_{k-1}^k}} e^{-\frac{1}{2}\left\{|x_j|^2 - 2x_j \cdot s_{-1+1} + |s_{-1+1}|\right\}^2}}{\dfrac{K}{1+e^{L_{k-1}^k}} e^{-\frac{1}{2}\left\{|x_j|^2 - 2x_j \cdot s_{-1-1} + |s_{-1-1}|\right\}^2}}$$

$$+ \frac{\dfrac{Ke^{L_{k-1}^k}}{1+e^{L_{k-1}^k}} e^{-\frac{1}{2}\left\{|x_j|^2 - 2x_j \cdot s_{+1+1} + |s_{+1+1}|\right\}^2}}{\dfrac{Ke^{L_{k-1}^k}}{1+e^{L_{k-1}^k}} e^{-\frac{1}{2}\left\{|x_j|^2 - 2x_j \cdot s_{+1-1} + |s_{+1-1}|\right\}^2}}$$

$$(j=k\neq 0) \qquad \text{(B.1)}$$

Canceling factors common to the numerator and denominator we have

$$\ln l_k(x_j) = \ln \frac{e^{x_j \cdot s_{-1+1} - \frac{1}{2}|s_{-1+1}|^2} + e^{L_{k-1}^k + x_j \cdot s_{+1+1} - \frac{1}{2}|s_{+1+1}|^2}}{e^{x_j \cdot s_{-1-1} - \frac{1}{2}|s_{-1-1}|^2} + e^{L_{k-1}^k + x_j \cdot s_{+1-1} - \frac{1}{2}|s_{-1-1}|^2}}$$

$$(j = k \neq 0) \qquad \text{(B.2)}$$

Squaring Equation 5.17 we have

$$|s_{b_{j-1}b_j}|^2 = |\rho_1^{j-1}|^2 + 2 b_{j-1} b_j \rho_1^{j-1} \cdot \rho_0^j + |\rho_0^j|^2 \qquad \text{(B.3)}$$

Inserting Equations B.3 and 5.17 into Equation B.2 and canceling common factors in the numerator and denominator gives:

$$\ln l_k(x_j) =$$

$$\ln \frac{e^{x_j \cdot (\rho_0^j - \rho_1^{j-1}) + \rho_1^{j-1} \cdot \rho_0^j} + e^{L_{k-1}^k + x_j \cdot (\rho_0^j + \rho_1^j) - \rho_1^{j-1} \cdot \rho_0^j}}{e^{x_j \cdot (-\rho_0^j - \rho_1^{j-1}) - \rho_1^{j-1} \cdot \rho_0^j} + e^{L_{k-1}^k + x_j \cdot (-\rho_0^j + \rho_1^{j-1}) + \rho_1^{j-1} \cdot \rho_0^j}}$$

$$(j = k \neq 0) \qquad \text{(B.4)}$$

After multiplying numerator and denominator of Equation B.4 by $e^{-L_{k-1}^k/2 + x_j \cdot \rho_0^j}$ we obtain

$$\ln l_k(x_j) = \ln e^{2x_j \cdot \rho_0^j} \left\{ \frac{e^{+\rho_1^{j-1} \cdot (x_j - \rho_0^j) + \frac{L_{k-1}^k}{2}} + e^{-\rho_1^{j-1}(x_j - \rho_0^j) - \frac{L_{k-1}^k}{2}}}{e^{+\rho_1^{j-1} \cdot (x_j + \rho_0^j) + \frac{L_{k-1}^k}{2}} + e^{-\rho_1^{j-1}(x_j + \rho_0^j) - \frac{L_{k-1}^k}{2}}} \right\}$$

$$(j = k \neq 0) \qquad \text{(B.5)}$$

Since

$$\cosh u = \frac{e^{u} + e^{-u}}{2} \tag{B.6}$$

we may rewrite Equation B.5 in the desired form (5.19)

$$\mathrm{lnl}_k(x_j) = 2x_j \cdot \rho_0^j + \ln \frac{\cosh\left(\rho_1^{j-1} \cdot (x_j - \rho_0^j) + \frac{L_{k-1}^k}{2}\right)}{\cosh\left(\rho_1^{j-1} \cdot (x_j + \rho_0^j) + \frac{L_{k-1}^k}{2}\right)} \tag{5.19}$$

$$(j = k \neq 0)$$

Derivation of Equation 5.22

Substituting Equation 5.18 directly into Equation 5.14 we obtain for $j = k+1$:

$$\mathrm{lnl}_k(x_j) =$$

$$\ln \frac{\frac{1}{2} K\left[e^{-\frac{1}{2}\left\{|x_j|^2 - 2x_j \cdot s_{+1-1} + |s_{+1-1}|^2\right\}}\right.}{\frac{1}{2} K\left[e^{-\frac{1}{2}\left\{|x_j|^2 - 2x_j \cdot x_{-1-1} + |s_{-1-1}|^2\right\}}\right.}$$

$$\frac{\left. + \; e^{-\frac{1}{2}\left\{|x_j|^2 - 2x_j \cdot s_{+1+1} + |s_{+1+1}|^2\right\}}\right]}{\left. + \; e^{-\frac{1}{2}\left\{|x_j|^2 - 2x_j \cdot s_{-1+1} + |s_{-1+1}|^2\right\}}\right]}$$

$$(j = k+1) \tag{B.7}$$

Substituting Equation B. 3 into Equation B. 7 and canceling common factors in the numerator and denominator gives

$$lnl_k(x_j) = \ln \frac{e^{x_j \cdot s_{+1-1} + \rho_1^{j-1} \cdot \rho_0^j} + e^{x_j \cdot s_{+1+1} - \rho_1^{j-1} \cdot \rho_0^j}}{e^{x_j \cdot s_{-1-1} - \rho_1^{j-1} \cdot \rho_0^j} + e^{x_j \cdot s_{-1+1} + \rho_1^{j-1} \cdot \rho_0^j}}$$

$$(j = k+1) \qquad \text{(B. 8)}$$

By inserting Equation 5.17 into Equation B.8 and multiplying by $e^{x_j \cdot \rho_1^{j-1}}$ we obtain

$$lnl_k(x_j) = \ln e^{2x_j \cdot \rho_1^{j-1}} \left\{ \frac{e^{-\rho_0^j \cdot (x_j - \rho_1^{j-1})} + e^{\rho_0^j \cdot (x_j - \rho_1^{j-1})}}{e^{\rho_0^j \cdot (x_j + \rho_1^{j-1})} + e^{-\rho_0^j \cdot (x_j + \rho_1^{j-1})}} \right\}$$

$$(j = k+1) \qquad \text{(B. 9)}$$

We may rewrite Equation B. 9 in the desired form (5.22):

$$lnl_k(x_j) = 2x_j \cdot \rho_1^{j-1} + \ln \frac{\cosh\left[\rho_0^j \cdot (x_j - \rho_1^{j-1})\right]}{\cosh\left[\rho_0^j \cdot (x_j + \rho_1^{j-1})\right]} \qquad (5.22)$$

$$(j = k+1)$$

Derivation of Equation 5.26

From Equation 5.18 we have

$$\left\{ p(x_j | b_{j-1},\ b_j = +1) + p(x_j | b_{j-1}\, b_j = -1) \right\}$$

$$= K \left\{ e^{-\frac{1}{2}\left\{ |x_j|^2 - 2x_j \cdot s_{b_{j-1},+1} + |s_{b_{j-1},+1}|^2 \right\}} \right.$$

$$\left. + \quad e^{-\frac{1}{2}\left\{ |x_j|^2 - 2x_j \cdot s_{b_{j-1},-1} + |s_{b_{j-1},-1}|^2 \right\}} \right\} \qquad \text{(B.10)}$$

By substituting Equations B. 3 and 5.17 into Equation B.10 and extracting common factors we obtain

$$\left\{ p(x_j | b_{j-1},\ b_j = +1) + p(x_j | b_{j-1},\ b_j = -1) \right\}$$

$$= Ke^{-\frac{1}{2}\left\{ |x_j|^2 + |\rho_1^{j-1}|^2 + |\rho_0^j|^2 - 2b_{j-1} x_j \cdot \rho_1^{j-1} \right\}}$$

$$\left\{ e^{\rho_0^j \cdot (x_j - b_{j-1}\rho_1^j)} + e^{-\rho_0^j \cdot (x_j - b_{j-1}\rho_1^j)} \right\} \qquad \text{(B.11)}$$

$$= 2Ke^{-\frac{1}{2}\left\{ |x_j|^2 + |\rho_1^{j-1}|^2 + |\rho_0^j|^2 - 2b_{j-1} x_j \cdot \rho_1^{j-1} \right\}}$$

$$\left\{ \cosh \rho_0^j \cdot (x_j - b_{j-1}\rho_1^j) \right\} \qquad \text{(B.12)}$$

Equation 5.25 can be inverted to give

$$P(b_{j-1} | X_j b_k) = \frac{e^{\frac{1}{2}(b_{j-1}+1)\, L^j_{j-1}(b_k)}}{1 + e^{L^j_{j-1}(b_k)}} \qquad \text{(B.13)}$$

Substituting Equations B.12 and B.13 into Equation 5.15 and canceling common factors in the numerator and denominator, we obtain

$$\ln l_k(x_j) = \ln \frac{1 + e^{L^j_{j-1}(+1)}}{1 + e^{L^j_{j-1}(-1)}}$$

$$\frac{\left\{ e^{-x_j \cdot \rho_1^{j-1}} \cosh \rho_0^j (x_j + \rho_1^j) + e^{L^j_{j-1}(+1) + x_j \cdot \rho_1^{j-1}} \cosh \rho_0^j (x_j - \rho_1^{j-1}) \right\}}{\left\{ e^{-x_j \cdot \rho_1^{j-1}} \cosh \rho_0^j (x_j + \rho_1^{j-1}) + e^{L^j_{j-1}(-1) + x_j \cdot \rho_1^{j-1}} \cosh \rho_0^j (x_j - \rho_1^{j-1}) \right\}}$$

$$(j > k+1) \qquad \text{(B.14)}$$

By removing a factor of $e^{\frac{1}{2} L^j_{j-1}(+1)}$ from the numerator and a factor of $e^{\frac{1}{2} L^j_{j-1}(-1)}$ from the denominator and changing the resulting product into a sum of logarithms gives the desired form of Equation 5.26.

$$\ln l_k(x_j) = .5\left(L^j_{j-1}(+1) - L^j_{j-1}(-1)\right) + \ln \frac{1+e^{L^j_{j-1}(-1)}}{1+e^{L^j_{j-1}(+1)}}$$

$$+ \ln \frac{\left\{ \begin{matrix} .5\,(L^j_{j-1}(+1) + 2x_j \cdot \rho^j_0) & -.5\,(L^j_{j-1}(+1) + 2x_j \cdot \rho^j_0) \\ e \quad \cosh(\rho^{j-1}_1 \cdot (x_j - \rho^j_0)) & + e \quad \cosh(\rho^{j-1}_1 \cdot (x_j + \rho^j_0)) \end{matrix} \right\}}{\left\{ \begin{matrix} .5\,(L^j_{j-1}(-1) + 2x_j \cdot \rho^j_0) & -.5\,(L^j_{j-1}(-1) + 2x_j \cdot \rho^j_0) \\ e \quad \cosh(\rho^{j-1}_1 \cdot (x_j - \rho^j_0)) & + e \quad \cosh(\rho^{j-1}_1 \cdot (x_j + \rho^j_0)) \end{matrix} \right\}}$$

$$(j > k+1) \qquad (5.26)$$

Derivation of Equation 5.81

We have, from Equation 5.70

$$\rho^k_0 = \rho'_{00}\,\hat{u}_0 \qquad (B.15)$$

$$\rho^{k-1}_1 = \rho'_{10}\,\hat{u}_0 + \rho'_{11}\,\hat{u}_1 \qquad (B.16)$$

Then from Equations B.15, B.16 and 5.71 we obtain

$$x_k \cdot \rho^k_0 = x^0_k\,\rho'_{00} \qquad (B.17)$$

$$x_k \cdot \rho^{k-1}_1 = x^0_k\,\rho'_{10} + x^1_k\,\rho'_{11} \qquad (B.18)$$

Let

$$R = \rho^k_0 \cdot \rho^{k-1}_1 \qquad (B.19)$$

$$= \rho'_{00}\,\rho'_{10} \qquad (B.20)$$

from Equations B.15 and B.16. Then Equation 5.19 can be rewritten (with j=k) as

$$\ln l_k(x_k) = 2x_k^0 \rho'_{00} + \ln \frac{\cosh\left\{\frac{L_{k-1}^k}{2} + x_k^0 \rho'_{10} + x_k^1 \rho'_{11} - R\right\}}{\cosh\left\{\frac{L_{k-1}^k}{2} + x_k^0 \rho'_{10} + x_k^1 \rho'_{11} + R\right\}} \tag{B.21}$$

$$= L_k^{k+1} \tag{B.22}$$

from Equations 5.6 and 5.10. Define

$$\xi = \tfrac{1}{2}\left[L_{k-1}^k + 2x_k^0 \rho'_{10}\right] \tag{B.23}$$

$$\zeta = \tfrac{1}{2}\left[L_k^{k+1} - 2x_k^0 \rho'_{00}\right] \tag{B.24}$$

Then from Equations B.21 and B.22 we have

$$e^{2\zeta} = \frac{\cosh(\xi + x_k^1 \rho'_{11} - R)}{\cosh(\xi + x_k^1 \rho'_{11} + R)} \tag{B.25}$$

$$= \frac{e^{\xi + x_k^1 \rho'_{11} - R} + e^{-\xi - x_k^1 \rho'_{11} + R}}{e^{\xi + x_k^1 \rho'_{11} + R} + e^{-\xi - x_k^1 \rho'_{11} + R}} \tag{B.26}$$

Rearranging terms in Equation B.26 gives

$$e^{2x_k^1 \rho'_{11} + 2\xi} = \frac{e^{R-\zeta} - e^{-(R-\zeta)}}{e^{R+\zeta} - e^{-(R+\zeta)}} \tag{B.27}$$

Taking the logarithm of both sides of Equation B. 27 and solving for x'_k gives

$$x_k^1 = \frac{1}{2\rho'_{11}} \left\{ -2\xi + \ln \frac{\sinh R - \zeta}{\sinh R + \zeta} \right\} \qquad \text{(B. 28)}$$

The desired Equation 5.81 is obtained by inserting Equations B. 22, B. 23 and B. 24:

$$x_k^1 = \frac{1}{2\rho'_{11}} \left\{ -L_{k-1}^k - 2x_k^0 \rho'_{10} + \ln \frac{\sinh\left(\rho'_{00}\rho'_{10} - \frac{L_k^{k+1}}{2} - x_k^0 \rho'_{00}\right)}{\sinh\left(\rho'_{00}\rho'_{10} + \frac{L_k^{k+1}}{2} - x_k^0 \rho'_{00}\right)} \right\}$$

(5. 81)

REFERENCES

1. W.W. Peterson, T.G. Birdsall and W.C. Fox, "The Theory of Signal Detectability," IRE Trans. on Information Theory, IT-4, 1954.

2. J.M. Aein and J.C. Hancock, "Reducing the Effects of Intersymbol Interference with Correlation Receivers," IEEE Trans. on Information Theory, July 1963.

3. M.R. Aaron and D.W. Tufts, "Intersymbol Interference and Error Probability," IEEE Trans. on Information Theory, January 1966.

4. D.C. Coll, A System for the Optimumization of Pulse Communication Channels, Defense Research Telecommunications Establishment Report No. 168, Ottawa, Canada, December 1966.

5. J.C. Steinberg and T.G. Birdsall, "Underwater Sound Propagation in the Straits of Florida," Journal of the Acoustic Society of America, 39, pp. 301-315, 1966.

6. M.P. Ristenbatt, et al., Digital Communication Studies, Part I: Comparative Probability of Error and Channel Capacity, Cooley Electronics Laboratory Report No. 133, University of Michigan, Ann Arbor, Michigan, March 1962.

7. R. Price and P.E. Green, "A Communication Technique for Multipath Channels," Proceedings of the IRE, March 1958.

8. A. Papoulis, The Fourier Integral and Its Applications, McGraw-Hill Book Co., New York, 1962.

9. C.W. Helstrom, Statistical Theory of Signal Detection, Pergamon Press, New York, 1960.

10. H. Rudin Jr., "Automatic Equalization Using Transversal Filters," IEEE Spectrum, Vol. 4, No. 1, January 1967, pp. 53-59.

11. S.W. Golomb, et al., Digital Communications with Space Applications, Prentice Hall, Inc., Englewood Cliffs, N.J., 1964.

REFERENCES Cont.

12. U. Grenander, "Stochastic Processes and Statistical Inference," Arkiv det Mat., 1, 1950, pp. 195-277.

DISTRIBUTION LIST

	No. of Copies
Office of Naval Research (Code 468) Navy Department Washington, D. C. 20360	2
Director, Naval Research Laboratory Technical Information Division Washington, D. C. 20360	6
Director Office of Naval Research Branch Office 1030 East Green Street Pasadena, California 91101	1
Office of Naval Research San Francisco Annex 1076 Mission Street San Francisco, California 94103	1
Office of Naval Research New York Annex 207 West 24th Street New York, New York 10011	1
Director Office of Naval Research Branch Office 219 South Dearborn Street Chicago, Illinois 60604	1
Commanding Officer Office of Naval Research Branch Office Box 39 FPO New York 09510	8
Commander, Naval Ordnance Laboratory Acoustics Division White Oak, Silver Spring, Maryland 20910	1
Commanding Officer and Director Naval Electronics Laboratory San Diego, California 92152	1

DISTRIBUTION LIST (Cont.)

	No. of Copies
Commanding Officer and Director Navy Underwater Sound Laboratory Fort Trumball New London, Connecticut 06321	1
Commanding Officer Naval Air Development Center Johnsville, Warminister, Pennsylvania	1
Commanding Officer and Director David Taylor Model Basin Washington, D. C. 2007	1
Superintendent Naval Postgraduate School Monterey, California 93940 Attn: Prof. L. E. Kinsler	1
Commanding Officer Navy Mine Defense Laboratory Panama City, Florida 32402	1
Superintendent Naval Academy Annapolis, Maryland 21402	1
Commander Naval Ordnance Systems Command Code ORD-0302 Navy Department Washington, D. C. 20360	1
Commander Naval Ship Systems Command Code SHIPS-03043 Navy Department Washington, D. C. 20360	1

DISTRIBUTION LIST (Cont.)

	No. of Copies
Commander Naval Ship Systems Command Code SHIPS-1630 Navy Department Washington, D. C. 20360	1
Chief Scientist Navy Underwater Sound Reference Div. Post Office Box 8337 Orlando, Florida 38200	1
Defense Documentation Center Cameron Station Alexandria, Virginia	20
Dr. Melvin J. Jacobson Rensselaer Polytechnic Institute Troy, New York 12181	1
Dr. Charles Stutt General Electric Company P. O. Box 1088 Schenectady, New York 12301	1
Dr. J. V. Bouyoucos General Dynamics/Electronics 1400 N. Goodman Street P. O. Box 226 Rochester, New York 14609	1
Mr. J. Bernstein EDO Corporation College Point, New York 11356	1
Dr. T. G. Birdsall Cooley Electronics Laboratory The University of Michigan Ann Arbor, Michigan 48105	1

DISTRIBUTION LIST (Cont.)

	No. of Copies
Dr. John Steinberg Institute of Marine Science The University of Miami Miami, Florida 33149	1
Mr. William Stalford Bendix Corporation Bendix-Pacific Division North Hollywood, California 91605	1
Commander Naval Ordnance Test Station Pasadena Annex 3203 E. Foothill Boulevard Pasadena, California 91107	1
Dr. Stephen Wolff Johns Hopkins University Baltimore, Maryland 21218	1
Dr. M. A. Basin Litton Industries 8000 Woodley Avenue Van Nuys, California 91409	1
Dr. Albert Nuttall Litton Systems, Inc. 335 Bear Hill Road Waltham, Massachusetts 02154	1
Dr. Philip Stocklin Box 360 Raytheon Company Newport, Rhode Island 02841	1
Dr. H. W. Marsh Raytheon Company P. O. Box 128 New London, Connecticut 06321	1

DISTRIBUTION LIST (Cont.)

	No. of Copies
Mr. Ken Preston Perkin-Elmer Corporation Electro-Optical Division Norwalk, Connecticut 06852	1
Mr. Tom Barnard Texas Instruments Incorporated 100 Exchange Park North Dallas, Texas 75222	1
Dr. John Swets Bolt, Beranek and Newman 50 Moulton Street Cambridge 38, Massachusetts	1
Dr. H. S. Hayre The University of Houston Cullen Boulevard Houston, Texas 77004	1
Dr. Robert R. Brockhurst Woods Hole Oceanographic Inst. Woods Hole, Massachusetts	1
Cooley Electronics Laboratory The University of Michigan Ann Arbor, Michigan	50
Director Office of Naval Research Branch Office 495 Summer Street Boston, Massachusetts 02210	1
Dr. L. W. Nolte Dept. of Elec. Eng. Duke University Durham, N. Carolina	1

DISTRIBUTION LIST (Cont.)

	No. of Copies
Mr. F. Briggson Office of Naval Research Representative 121 Cooley Building The University of Michigan Ann Arbor, Michigan	1
Dr. R. A. Roberts Dept. of Elec. Eng. University of Colorado Boulder, Colorado	1

Security Classification

DOCUMENT CONTROL DATA - R&D

(Security classification of title, body of abstract and indexing annotation must be entered when the overall report is classified)

1. ORIGINATING ACTIVITY *(Corporate author)*
Cooley Electronics Laboratory
The University of Michigan
Ann Arbor, Michigan 48105

2a. REPORT SECURITY CLASSIFICATION
UNCLASSIFIED

2b. GROUP

3. REPORT TITLE
Intersymbol Interference in Binary Communication Systems

4. DESCRIPTIVE NOTES *(Type of report and inclusive dates)*
Technical Report No. 195 - 3674-18-T

5. AUTHOR(S) *(Last name, first name, initial)*
Kimball, Christopher V.

6. REPORT DATE	7a. TOTAL NO. OF PAGES	7b. NO. OF REFS
August 1968	217	12

8a. CONTRACT OR GRANT NO.	9a. ORIGINATOR'S REPORT NUMBER(S)
Nonr-1224(36)	3674-18-T
b. PROJECT NO.	
c.	9b. OTHER REPORT NO(S) *(Any other numbers that may be assigned this report)*
d.	TR 195

10. AVAILABILITY/LIMITATION NOTICES
Reproduction in whole or in part is permitted for any purpose of the U. S. Government.

11. SUPPLEMENTARY NOTES	12. SPONSORING MILITARY ACTIVITY
	Office of Naval Research Department of the Navy Washington, D.C.

13. ABSTRACT When a binary communication system transmits symbols through a bandlimited channel, the received symbols will generally overlap in time, giving rise to intersymbol interference. In the presence of noise, intersymbol interference produces a significant increase in the system probability of error. The problem of intersymbol interference and noise is considered here for known, linear, time invariant channels and with added white Gaussian noise. Although a particular underwater acoustic channel is used as a source of motivation, the results presented are equally applicable to other communication channels. Traditional approaches to the intersymbol interference problem--spectrum and transversal (time) equalization are examined. A basis for the comparison of intersymbol interference problems using the concept of phase equalization, is given. A major assumption which limits the interference to that caused by adjacent symbols is made. This assumption is shown to be equivalent to restricting the transmitter to reasonable signalling rates relative to the bandwidth of the channel power spectrum. All subsequent analysis and evaluation are done under this assumption. Several linear filter receivers prevalent in the literature are reviewed and evaluated. Two easily implemented nonlinear receivers are considered as alternatives to the more complex optimized linear filter receivers. The iterated switched-mode receiver is shown to perform better than any optimized linear receiver when intersymbol interference is moderate.

DD FORM 1 JAN 64 1473

Security Classification

14. KEY WORDS	LINK A		LINK B		LINK C	
	ROLE	WT	ROLE	WT	ROLE	WT
Underwater Communications Binary Communications Intersymbol Interference Multipath Effects Selective Fading Signal Detection						

INSTRUCTIONS

1. ORIGINATING ACTIVITY: Enter the name and address of the contractor, subcontractor, grantee, Department of Defense activity or other organization *(corporate author)* issuing the report.

2*a*. REPORT SECURITY CLASSIFICATION: Enter the overall security classification of the report. Indicate whether "Restricted Data" is included. Marking is to be in accordance with appropriate security regulations.

2*b*. GROUP: Automatic downgrading is specified in DoD Directive 5200.10 and Armed Forces Industrial Manual. Enter the group number. Also, when applicable, show that optional markings have been used for Group 3 and Group 4 as authorized.

3. REPORT TITLE: Enter the complete report title in all capital letters. Titles in all cases should be unclassified. If a meaningful title cannot be selected without classification, show title classification in all capitals in parenthesis immediately following the title.

4. DESCRIPTIVE NOTES: If appropriate, enter the type of report, e.g., interim, progress, summary, annual, or final. Give the inclusive dates when a specific reporting period is covered.

5. AUTHOR(S): Enter the name(s) of author(s) as shown on or in the report. Enter last name, first name, middle initial. If military, show rank and branch of service. The name of the principal author is an absolute minimum requirement.

6. REPORT DATE: Enter the date of the report as day, month, year; or month, year. If more than one date appears on the report, use date of publication.

7*a*. TOTAL NUMBER OF PAGES: The total page count should follow normal pagination procedures, i.e., enter the number of pages containing information.

7*b*. NUMBER OF REFERENCES: Enter the total number of references cited in the report.

8*a*. CONTRACT OR GRANT NUMBER: If appropriate, enter the applicable number of the contract or grant under which the report was written.

8*b*, 8*c*, & 8*d*. PROJECT NUMBER: Enter the appropriate military department identification, such as project number, subproject number, system numbers, task number, etc.

9*a*. ORIGINATOR'S REPORT NUMBER(S): Enter the official report number by which the document will be identified and controlled by the originating activity. This number must be unique to this report.

9*b*. OTHER REPORT NUMBER(S): If the report has been assigned any other report numbers *(either by the originator or by the sponsor)*, also enter this number(s).

10. AVAILABILITY/LIMITATION NOTICES: Enter any limitations on further dissemination of the report, other than those imposed by security classification, using standard statements such as:

(1) "Qualified requesters may obtain copies of this report from DDC."

(2) "Foreign announcement and dissemination of this report by DDC is not authorized."

(3) "U. S. Government agencies may obtain copies of this report directly from DDC. Other qualified DDC users shall request through _____."

(4) "U. S. military agencies may obtain copies of this report directly from DDC. Other qualified users shall request through _____."

(5) "All distribution of this report is controlled. Qualified DDC users shall request through _____."

If the report has been furnished to the Office of Technical Services, Department of Commerce, for sale to the public, indicate this fact and enter the price, if known.

11. SUPPLEMENTARY NOTES: Use for additional explanatory notes.

12. SPONSORING MILITARY ACTIVITY: Enter the name of the departmental project office or laboratory sponsoring *(paying for)* the research and development. Include address.

13. ABSTRACT: Enter an abstract giving a brief and factual summary of the document indicative of the report, even though it may also appear elsewhere in the body of the technical report. If additional space is required, a continuation sheet shall be attached.

It is highly desirable that the abstract of classified reports be unclassified. Each paragraph of the abstract shall end with an indication of the military security classification of the information in the paragraph, represented as *(TS), (S), (C), or (U)*.

There is no limitation on the length of the abstract. However, the suggested length is from 150 to 225 words.

14. KEY WORDS: Key words are technically meaningful terms or short phrases that characterize a report and may be used as index entries for cataloging the report. Key words must be selected so that no security classification is required. Identifiers, such as equipment model designation, trade name, military project code name, geographic location, may be used as key words but will be followed by an indication of technical context. The assignment of links, rules, and weights is optional.